

# **Elucidating the role of Clusterin in human oral cancers**

**By**

**Ms. Rajashree Chittaranjan Kadam**

**[LIFE09201304006]**

**TATA MEMORIAL CENTRE**

**MUMBAI**

*A thesis submitted to the  
Board of Studies in Life Sciences  
in partial fulfillment of requirements  
for the Degree of*

**DOCTOR OF PHILOSOPHY**

*of*

**HOMI BHABHA NATIONAL INSTITUTE**



**May, 2021**

# Homi Bhabha National Institute

## Recommendations of the Viva Voce Committee

As members of the Viva Voce Committee, we certify that we have read the dissertation prepared by Ms. Rajashree Chittaranjan Kadam entitled "Elucidating the Role of Clusterin in Human Oral Cancers" and recommend that it may be accepted as fulfilling the thesis requirement for the award of Degree of Doctor of Philosophy.

-----  
Chairperson – Dr. Sorab N. Dalal *S. N. Dalal* Date: 17/05/2021  
-----  
Guide/Convener – Dr. Tanuja Teni *TR Teni* Date: 17/05/2021  
-----  
External Examiner – Dr. Sharmila Bapat *S. Bapat* Date: 17/05/2021  
-----  
Member – Dr. Manoj Mahimkar *M. Mahimkar* Date: 17/05/2021  
-----  
Member -Dr. Abhijit De *Abhijit De* Date: 17/05/2021

Final approval and acceptance of this thesis is contingent upon the candidate's submission of the final copies of the thesis to HBNI.  
I hereby certify that I have read this thesis prepared under my direction and recommend that it may be accepted as fulfilling the thesis requirement.

Date: 17.05.2021

Place: Navi Mumbai

*TR Teni*  
Dr. Tanuja Teni  
Guide

## STATEMENT BY AUTHOR

This dissertation has been submitted in partial fulfillment of requirements for an advanced degree at Homi Bhabha National Institute (HBNI) and is deposited in the Library to be made available to borrowers under rules of the HBNI. Brief quotations from this dissertation are allowable without special permission, provided that accurate acknowledgement of source is made. Requests for permission for extended quotation from or reproduction of this manuscript in whole or in part may be granted by the Competent Authority of HBNI when in his or her judgment the proposed use of the material is in the interests of scholarship. In all other instances, however, permission must be obtained from the author.

Rekadam

Rajashree Chittaranjan Kadam

## DECLARATION

I, hereby declare that the investigation presented in the thesis has been carried out by me. The work is original and has not been submitted earlier as a whole or in part for a degree / diploma at this or any other Institution / University.



Rajashree Chittaranjan Kadam

## List of Publications arising from the thesis

### Journals

1. Novel nucleolar localization of clusterin and its associated functions in human oral cancers: An in vitro and in silico analysis.

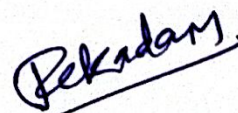
Rajashree Kadam, Mahalakshmi Harish, Kajal Dalvi and Tanuja Teni, Cell Biochemistry and Function, 2020, 1-12. DOI: 10.1002/cbf.3600

2. Clusterin in cancer: Dual role as a tumor suppressor gene and an oncogene (review article)

Rajashree Kadam and Tanuja Teni. Biomedical Research Journal, 2016; 3(2):130-156.  
DOI: 10.4103/2349-3666.240609

### Conferences

1. Cold Spring Harbor Laboratory meeting on 'Mechanisms & Models of Cancer', New York, August 2018
2. The International Conference of Cell Biology at Hyderabad, India, January 2018
3. TMC Platinum Jubilee Conference entitled "A Conference of New Ideas in Cancer – Challenging Dogmas", Mumbai, India, February 2016.



Rajashree Chittaranjan Kadam

*Dedicated to Aai, Papa and Sourabh*

## Acknowledgement

*I wish to express my sincere gratitude to my guide and mentor Dr. Tanuja Teni for giving me an opportunity to work under her kind guidance. This journey would not have been easy without her constant support, encouragement, and scientific inputs. She has always been very supportive at both the professional and personal front and has played an important role in bringing the best out of me. Despite all the challenges in this Ph.D. journey, her smiling face and reassuring words always used to motivate me to keep going.*

*I would also like to thank Dr. Sudeep Gupta (Director), Dr. Prasanna Venkatraman (Dy. Director), Dr. S.V Chiplunkar (Ex-Director) for giving me an opportunity to work in the institute and providing the research infrastructure. I would like to thank them for their support and encouragement in organizing National Research Scholars Meet and resolving issues taken up by Students Council of ACTREC. I sincerely thank ACTREC for providing me the fellowship, Sam Mistry Fund (TMC), HBNI, and Patel Kantaben Kantilal Charitable Trust for providing financial assistance to attend the international conference during my Ph.D. tenure.*

*I would like to thank my doctoral committee members Dr. Sorab Dalal (Chairperson), Dr. Manoj Mahimkar, Dr. Abhijit De, and late Dr. Anjali Shiras (NCCS-Pune) for their valuable suggestions, critical comments, and constant encouragement in this journey. I also thank Dr. Poonam Gera (Pathologist, ACTREC) for providing patient tissue samples from ACTREC biorepository and help in initial immunohistochemistry standardization. Also special thanks to Dr. Swapnil Rane (Pathologist, TMC) for scoring IHC slides and his constant support. I am thankful to Pallavi ma'am for her help with the statistical analysis of the patient data.*

*I wish to thank Mr. Uday Dandekar and other staff at the common instrument facility for all technical assistance. I would especially like to thank Mrs. Vaishali Kailaje and Mrs. Tanuja from the ACTREC imaging facility for all their help with microscopy related experiments and constant motivation. Also, I thank the histology department staff at ACTREC for their help with tissue processing and slide*

preparation. I am thankful to staff of IT, Library, Photography, Administration, Accounts, Steno pool, SCOPE, and security department for their prompt help and support whenever needed.

I am also indebted to Dr. Mahalakshmi Ram for her help with the structure prediction and docking analysis of CLU. I also would like to thank Dr. Dibyendu Bhattacharyya (ACTREC) and Dr. Kristel Sleeper (University of Antwerp, Belgium) for providing pEGF-C1-Fibrillarin and pEGFP-C1-Clusterin constructs for this study. I also thank Prof. Sussane Gollin (University of Pittsburgh) for providing oral cancer cell lines used in this study.

My special thanks to Teni Lab members Yashwant sir, Sagar sir, Rupa, Prasad, Yasser, Dhanashree, Dipti, Abhay, Swapnil and Reshma for making this workplace so comfortable and joyous. Also would like to specially mention ex-members of Teni Lab Prajakta, Rohit, Pritha and Farheen for all the love and support you offered in this journey. I will always cherish all the scientific discussions and sharing-caring moments spent with you guys forever. This journey would not have been easy without the help of some of my trainees (now turned into friends) Kajal, Ambika, Aniruddha, Anushka, Mitali, Sanika and Aishwarya.

I also take this as an opportunity to thank batch-2013 members for making this Ph.D. journey memorable. I have shared a special bond with each and everyone in this batch and words will fall short to thank you guys enough. I would especially like to thank Pravin, Asmita, Shalini, Rai, and my juniors Roma, Nazia, Sayoni, and Naini for your selfless love and countless help.

In the end, I would like to thank my special people Aai, Papa, Aaji, and my husband Sourabh. They are pillars of my life who never let me fall down. Without their love, support and sacrifices this would not have been possible. Words will fall short to express my gratitude towards them. I also thank my in-laws, friends and family for their encouragement and love. Last but not least I thank God, the almighty who has showered countless blessings and granted the knowledge and opportunities to me.

# CONTENTS

	<b>Page No.</b>
<b>Synopsis</b> .....	<b>14</b>
<b>List of Abbreviations</b> .....	<b>28</b>
<b>List of Tables</b> .....	<b>31</b>
<b>List of Figures</b> .....	<b>32</b>
<b>Chapter 1: Introduction</b> .....	<b>35</b>
<b>Chapter 2. Review of Literature</b> .....	<b>39</b>
2.1 Oral Cancer.....	40
2.1.1 Oral cancer epidemiology.....	40
2.1.2 Oral cancer pathogenesis.....	40
2.1.3 Oral premalignant lesions.....	41
2.1.4 Etiology and risk factors.....	42
2.1.5 Treatment modalities for oral cancer.....	45
2.2 Apoptosis and dysregulation in cancer.....	47
2.2.1 Intrinsic and extrinsic pathways of apoptosis.....	48
2.2.2 Inhibitors of apoptosis proteins (IAPs).....	50
2.2.3 Apoptosis as a therapeutic target in cancer.....	50
2.3 Clusterin.....	51
2.3.1 Origin and associated functions.....	51
2.3.2 Genomic organization and biogenesis of splice variants of CLU.....	51
2.3.3 Structure of Clusterin.....	54
2.3.4 Expression and role of CLU in different cancers.....	55

2.3.4.1 CLU as a tumor suppressor gene.....	56
2.3.4.2 CLU as an oncogene.....	58
2.3.5 Localization studies of CLU.....	61
2.4 Nucleolus: structural organization and associated functions.....	61
2.4.1 Nucleolar proteins.....	62
2.4.2 Cajal body.....	64
2.4.3 Nucleolar stress response.....	65
2.4.3.1 p53 dependent nucleolar stress response.....	67
2.4.3.2 p53 independent nucleolar stress response.....	67
2.5 Ribosome biogenesis.....	68
<b>Chapter 3 Aims and Objectives.....</b>	<b>71</b>
<b>Chapter 4 Materials and Methods.....</b>	<b>73</b>
4.1 Materials.....	74
4.2 Methods.....	78
4.2.1 Mammalian cell culture.....	78
4.2.2 Oral tissue sample collection and processing.....	79
4.2.3 RNA extraction from cell lines using RNAiso Plus reagent.....	81
4.2.4 RNA extraction from tissues using GeneJET RNA purification kit.....	82
4.2.5 cDNA synthesis.....	83
4.2.6 Quantitative real time PCR (qRT-PCR).....	84
4.2.7 Immunohistochemistry (IHC).....	85
4.2.8 Immunofluorescence microscopy.....	86
4.2.9 siRNA and shRNA transfection.....	87

4.2.10 5-Fluorouridine incorporation assay.....	88
4.2.11 Protein extraction and western blotting.....	88
4.2.12 Cycloheximide chase assay.....	92
4.2.13 Cell proliferation assay (MTT assay).....	92
4.2.14 Loss of heterozygosity detection using Sequenom MassARRAY iPLEX Platform.....	93
4.2.15 Methylation specific PCR (MSP).....	96
4.2.16 miRNA expression analysis oral tumor samples.....	96
4.2.17 Analysis of CLU amino acid sequence for the detection of nuclear and nucleolar localization sequence.....	98
4.2.18 Analysis of CLU amino acid sequence for the detection RNA binding motif.....	98
4.2.19 In silico analysis of CLU.....	99
4.2.20 Statistical Analysis.....	99
4.2.21 Molecular cloning methods.....	100
<b>Chapter 5 Results.....</b>	<b>103</b>
5.1 To assess the expression of CLU in oral tumor samples.....	104
5.1.1 Evaluation of different CLU transcripts in oral tumor samples using isoform specific quantitative real-time PCR (qRT-PCR).....	104
5.1.2 Evaluation of CLU protein expression in oral tumor samples using western blotting and immunohistochemistry.....	105
5.2 Understanding the possible mechanisms of CLU downregulation in oral tumor samples...	110
5.2.1 Detecting methylation of CLU promoter using methylation specific PCR (MSP).....	110
5.2.2 Detecting loss of heterozygosity at CLU locus chromosome 8p21 using Sequenom Mass ARRAY system.....	111

5.2.3 Expression profiling of miRNA predicted to target CLU in oral tumors samples.....	113
5.3 To assess the expression of CLU in oral cancer cell lines.....	115
5.3.1 To check the expression of different CLU variants in oral cancer cell lines using isoform specific qRT-PCR.....	115
5.3.2 Evaluating the expression of CLU protein in different oral cancer cell lines.....	115
5.3.3 Assessing the CLU protein stability and possible mechanisms associated with the stability.....	116
5.3.3.1 Cycloheximide (CHX) chase assay to determine the CLU protein stability.....	116
5.3.3.2 Mechanisms of CLU degradation in oral cancer cells.....	117
5.3.3.3 Understanding the role of glycosylation in the stability of CLU in oral cancer cells.....	118
5.4 To study the localization of CLU in oral cancer cell lines.....	119
5.5 Overexpression of GFP tagged CLU construct and its localization study in oral cancer cells.....	123
5.5.1 Molecular cloning of sCLU coding region (CDS) in pEGFP-N1 construct.....	123
5.5.2 Overexpression of pFGFP-N1-sCLU in oral cancer cell lines.....	127
5.5.3 Overexpression of pFGFP-C1-sCLU in oral cancer cell lines.....	127
5.6 Identification of nucleolar and nuclear localization sequence of CLU using bioinformatics tools.....	129
5.7 Effect of nuclease treatment on nucleolar localization of CLU.....	131
5.8 Effect of stress on expression and nucleolar localization of sCLU.....	133
5.9 Effect of CLU knockdown in oral cancer cell lines.....	140
5.9.1 Effect of CLU knockdown on ribosome biogenesis.....	140
5.9.2 Effect of CLU knockdown on proliferation.....	142

5.9.3 Effect of CLU knockdown on nuclear morphology.....	143
5.10 In silico approach to predict the structure CLU and its interaction with nucleolar proteins.....	145
<b>Chapter 6 Discussion.....</b>	<b>152</b>
<b>Chapter 7 Summary and Conclusions.....</b>	<b>164</b>
<b>Chapter 8 References.....</b>	<b>169</b>
<b>Chapter 9 Appendix.....</b>	<b>200</b>
<b>Chapter10 Publication.....</b>	<b>204</b>

## List of Tables

	<b>Page No.</b>
<b>Table 1:</b> Primary and secondary antibodies used in the study.....	76
<b>Table 2:</b> Instruments used in the study.....	77
<b>Table 3:</b> List of different oral cancer cell lines used in the study.....	79
<b>Table 4:</b> Clinicopathological characteristics of the oral cancer patient samples used for immunohistochemistry study.....	81
<b>Table 5:</b> Preparation of 2X RT mastermix for cDNA synthesis.....	83
<b>Table 6:</b> Thermal cycler conditions for cDNA synthesis using high capacity cDNA synthesis kit.....	83
<b>Table 7:</b> The list of primers used for quantitative real time PCR.....	84
<b>Table 8:</b> Reaction set up for Real Time PCR using SYBR Green Chemistry.....	85
<b>Table 9:</b> Folin-Lowry protein estimation assay.....	89
<b>Table 10:</b> Bradford protein estimation assay.....	90
<b>Table 11:</b> Composition of resolving and stacking gel for SDS-PAGE.....	91
<b>Table 12:</b> Primers used for MSP assay.....	96
<b>Table 13:</b> Primers used for miRNA specific cDNA synthesis and real-time PCR.....	97
<b>Table 14:</b> Restriction enzyme digestion of of CLU CDS and pEGFP-N1 plasmid.....	101
<b>Table 15:</b> Ligation reaction.....	102
<b>Table 16:</b> Association of sCLU with clinopathological parameters in oral tumors.....	108
<b>Table 17:</b> Potential additional interactions between CLU and nucleolar proteins.....	151

## List of Figures

	Page No.
<b>Figure 1:</b> Apoptosis: The intrinsic and extrinsic pathways to activate caspase.....	50
<b>Figure 2:</b> Schematic representation of different splice variants of Clusterin.....	52
<b>Figure 3:</b> CLU biogenesis pathway.....	53
<b>Figure 4:</b> Different sub-compartments of the nucleolus.....	62
<b>Figure 5:</b> Classification of nucleolar proteins involved in various cellular functions identified by quantitative proteome analysis.....	63
<b>Figure 6:</b> Immunofluorescence photograph showing SMN (survival of motor neuron protein), a cajal body marker.....	65
<b>Figure 7:</b> Different types of nucleolar stress inducers.....	66
<b>Figure 8:</b> Nucleolar segregation or cap formation in response to nucleolar stress.....	67
<b>Figure 9:</b> Eukaryotic ribosome biosynthesis.....	70
<b>Figure 10:</b> The Schematic of MassEXTEND iPLEX reaction.....	95
<b>Figure 11:</b> qRT-PCR analysis for the expression of sCLU in paired oral tumor samples.....	104
<b>Figure 12:</b> Expression of sCLU protein in oral tumor samples.....	105
<b>Figure 13:</b> Immunohistochemical analysis of CLU expression in oral tumor Samples.....	106-107
<b>Figure 14:</b> Kaplan-Meier curves of OS and RFS for CLU expression in tumor epithelial and stromal compartment.....	109
<b>Figure 15:</b> Methylation specific PCR in oral tumor samples.....	111
<b>Figure 16:</b> Study of LOH in oral tumor samples using Sequenom MassEXTEND genotyping assay.....	112
<b>Figure 17:</b> miRNA expression profiling in oral tumor samples.....	114

<b>Figure 18:</b> Expression of sCLU transcripts in oral cancer cell lines.....	115
<b>Figure 19:</b> Expression of sCLU protein in oral cancer cell lines.....	116
<b>Figure 20:</b> Cycloheximide chase assay to assess the CLU stability.....	117
<b>Figure 21:</b> Effect of inhibition of proteasome and lysosomal degradation pathways on CLU levels.....	117
<b>Figure 22:</b> Effect of N-linked glycosylation inhibitors on CLU expression.....	118
<b>Figure 23:</b> Immunofluorescence based localization study of CLU in oral cancer cell line AW8507.....	119
<b>Figure 24:</b> Co-localization of CLU with different nucleolar markers.....	119-121
<b>Figure 25:</b> Confirmation of CLU antibody used for western blotting and immunofluorescence.....	122
<b>Figure 26:</b> Nucleolar fractionation studies in AW8507 oral cancer cell line.....	123
<b>Figure 27:</b> Molecular cloning of CLU CDS in pEGFP-N1 mammalian expression Construct.....	125
<b>Figure 28:</b> Screening of positive clones for the presence of CLU CDS.....	126
<b>Figure 29:</b> Overexpression of pEGFP-N1-CLU construct in AW8507 cell line.....	127
<b>Figure 30:</b> Overexpression of pFGFP-C1-sCLU in AW8507 cells.....	128
<b>Figure 31:</b> Identification of Nucleolar and nuclear localization sequence in CLU amino acid sequence.....	130
<b>Figure 32:</b> Effect of RNase A treatment on localization of CLU.....	132
<b>Figure 33:</b> Effect of ribosome biogenesis inhibitors actinomycin D and doxorubicin on 45S rRNA and sCLU transcripts.....	134
<b>Figure 34:</b> Effect of Actinomycin D and Doxorubicin on nucleolar localization of CLU.....	135-137
<b>Figure 35:</b> Effect of Actinomycin D treatment on localization of CLU and Coilin.....	138

<b>Figure 36:</b> Effect of radiation on sCLU expression.....	139
<b>Figure 37:</b> Effect of hypoxia inducing agent COCl <sub>2</sub> on CLU expression and Localization.....	140
<b>Figure 38:</b> Effect of CLU knockdown on ribosome biogenesis.....	141
<b>Figure 39:</b> Effect of CLU knockdown on proliferation in oral cancer cells.....	142
<b>Figure 40:</b> Effect of CLU knockdown on downstream signaling components.....	143
<b>Figure 41:</b> Effect of CLU knockdown on nuclear morphology and nucleolar proteins in oral cancer cells.....	144-145
<b>Figure 42:</b> Predicted structures of sCLU using trRosetta tool.....	147
<b>Figure 43:</b> Sequence alignment of sCLU sequences across different species using PRALINE tool.....	148
<b>Figure 44:</b> Docking analysis of CLU with different nucleolar client proteins using Z-DOCK.....	150

*Chapter 7*  
*Summary and*  
*Conclusions*

The present study aimed to identify the expression of different transcript variants of CLU and its functional significance in human oral cancer cells. This is the first comprehensive study to understand the expression, localization, and intracellular function of CLU in human oral cancer tissues and cell lines.

**The important findings from this study are as follow:**

- The isoform specific qRT-PCR in oral cancer tissues and cell lines showed the presence of sCLU as the predominant isoform. The transcript levels of other transcript variants including nCLU, NR\_038335.1, and NR\_045494.1 were very low or undetectable.
- The sCLU transcript levels were significantly downregulated in oral tumors compared to their adjacent normal tissues and healthy control tissues obtained during minor dental surgeries. Similarly, we observed downregulation of pre-secretory form of CLU (psCLU) in the majority of the oral tumors compared to its adjacent normal tissue. Immunohistochemical analysis of CLU expression in oral tissue samples showed cytoplasmic staining in both epithelial and cancer associated stromal compartments. Interestingly, low epithelial and high stromal expression of CLU was found to be associated with poor overall and recurrence-free survival of the patients, highlighting its prognostic significance.
- To understand the possible mechanisms for CLU downregulation in oral tumors, we studied methylation of CLU promoter, LOH at chromosome 8p, and miRNA mediated regulation in 10 randomly selected paired oral tissue samples. However, data obtained from methylation- specific PCR and LOH was inconclusive possibly due to the smaller sample size; hence needs to be performed in a larger sample cohort to understand its role in CLU regulation if any. The expression analysis of miRNAs which are predicted to target the CLU gene, showed overexpression of miR-21, miR-15a, and miR-17-3p, which may have a role in CLU downregulation in oral tumors. This needs to be performed in a larger sample cohort

and needs further validation using luciferase-based assay to confirm the binding of miRNA to CLU 3'-UTR.

- All oral cancer cell lines showed downregulation of sCLU transcripts compared to HaCaT, an immortalized skin keratinocyte cell line. However, at the protein level, all oral cancer cell lines showed the presence of a significant amount of protein possibly due to its increased stability. Cycloheximide chase assay in oral cancer cell lines revealed that sCLU is stable for up to 24 hr. Further, treatment of these cells with N-linked glycosylation inhibitor tunicamycin showed a decrease in sCLU levels, suggesting the possible role of glycosylation in imparting stability to sCLU. sCLU degradation was shown to be mediated by the proteasome and lysosomal pathways.
- We demonstrated for the first time the nucleolar localization of CLU in oral cancer cell lines. The nucleolar localization of CLU was confirmed by its co-localization with different nucleolar markers and different fixation-permeabilization techniques. sCLU was mainly localized at the FC and DFC compartments of the nucleolus, the site of rDNA transcription and processing. Nucleolar fractionation studies indisputably confirmed the presence of sCLU in the nucleolar fraction. Also, CLU knockdown studies confirmed the specificity of the CLU antibody used for western blotting and immunofluorescence based studies.
- The study involving overexpression of N- and C-terminally GFP tagged CLU protein in oral cancer cells either showed pan-cellular localization or in the ER and golgi, the secretory pathway components. We did not observe the nucleolar localization of GFP tagged CLU either due to sterically hindered NLS or poor exchange with intracellular endogenous CLU present in the nucleolus.
- Analysis of the sCLU amino acid sequence showed the presence of NLS but no NoLS was detected, suggesting that transport of CLU to nucleolus may be NLS dependent. Further

studies involving site-directed mutagenesis of NLS of sCLU and its effect on the nucleolar localization are currently ongoing in the lab.

- sCLU, like other nucleolar proteins, showed the formation of ‘nucleolar caps’ or ‘nucleolar segregation pattern’ post-treatment with actinomycin D or doxorubicin, a characteristic phenomenon observed post ribosome biosynthesis inhibition. Also, sCLU was associated with cajal bodies at the nucleolar caps post ribogenesis inhibition, suggesting its possible role in nucleolar stress response. However, such types of nucleolar caps were not seen post metabolic stress conditions like radiation and hypoxia.
- RNase A treatment showed translocation of nucleolar CLU to the nucleoplasm, indicating that nucleolar localization of CLU may be rRNA or ribonucleoprotein dependent. This was supported by the presence of putative RNA binding regions at the N and C terminus of sCLU predicted by RNABindR and PPRInt.
- CLU knockdown studies in oral cancer cells showed a significant increase in 28S and 18S rRNAs. The increase in 45S rRNA was not statistically significant. This was also confirmed by the 5-FUrd incorporation assay which showed increased uptake of 5-FUrd in CLU knockdown cells, suggesting the role of nucleolar CLU in the negative regulation of ribogenesis. On a similar line, CLU knockdown clones showed increased proliferation. This suggests the possible tumor suppressor like role of sCLU in oral cancer cells.
- Intriguingly, we also observed altered nuclear shapes post knockdown of CLU. CLU silencing resulted in aberrant nuclear morphologies like ruffled, irregular, and lobulated. The knockdown of CLU resulted in a decrease in the expression of nucleolar proteins NPM1 and Fibrillarin. These two proteins were earlier reported to regulate the nuclear shape possibly by maintaining the cytoskeletal structures like tubulin and actin filaments. In this study, we observed shrunk tubulin filaments in CLU silenced cells resulting in abnormal nuclear shape.

This suggests the role of CLU in nuclear shape maintenance mediated by regulating the levels of nucleolar proteins like NPM1 and Fibrillarin.

- Since NPM1 and Fibrillarin levels were downregulated post sCLU knockdown, we wanted to assess whether sCLU can interact with these nucleolar proteins and mediate chaperonic functions. Hence, to explore this possibility we predicted the structure of sCLU and studied its interaction with different nucleolar proteins like NPM1, Fibrillarin, UBF, and Nucleolin using an *in silico* approach. Interestingly, docking studies revealed the involvement of the amino acid region 140-155 of sCLU in interaction with all the complexes studied. Notably, all the docking complexes showed that the Phe152 residue of sCLU is held in a hydrophobic core created by the residues of the interacting partners.

## Thesis Summary

Clusterin (CLU) is stress induced chaperonic glycoprotein associated with various physiological functions like cell cycle regulation, apoptosis, DNA repair, etc. The two spliced variants of CLU namely the secretory and nuclear forms serve anti- and pro-apoptotic functions respectively. Previous studies done in the lab using ribonuclease protection assay have shown downregulation of CLU transcripts in oral cancer cells unlike its overexpression in other carcinomas which prompted us further to investigate the role of CLU in oral tumorigenesis.

We demonstrated the downregulation of secretory CLU (sCLU) transcript and protein in human oral cancer tissues. Immunohistochemical analysis in oral tumor samples has shown that low expression of sCLU in the epithelium and high expression in stroma is associated with poor overall and recurrence-free survival of patients. Oral cancer cell lines showed downregulation of sCLU transcripts compared to normal tissues; however, we observed high expression of sCLU protein in oral cancer cell lines possibly due to its increased stability. Nuclear CLU (nCLU) was not detected at transcript and protein levels in oral cancer cells. In the present study, we report for the first time the RNA-dependent nucleolar localization of sCLU protein in oral cancer cell lines. sCLU has been shown to form 'nucleolar cap' like structures in response to nucleolar stress conditions which affect the ribosome biosynthesis. Interestingly, post-CLU knockdown we observed an increase in ribogenesis and proliferation which suggests its possible tumor-suppressive role in oral cancer. Also knockdown of sCLU resulted in a decrease in NPM1 and Fibrillarin levels which concomitantly result in abnormal shapes of nuclei and shrunk cytoskeletal filaments indicative of its role in nuclear shape maintenance. Further *in silico* analysis revealed the hydrophobic interaction of Phe152 residue of CLU with different nucleolar proteins like NPM1, Fibrillarin, Nucleolin, and UBF suggesting the possible chaperonic function of CLU in the stabilization of these nucleolar proteins.

# *Chapter 1*

## *Introduction*

In some of the South-Central Asian countries including India, oral cancer is one of the most common cancers worldwide and a leading cause of mortality. It is a significant public health concern [1]. The worldwide annual incidence of oral cancer is above 300,000 cases with a mortality rate of 48% [2]. More than 90% of the oral tumors in this anatomical site arise from premalignant lesions like leukoplakia and submucous fibrosis [3]. Apart from tobacco and alcohol consumption habits, factors like micronutrient deficiencies, poor oral hygiene, chronic traumatism, and viruses have been shown to increase the risk of oral cancer development[3].

Even though the oral cavity is easily accessible, most of the oral cancers are detected at a later stage either due to lack of awareness, ignorance, or remoteness of medical care resulting in lower survival rates. Despite the advancement in treatment modalities of oral cancer, no significant change in the 5-year survival rate has been observed since the last decade due to development of tumor recurrence and treatment resistance. Eventually, more than 50% of patients develop local recurrence or metastasis typically within the first 2 years after completion of treatment [4,5].

Oral carcinogenesis is a multistep process in which numerous genetic alterations abrogate the normal functions of tumor suppressor genes and proto-oncogenes/oncogenes. Moreover, these genetic changes result in an increase in the synthesis of growth factors or their cell surface receptors, enhanced intracellular signaling, and production of mutated transcription factors that disturb the well regulated signaling pathways of a normal cell [6]. Therefore, identification of the key molecules involved in oral cancer progression may assist in early detection and better prognosis. To understand the molecular basis for the progression of oral cancers, previous studies in the lab identified the differences in the expression of various inhibitors of apoptosis proteins (IAPs) in oral cancer cell lines and tissues using

ribonuclease protection assay (RPA). This revealed decreased levels of TRPM2/Clusterin transcript in tumor tissues and cell lines as compared to the normal tissues.

Clusterin (CLU) is a heterodimeric, sulfated chaperone glycoprotein associated with various physiological functions like cell-cell interaction, cell cycle regulation, apoptosis, lipid transport, complement inhibition, etc. [7]. Different splice variants of CLU are described in the literature of which secretory (sCLU) and nuclear (nCLU) isoforms are well studied. These two isoforms of CLU have antagonistic functions in the context of apoptosis i.e. sCLU is an anti-apoptotic whereas nCLU is pro-apoptotic in nature. The secretory form of CLU (sCLU) is the full length isoform which is reported to be overexpressed in different cancers like pancreatic, breast, hepatocellular, and melanoma [8,9] and its role as an oncogene is well reported. Conversely, in few cancers like neuroblastoma, testicular seminoma, and esophageal carcinoma CLU is downregulated suggesting its context-dependent tumor-suppressor like role in these cancers [10–12], although the exact mechanism of CLU downregulation and its effect on downstream signaling is obscure. The exact mechanism by which the cell regulates the production of these CLU isoforms and their localization is not completely understood. Furthermore, the existence of different transcript variants of CLU, ambiguity in their nomenclature, lack of structural details, and isoform specific antibody contributes to the complexity of CLU research.

Studies carried out in the head and neck carcinoma tissue samples have shown downregulation of sCLU transcripts due to overexpression of miR-21 [13], however, the expression of sCLU at protein level is not described in this study. Another study involving serum proteomic analysis of oral cancer patients showed significant downregulation of CLU protein [14]; however, it lacks clear information about the isoform of CLU expressed. Contrarily, a recent study by Naik *et al* showed upregulation of CLU with an increase in tumor grade in oral cancer patients of India [15]. Such kind of discrepancies arises from the

fact that in human tissues and fluids there are differentially expressed CLU transcript variants that may exhibit distinct context-dependent functions. Hence, this demands the need for isoform-specific expression analysis of CLU in oral cancer samples. The present study aimed to perform the isoform-specific expression analysis of CLU in both oral tumor tissues and cell lines and understand its functional relevance in oral tumorigenesis. We have reported for the first time the nucleolar localization of CLU in oral cancer cell lines and its nucleolar related functions in oral cancer cells. Further, with the help of *in silico* approach, the structure of CLU was predicted and further, docking studies were performed to understand the interaction of CLU with different nucleolar client proteins which highlighted the plausible chaperone-like function of CLU in maintaining the stability of these nucleolar proteins in oral cancer cells.

*Chapter 2*  
*Review*  
*of Literature*

## **2.1 Oral cancer**

### **2.1.1 Oral cancer epidemiology**

Oral cancer is the sixth most common malignancy in the world with a much more common incidence in developing countries including South-Central Asian countries compared to developed countries [16]. Oral cancers are the most common type of head and neck squamous cell carcinomas with high prevalence in South-Central Asian countries like India, Sri Lanka, Pakistan, Bangladesh, whereas, the cancers of the tongue and oropharynx are more common in the western countries[17]. This difference in the predominant sites affected in different countries is attributed to the different habits prevailing in respective geographic regions [17]. As per GLOBOCAN 2018 report, oral cancer is the eleventh most common cancer in Asia with an estimated 227,906 newly diagnosed cases. In India, oral cancer is the most common cancer among males and the fourth most common cancer among females. This is a major health concern in the Indian subcontinent, which accounts for over 30% of the total cancer burden in India [18]. GLOBOCAN 2018 report shows that it is the second common reason for death in India with an age-standardized mortality rate of 5.6 per 100,000. Despite advancements in treatment modalities of oral cancer, the overall 5-year survival rate of oral cancer patients after treatment is around 50%. The loco-regional recurrence is the most common reason for treatment failure [19].

### **2.1.2 Oral cancer pathogenesis**

Oral tumorigenesis is a multistep process in which genetic and molecular events alter the normal regulatory signaling that controls cellular processes like cell division, differentiation, and death leading to uncontrolled proliferation of cells and transformation of a normal keratinocyte into a potentially malignant keratinocyte [6]. These alterations are driven by genomic alterations, chronic inflammation due to exposure to different carcinogens, poor dental hygiene, dietary factors, and immunosuppression [20]. Most of the oral cancer cases

are preceded by oral potentially malignant disorder (OPMD), an asymptomatic clinical condition [21].

### **2.1.3 Oral premalignant lesions**

Precancerous lesions of oral mucosa with a predisposition to the development of oral cancer are defined as “potentially malignant disorders”, which mainly include different conditions like leukoplakia, erythroplakia, oral submucous fibrosis, and lichen planus [22]. However, the majority of these premalignant lesions do not progress to cancer. In India, leukoplakia and oral submucous fibrosis are the most commonly found premalignant lesions as opposed to leukoplakia and erythroplakia common in western countries [23].

#### **Leukoplakia:**

As defined by World Health Organization (WHO), oral leukoplakia is a white patch of the mucosal region of the oral cavity that cannot be scrubbed off and cannot be classified either histologically or clinically [24]. It does not indicate the presence or absence of any stage of oral epithelial dysplasia, as it is a clinical condition that cannot be characterized histologically [21,24]. The most commonly affected regions of the oral cavity include alveolar-buccal mucosa, floor of the mouth, palate, and tongue. Oral leukoplakia is reported to undergo malignant transformation at a rate from 0.13 to 17.5% [25]. This rate of malignant transformation varies in different parts of the world depending on cultural diversity, tobacco, and dietary habits. In patients with such types of lesions, malignant transformation can occur in different oral subsites apart from the original site of the lesion [26]. Oral leukoplakia can be clinically categorized as homogeneous and non-homogeneous lesions. The homogeneous leukoplakias are more common and benign in nature, whereas the non-homogeneous leukoplakias are flat or speckled, white or red in color (erythroleukoplakia), exophytic, nodular, or papillary/verrucous [27].

## **Erythroplakia**

Erythroplakia is described as “A fiery red patch that cannot be characterized clinically or pathologically as any other definable disease”. Erythroplakia prevalence varies between 0.02% and 0.83%. It commonly affects the floor of the mouth, soft palate, and the buccal mucosa [28]. The malignant transformation rate of erythroplakia is considered higher than leukoplakia [22]. Histopathologically, it shows at least some degree of dysplasia and even frequently carcinoma *in situ* or invasive carcinoma [27].

## **Oral submucous fibrosis**

Oral submucous fibrosis (OSMF) is defined as “a chronic and potentially malignant disorder characterized by juxtaepithelial fibrosis of the oral cavity” [29]. In this condition, there is a loss of fibroelasticity in the affected tissue that limits the mobility of the tongue and mouth opening [30]. In India and other East-Asian countries, betel quid chewing has been found to be the main etiological factor [31]. The arecoline present in the areca nut causes fibrosis in the lamina propria which leads to loss of fibroelasticity [21]. This kind of fibrotic lesion is known to have malignant potential with an estimated transformation rate of 9% [30,32].

### **2.1.4 Etiology and risk factors:**

In the Indian subcontinent, the high incidence of oral submucous fibrosis and oral cancers is largely due to the use of smokeless types of tobacco in combination with alcohol intake [33].

The major risk factors associated with oral carcinogenesis are described below:

#### **A) Tobacco**

Tobacco consumption remains to prevail as the most key risk factor for the development of oral cancers. The association between smoking and oral cancer has been recognized by epidemiological studies [34]. The presence of a psychoactive alkaloid makes tobacco addictive. "Nicotine" present in the leaves of tobacco plant causes vasoconstriction, anxiety, and alertness. There exist more than 300 identified carcinogens in tobacco belonging to

aromatic hydrocarbon benzopyrene and tobacco-specific nitrosamines (TSN) family in tobacco smoke. 4-(nitrosomethylamino)-1-(3-pyridyl)-1-butanone (NNK) and N'-nitrosonornicotine (NNN) are the most commonly found carcinogens in tobacco smoke [33]. NNK, NNN, and their derived metabolites covalently bind with the DNA of keratinocytes and form DNA adducts which introduce mutations during the DNA replication process [35]. The metabolism of these tobacco carcinogens mainly involves oxygenation by cytochrome P450 enzyme (CYP) and conjugation by glutathione- s-transferase. The polymorphisms in the genes encoding for these enzymes have been suspected to modulate the individual susceptibility to oral cancers [33,36].

#### **B) Betel quid**

Chewing of betel quid along with different ingredients like slaked lime, areca nut ('supari'), and tobacco is the most common habit in South-Central Asian countries, especially in India [37]. Betel vine leaf contains an aromatic unsaturated volatile substance named eugonal which is a central nervous system stimulant. It is generally chewed to extract out alkaloids such as arecoline (similar to nicotine), arecaidine, guvacine and guvacoline which interact with muscarinic receptors and function via acetylcholine [38]. Areca nut contains carcinogens like N-nitrosamines and chewing results in the production of reactive oxygen species (ROS) due to oxidation of polyphenols present in areca nut and enhanced by slaked lime alkaline pH [39]. Additionally, arecoline in areca nut extracts causes genotoxicity and teratogenicity, which plays an imperative role in oral carcinogenesis [40].

#### **C) Alcohol**

The synergistic action of alcoholic drinks with tobacco increases the risk of oral cancer. Excess alcohol consumption can lead to an increased risk of oral cancer, because alcohol acts as a solvent that causes movement of carcinogens via oral cell membranes, and alters the intracellular metabolism of the epithelial cells, leading to impaired cellular functions (e.g.,

enhanced DNA alkylation and reduced mitochondrial function) in the earlier phase of oral carcinogenesis [41]. The alcohol dehydrogenase (ADH) carries out the conversion of alcohol to acetaldehyde, which is further oxidized to acetate by aldehyde dehydrogenase (ALDH) enzymes. Acetaldehyde has been shown to cause DNA damage and impairment in DNA repair by inhibiting the enzyme O-6-methylguanine-DNA methyltransferase required for DNA repair caused by alkylating agents [42]. Also, in addition to ethanol, alcoholic beverages are known to contain other potential carcinogens like N-nitroso compounds, urethane, mycotoxins, inorganic arsenic, etc. [43].

#### **D) Viral infections**

Epstein–Barr virus (EBV) and human papillomavirus (HPV) have been shown to be associated with the development of oral cancers [44–46]. In immunosuppressed patients, EBV causes hairy leukoplakia and "lymphoproliferative diseases" [47]. However, the causal relationship of EBV with oral cancer is still unclear. HPV is the most common viruses involved in oral tumorigenesis. Certain 'high-risk' HPV types (16, 18, 31, 33, and 35) have been shown to be associated with oral premalignant lesions and OSCC [48]. HPV derived oncoproteins E6 and E7 mainly interfere with the cell cycle machinery by binding and inhibiting tumor-suppressive functions of p53 and pRb [49].

#### **E) Dietary deficiency**

Poor dietary intake of vegetables and fruits together with low intake of beta-carotene, riboflavin, thiamine, folate, vitamin C, iron, and copper, modify the risk associated with oral cancer. The plasma levels of vitamin A, E, and zinc were shown to be reduced in oral cancer patients [50]. The experimental evidences suggest a higher risk of cancer development in zinc-deficient subjects primarily in nitrosamine induced cancers. Zinc is known to regulate glutathione-S transferase expression which is crucial for DNA repair mechanism [51].

### **2.1.5 Treatment modalities for oral cancer**

All three treatment modalities i.e. surgery, radiation, and chemotherapy are used to treat oral cancers either alone or in combination. In general, single modalities are normally used in early stage I and II types of SCC and carcinoma *in situ*, while for patients with advanced stage III and IV types of cancers, a combination of therapies are employed. Different factors like age of the patient, overall health and medical history, type of carcinoma (oral subsite affected, clinical size and stage of the tumor, the extent of invasion, involvement of regional lymph nodes, and metastasis) primarily decide the therapy to be used for oral cancer treatment [52,53].

#### **Surgery**

Surgery is the primary treatment choice for oral cancers. Surgery attempts to remove the tumor tissue leaving histologically normal tumor margins and preserve the normal tissue and its function. Surgical techniques vary depending on the size and accessibility of the tumor to be excised. Smaller tumors are excised from within the oral cavity; but, for large and difficult to access tumors, a surgical procedure may involve regions outside of the oral cavity and the removal of soft tissue and bone. Lower cheek flap approach, mandibulotomy, upper cheek flap, or visor flap approach are the most regularly used surgical procedures for surgical resection of the primary tumor of the oral cavity. Radical neck dissection surgery may be required in the case of an advanced disease stage when there is the involvement of a positive or suspicious lymph node. [54,55].

Recently an autofluorescence imaging-based surgical techniques have been used for the visualization and tracking the spread of the tumor. In direct fluorescence visualization technique (FV), normal mucosa emits green autofluorescence when exposed to fluorescent light of wavelength 400-460 nm due to the presence of naturally occurring fluorophores, whereas tumors with abnormal mucosa appear dark due to change in the quantity and quality

of fluorophores due to neoplastic transformation. A study in 2009 by Poh *et al* have shown that none of the patients who underwent FV-guided surgery showed recurrence compared to 25% of the patients who underwent surgery without FV-assisted technology [56]. A reconstructive surgery is essential when resection of a primary tumor in the oral cavity leads to loss of function and/ or aesthetics e.g. loss of a significant part of the tongue, buccal mucosa or mandible in the oral cavity [52].

### **Radiotherapy**

Radiation alone may not be used for the treatment of oral cancers, but has been used for the difficult to access sites such as the oropharynx. The main principle for using radiotherapy is to destroy DNA in rapidly dividing cancer cells in a confined region while conserving the function of adjacent healthy tissue. The use of surgery and post-surgery radiation is a common combination used for oral cancer treatment [57]. Currently, treatment of radiation involves administration of a fractionated dose, i.e. 1.8-2 Gray (Gy) radiation delivered daily (5 days a week) for the duration of 6 weeks in 30 fractions until a maximum of 60 Gy dose is delivered [52]. New advances in radiotherapy also include 3-dimensional conformal radiation therapy (3D-CRT), intensity modulated radiation therapy (IMRT), and volumetric arc therapy (VMAT). These techniques have been established to deliver radiation precisely at the tumor site with minimum damage to the adjacent healthy tissue and allow flexibility to alter the dose [52,58]. In brief, 3D-CRT delivers beams from 3 dimensions while IMRT provides greater control by using different intensities beams from a variety of dimensions. VMAT is a modification of IMRT which delivers a higher dose faster to the whole tumor volume concurrently either in a single arc or series of arcs [59]. In the case of concurrent chemoradiotherapy, the use of chemotherapeutic drug has been shown to increase the radiation sensitivity of tumors [52].

## **Chemotherapy**

Earlier chemotherapy was mostly used as a palliative treatment for oral cancers. But with advances in the new drugs, it is now widely used in curative treatment regimens. Chemotherapeutic drugs destroy dividing cancer cells in order to control tumor spread and metastasis. Chemotherapy can be divided into three categories:

1. Induction chemotherapy (before surgery)
2. Concurrent chemotherapy (in combination with radiation)
3. Adjuvant chemotherapy (after surgery and/or radiation)

Concurrent chemotherapy has been shown to more effective than induction chemotherapy.

The combination of a chemotherapeutic agent with radiation increases the efficacy of radiotherapy resulting in better tumor control and survival rates [57,60]. The common classes of chemotherapeutic agents include antimetabolites (methotrexate and 5-fluorouracil), platinum compounds (cisplatin and carboplatin), plant alkaloids, taxanes (docetaxel), and most recently taxoids. A combination of cisplatin, 5-fluorouracil, and docetaxel drugs has been used in oral cancer treatments [52].

Recently Cetuximab, a monoclonal antibody targeting the epidermal growth factor receptor (EGFR) has been used in targeted therapy for oral cancers. The EGFR is overexpressed in epithelial cancers such as oral cancers and is enhanced post radiotherapy leading to poor treatment outcome. Cetuximab increases the efficacy of radiotherapy by inhibiting EGFR [54,61].

## **2.2 Apoptosis and dysregulation in cancer**

Apoptosis is the cell's natural mechanism for programmed cell death which plays a critical role in homeostasis as well as the development process [62]. The death of a mammalian cell in an ordered and orchestrated manner under physiological and pathological conditions is termed as 'apoptosis'. Resisting cell death is one of the eight hallmarks of

cancer cells due to which they are resistant to the death-inducing stimuli [63]. Dysregulation in the apoptotic process leads to cancer development and is a major obstacle to anticancer therapeutics. The dysregulation of apoptosis is reported in a wide variety of diseases. Enhanced apoptosis is found in immunodeficiency, acute and chronic degenerative diseases, and infertility and inhibited or delayed apoptosis is present in cancer and autoimmune disorders [64].

### **2.2.1 Intrinsic and extrinsic pathways of apoptosis**

Figure 1 describes the apoptotic pathway which is triggered by both intracellular and extracellular signals. There are two different pathways that lead to apoptosis: A) The death receptor mediated or extrinsic pathway which receives and processes the extracellular death-inducing stimuli (e.g. TNF receptor/TNF and the Fas receptor/FasL). B) The mitochondrial or intrinsic pathway which senses and assimilates different intracellular stimuli (e.g. growth factor deprivation, DNA damage, and cytokine deprivation). Both pathways ultimately culminate into the activation of ‘caspases’ i.e. cysteine aspartyl-specific proteases in a cascade of events which lead to cell death characterized by membrane blebbing, DNA fragmentation, and chromatin condensation [65].

- **Extrinsic pathway of apoptosis**

The extrinsic pathway requires extracellular signals to induce apoptosis. Death ligands or cell death signals like tumor necrosis factor (TNF), Fas ligand (Fas-L), TNF-related apoptosis-inducing ligand (TRAIL) bind to tumor necrosis factor (TNF) family death receptors [66]. Further, adaptor proteins like TNF receptor-associated death domain (TRADD) and Fas-associated death domain (FADD) are recruited to the death receptor followed by recruitment of initiator pro-caspases-8 and -10 at adaptor protein, thus forming death-inducing signaling complex (DISC). Pro-caspases 8 and 10 are activated by DISC followed by activation of

executioner caspases-3, 6, and 7. The activated effector caspases then carry out proteolytic degradation of intracellular proteins leading to cell death [67,68].

- **Intrinsic pathway of apoptosis**

The intrinsic or mitochondria mediated pathway of apoptosis is activated post internal stress signals such as DNA damage, growth factor deprivation, cytoskeletal damage, ER stress, loss of adhesion, macromolecular synthesis inhibition [66]. This pathway is regulated by the Bcl-2 family members [69]. Different apoptotic signals lead to the up regulation of BH3-only proteins, which activate both Bax and Bak. The oligomerization of BAX and BAK causes mitochondrial outer membrane permeabilization (MOMP) [66,70]. The mitochondrial permeabilization causes the release of cytochrome c which binds with Apoptotic protease activating factor – 1 (Apaf-1) and ATP. This binds to pro-caspase-9 to form a protein complex termed as an ‘apoptosome’ which cleaves the pro-caspase 9 to its active form of caspase-9, which subsequently cleaves and activates pro-caspase 3 into the effector caspase-3. The permeabilized mitochondria membrane also releases SMACs (second mitochondria-derived activator of caspases) into the cytoplasm. SMAC binds to the inhibitor of apoptosis family proteins (IAPs) thereby inactivating them, and preventing the IAPs from inhibiting apoptosis [66].

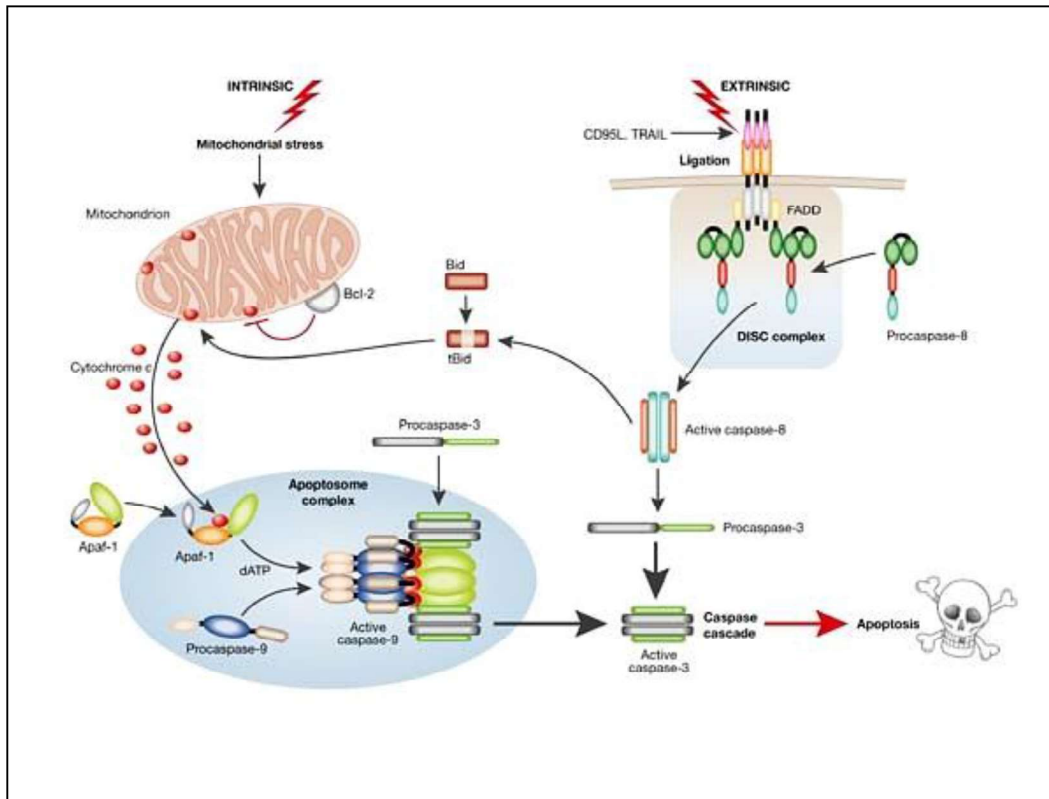


*Figure 1: Apoptosis: The intrinsic and extrinsic pathways to activate caspase (Adopted from MacFarlane et al., 2004) [65].*

### 2.2.2. Inhibitors of apoptosis proteins (IAPs)

Inhibitors of apoptosis (IAP) family of proteins are intracellular proteins involved in inhibiting the caspase cascade. Till date, eight members have been identified in the IAP family. Survivin and X-linked IAP (XIAP) have the ability to directly impede caspases [71,72]. Binding of XIAP and Survivin to caspases 3 and 7 in their dimeric state sterically hinders the catalytic site, as a result of which the proteolytic activities of these effector caspases become nonfunctional [73].

### 2.2.3 Apoptosis as a therapeutic target in cancer

The increasing knowledge of some of the molecular components of the apoptotic signaling pathways has opened the way for generating more specific agents which target one critical

signaling element. This has allowed a revolution in anticancer therapy trends, from classical cytotoxic drugs to the development of new non-toxic therapies which target the tumor-specific apoptosis response. Potential future cancer therapies target both intrinsic and extrinsic pathways of apoptosis, where antagonists of the anti-apoptotic Bcl-2 family and pro-apoptotic receptor agonists (PARA) are in focus [74,75]. Targeting extrinsic pathway has the advantage over intrinsic pathway as it triggers p53 independent tumor cell apoptosis and mutations inactivating the extrinsic pathway are less common [74].

## **2.3 Clusterin**

### **2.3.1 Origin and associated functions**

Clusterin (CLU) is a sulfated chaperone glycoprotein present in different tissues and physiological body fluids. This was first identified in ram rete testis fluid and named so because of its ability to cause clustering of sertoli cells and erythrocytes *in vitro* [76]. Due to its wide presence in different species and tissues with varied functions, initially different alternative names were assigned to CLU which mainly includes sulfated glycoprotein 2 (SGP2), testosterone repressed prostate message protein 2 (TRPM2) in prostate and apolipoprotein J (ApoJ) [8]. CLU has been shown to be involved in different physiological functions like membrane recycling, cell-cell or cell-substratum interaction, lipid transport, cell proliferation and death, complement regulation, tissue differentiation, etc.[77–79]. Alteration in the expression of CLU has been shown to be associated with cardiovascular and metabolic disorders, aging, pseudoexfoliation glaucoma, Alzheimer's disease, and cancers of different origin [8,80].

### **2.3.2 Genomic organization and biogenesis of splice variants of CLU**

CLU gene is located at chromosome 8p21 location encompassing a total of nine exons, spanning a region of approximately 18 kb [81]. There are two major splice variants of CLU reported in the literature. The secretory form (sCLU) which most commonly found in

different tissues and fluids and the intracellular nuclear form (nCLU). These two different isoforms of CLU have antagonistic functions i.e. sCLU is anti-apoptotic whereas nCLU is pro-apoptotic in nature. Figure 2 is a schematic representation of different splice variants of CLU.

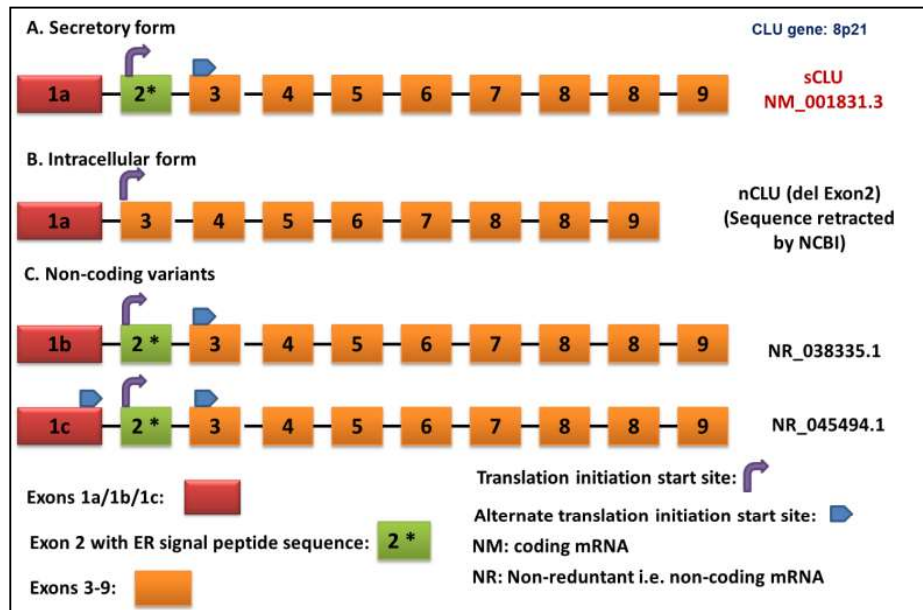


**Figure 2: Schematic representation of different splice variants of Clusterin**

*(Adopted from Kadam et al., 2016)[8]*

- **Secretory or Extracellular CLU (sCLU )**

sCLU (NM\_001831.3) is the most predominant isoform generated by the use of exon 1a. This NM\_001831.3 transcript is translated into 449 amino acid precursor protein using translation start site present upstream to ER signal peptide sequence in exon 2 [9,82]. As illustrated in figure 3, a 22 amino acids ER signal peptide sequence directs the CLU precursor protein to the endoplasmic reticulum where it undergoes post translational modification like N-linked glycosylation. This high mannose 60 kDa pre-secretory form of CLU (psCLU) is translocated to golgi apparatus for additional glycosylation which include the addition of complex sugar

moieties like fucose, galactose, mannose, N-acetylneuraminic acid, and N-acetylglucosamine [83]. Further, a Furin-like proprotein convertase enzyme recognizes the amino acid recognition motif RIVR present in 80 kDa CLU to cleave between Arg<sup>227</sup> and Ser<sup>228</sup> residues and produce N-terminal  $\alpha$ -chain and C-terminal  $\beta$ -chains linked by five disulfide bonds. Hence, the 80 kDa mature form of CLU (sCLU) is comprised of two subunits: 34-37 kDa  $\alpha$  subunit and 36–39 kDa  $\beta$  subunit, which are linked by five disulfide linkages [7,83].

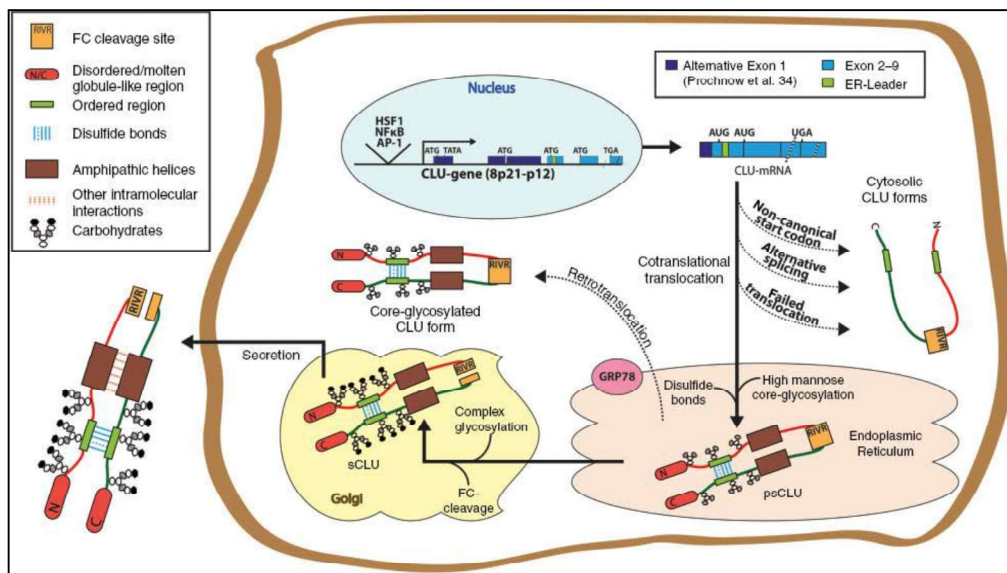


**Figure 3: CLU biogenesis pathway** (Adopted from Rohne et al., 2016) [83]

- **Nuclear or intracellular clusterin (nCLU)**

The intracellular isoform of CLU is generated by an alternative splicing event where exon 1 is spliced with exon 3 (i.e. skipping of exon 2). This generates an N-terminally truncated 49 kDa isoform of CLU which lacks ER signal peptide sequence located at exon 2 [8]. As a result, this form remains intracellular or gets targeted to the nucleus. However, the presence of nuclear localization sequences (NLS) has been shown to be not essential for its nuclear translocation [84]. This isoform was first identified in the MCF-7 breast cancer cell line and

later on, its presence was confirmed in prostate and colorectal cancers [82,85,86]. Intriguingly, in some cancer and non-cancer cells, it has been demonstrated that nCLU gets induced post proteotoxic stress conditions [9]. nCLU has been shown to bind to Ku-70, thus impairing the DNA repair pathway and thus inducing apoptosis [85]. Currently, the nCLU sequence is not available in the NCBI database questioning its existence and the mechanism of its biogenesis.

- **Non-coding/Non-redundant CLU isoforms**

As mentioned in the NCBI database, there are two other splice variants of CLU named variant 2 (NR\_038335.1) and variant 3 (NR\_045494.1). These two variants are generated by differential usage of exon 1b and 1c respectively and have been designated as ‘non-coding or non-redundant’ variants of CLU. As the name suggests, these two variants do not code for a functional protein due to the presence of an upstream open reading frame (ORF) that interferes with the translation process and as a result, it undergoes ‘nonsense-mediated mRNA decay’ (NCBI database). Although the NR\_038335.1 variant is classified as a non-coding isoform, it was detected in human brain cells of Alzheimer’s patients indicating its context-dependent expression and role, which is not explored yet [87].

### **2.3.3 Structure of Clusterin**

Despite extensive research in the field of CLU, there are no structural details available for this molecule possibly due to its aggregating nature. Numerous studies have shown that it has been very difficult to crystallize sCLU protein due to its heavy glycosylated nature. Approximately 30% of the CLU protein is glycosylated which results in its ‘sticky’ nature [7]. Apart from its interacting partners, CLU also forms aggregates with itself to form di-, tetra-, and higher-order oligomers depending on the pH of the solution [78,88]. sCLU can develop high molecular weight complexes up to 40,000 kDa with ligands like Fibrinogen having a diameter of between 50 and 100 nm [89]. Such properties of CLU along with its

heterogeneous glycosylation pattern make it difficult to obtain X-ray structures or reliable NMR spectra. Additionally, there are technical difficulties in obtaining purified sCLU protein in sufficient quantities with absolute glycosylation pattern as that is present *in vivo*. Most of the available information about the secondary structure of sCLU has been obtained through computational analysis tools, without any experimental evidences. sCLU is highly conserved in various species with the greatest homology displayed at the FC cleavage site and cysteine disulfide bonds [90,91]. Various attempts to characterize the sCLU-client protein complexes have been made using different techniques, such as dynamic light scattering, size exclusion chromatography, Circular dichroism, bis-ANS fluorescence spectroscopy, etc. These studies indicate the presence of 60%  $\alpha$ -helices. sCLU belongs to the intrinsically disordered proteins family signifying that it partially lacks a distinct tertiary structure and thus exposing the hydrophobic regions which are called molten-globule like regions, which allows the hydrophobic interaction of sCLU with other client proteins [92]. Notably, sCLU shares this feature with other intrinsically disordered proteins like heat shock protein 27 (Hsp-27) or  $\alpha$ -crystalline [78,93]. The intrinsically disordered molten globule structure and amphipathic  $\alpha$ -helical structure of sCLU attributes to its role as a “biological detergent” to clear unfolded/misfolded or undesired macromolecules in circulation [91].

The amino acid sequence analysis of nCLU identified a conserved BH3 motif at the C-terminal coiled-coil region (CC2) involved in the interaction with Bcl2 family proteins, as confirmed by NMR analysis [94]. This is the only study to date that demonstrated the interaction of nCLU with anti-apoptotic Bcl-2 family members using a structural modeling approach and confirmed the pro-apoptotic function of nCLU.

#### **2.3.4 Expression and role of CLU in different cancers**

sCLU is upregulated in the majority of the cancers including lung, hepatocellular, bladder, breast, and lymphomas [95]. On the other hand in few cancers like esophageal carcinoma,

neuroblastoma, and testicular seminoma it is downregulated [12,96,97]. This suggests the dual role of CLU either as an oncogene or tumor suppressor gene in a context-dependent manner.

#### **2.3.4.1 CLU as a tumor suppressor gene**

The study showing the development of skin cancers in CLU null mice provided the first evidence *in vivo* of the potential role of CLU as a tumor suppressor [96]. Further knockdown studies in prostate cancer cells demonstrated cell cycle progression with a concomitant increase in proliferation markers. Additionally, TRansgenic Adenocarcinoma of Mouse Prostate (TRAMP) mice (mouse model for prostate cancer) exhibited aggressive tumor development when crossed with CLU<sup>-/-</sup> mice with early metastasis, enhanced tumor homing, and poor survival [82]. These studies in prostate cancer suggested the possible role of CLU as a haploinsufficient tumor suppressor gene. Another study in neuroblastoma has shown that N-MYC overexpression induced expression of miR-17-92 cluster leads to sCLU suppression. Interestingly the incidences of neuroblastoma in MYCN transgenic mice were considerably increased which had zero or single allele of CLU, signifying its tumor suppressive role in neuroblastoma. Further xenograft studies in mice showed that sCLU siRNA-transfected neuroblastoma cells showed increased metastases with associated activation of NF-κB pathway leading to epithelial to mesenchymal transition (EMT) [96].

In testicular seminoma, CLU expression was significantly downregulated compared to the normal testis and these types of cancers are one of the most sensitive cancers being responsive to chemo and radiotherapy. This suggests the cytoprotective role of sCLU, which protects cells from anti-tumor therapy associated cell death [98]. In the case of colon cancers, copy number loss at CLU locus chromosome 8p21 leads to CLU downregulation [86].

The serum proteomic analysis done in the sera of oral cancer patients revealed CLU as one of the significantly downregulated proteins [14]. Also, miRNA-21 overexpression in

head and neck cancers has been shown to downregulate CLU indicating that CLU may have tumor suppressive functions in oral/head and neck cancers [13].

**Mechanisms of CLU regulation attributed to its tumor suppressive functions:**

- **Epigenetic regulation**

Epigenetics is defined as “mitotically and meiotically inherited gene expression changes that do not involve a change in the DNA sequence but play a key role in regulating gene expression by impacting the accessibility of DNA and the chromatin” [99]. H-Ras transformed rat fibroblasts cells showed downregulation of CLU mediated by deacetylation of the CLU promoter region followed by methylation via the MEK/ERK signaling [100]. Different studies have shown methylation of CpG island and histone deacetylation in the promoter region of CLU contributing to CLU downregulation in tumor endothelial cells, neuronal cells, and prostate cancer cells [101–103]. In the case of hepatocellular carcinoma, the hepatitis delta virus antigen (HDVg) induces CLU expression by histone H3 acetylation within the CLU promoter [104]. In another study carried out in prostate cancer cells revealed that induction of nCLU post hypoxia is dependent on the methylation status of its promoter region. This was demonstrated using two different prostate cancer cell lines PC3 and LNCaP. It was observed that nCLU is induced in only PC3 cells where CLU promoter region is unmethylated and thus HIF-1 $\alpha$  can directly bind to hypoxia responsive elements (HRE) in the promoter region as opposed to LNCaP cells where CLU promoter is methylated [105]. In breast cancer cells, CLU promoter region was found to be unmethylated as opposed to normal breast cells attributing to its overexpression in breast cancers [106]. In neuroblastoma cells, MYCN mediated CLU downregulation was shown to be a result of its interaction with lysine specific demethylase-1 (LSD1) contributing to CLU downregulation [107].

- **miRNA mediated post-transcriptional gene regulation**

“miRNAs are small, non-coding single stranded RNA (about 22 nucleotides in length), involved in post-transcriptional gene regulation, by binding to the 3'-UTR region of target mRNA". These miRNAs act either as an oncogene or tumor suppressive miRNA in a context dependent manner [108]. In neuroblastoma, downregulation of CLU has been attributed to the activation of miR-17-92 cluster by MYCN overexpression. Although miRNA target prediction tool miRanda predicted the binding of miR-17-5p and miR-92 to CLU promoter, validation studies including luciferase assay and miRNA mimics could not demonstrate direct binding of these miRNA at CLU promoter. This suggests the binding of these miRNA to some upstream activator of CLU which leads to CLU downregulation [96,109]. Another study in head and neck cancers showed that CLU is a direct target of miRNA-21 which plays a key role in the modulation of cell growth [13].

#### **2.3.4.2 CLU as an oncogene**

The oncogenic nature of sCLU is mainly attributed to its ability to inhibit apoptosis and promote cell growth. sCLU acts as a cytosolic retention factor for Bax by binding to Ku-70 and Bax complex, thereby impeding the oligomerization of Bax which inhibits the release of cytochrome C from mitochondria thus inhibiting activation of caspases [110]. Recent evidences suggest the role of CLU in pro-survival autophagy, where CLU has been shown to interact with LC-3B at autophagosome membrane resulting in LC-3B lipidation and formation of stable Atg-3 and LC-3B complex leading to autophagy initiation. Autophagy has been shown to be mitigated in CLU<sup>-/-</sup> mice and prostate cancer cells with CLU knockdown, signifying a role of CLU in pro-survival autophagy[111].

The oncogenic activity of CLU has been shown to be associated with the development of chemoresistance in different cancers. Downregulation of sCLU has been shown to affect the chemosensitivity of pancreatic cancer cells to gemcitabine by either

inhibiting activation of ERK1/2 or by modifying the NF- $\kappa$ B activity [112,113]. CLU overexpression has been shown to be associated with increased invasion and metastasis of cancer cells. Silencing of CLU resulted in decreased mesenchymal to epithelial transition (MET) as indicated by a decrease in Fibronectin with concomitant increase in E-cadherin [114]. CLU has been shown to modulate the levels of MMP-9 by regulating ERK1/2 and PI3K/AKT/NF- $\kappa$ B pathways in monocytes and macrophages which assist in tissue reorganization required for extracellular matrix degradation [115].

### **Signaling mechanisms involved in upregulation of CLU**

There exists more than one regulatory region in the CLU promoter which is possibly responsible for the diverse expression of CLU in different tissues. The proximal promoter region of CLU (P1) shows the presence of cis-regulatory elements like SP-1, AP-1, and AP-2 motifs. Also, it shows the presence of a 14 bp long conserved domain called Clusterin element (CLE), which is similar to heat-shock response element (HSE) present in heat shock proteins [116]. CLU promoter region located in the intron 1 (P2) shows the presence of TATA box, CAAT box, and cAMP responsive elements, which may have a role in context-dependent expression and regulation of CLU, which currently lacks experimental evidences.

### **TGF- $\beta$ signaling**

There are different mechanisms by which TGF- $\beta$  regulates the expression of CLU. TGF- $\beta$  signaling pathway activates different transcription factors like AP-1 and EGR-1 which are reported to upregulate CLU transcription. TGF- $\beta$  signaling also activates sCLU transcription by removal of suppression caused by c-FOS [117]. Yeast two-hybrid screening revealed that sCLU can bind to both TGF- $\beta$  type-I and II receptors and transmit signaling through the canonical pathway. TGF- $\beta$  causes translocation of sCLU to the nucleus from cytoplasm in HepG2 and CCL64 cancer cell lines [118]. Also, sCLU has been shown to control the stability of SMAD2/3 by preventing its proteasome-mediated degradation [119]. Conversely,

Twist-1 transcription factor mediated TGF- $\beta$  induced expression of CLU. Twist-1 binds to the E-boxes elements present in the distal promoter region of CLU and regulates basal and TGF- $\beta$  induced sCLU expression [120].

### **IGF-1/IGF-1R signaling**

CLU is a stress inducible chaperone protein known to get induced post treatment with low dose radiation (0.02-0.5 Gy), suggesting its role in radiation adaptive responses. One of the studies to investigate whether sCLU induction is a result of activation of IGF-1/IGF-1R signaling identified that ATM causes activation of IGF-1 transcription by removal of inhibitory p53-NF-YA complex, thus increasing IGF-1 levels which activate the IGF-1/IGF-1R pathway. This further leads to activation of downstream targets like PI3K/AKT or Src MEK/ERK [98,121], which in turn activates the EGR-1 transcription factor leading to induction of sCLU transcription [122]. Post serum deprivation, sCLU binds to and sequester IGF-1 and prevents its binding to the IGF-1R, thus negatively regulating the PI3K/AKT pathway [123]. In hepatocellular carcinoma, increased CLU expression has been shown to be associated with poor survival and high tumor recurrence, wherein CLU activates PI3K/AKT pathway by interacting with EIF3I causing activation of MMP-13 and metastasis [124]. In the case of castration resistant prostate cancer (CRPC), the STAT-Twist-1 signaling pathway induces sCLU expression. The binding of IGF-1 to IGF-1R leads to STAT protein phosphorylation and its translocation to the nucleus, which further leads to Twist-1 transcription. This Twist-1 further binds to the E-box elements present in CLU promoter region and induces sCLU expression [125].

### **NF- $\kappa$ B pathway**

Different reports in the literature suggest that CLU and NF- $\kappa$ B regulate each other. In the neuroblastoma cell line, the overexpression of CLU has been shown to stabilize NF- $\kappa$ B inhibitors, resulting in inhibition of NF- $\kappa$ B activity [126]. Also, CLU has been shown to

interact with phosphorylated I $\kappa$ B $\alpha$  thus preventing E3 ubiquitin ligase binding and I $\kappa$ B $\alpha$  stabilization, thereby preventing its degradation and activation of NF- $\kappa$ B signaling, indicating that CLU is a negative regulator of NF- $\kappa$ B activity [127]. Contrarily, in one of the studies in mouse embryo fibroblasts to identify NF- $\kappa$ B target genes, CLU was identified as one of the most upregulated genes [82].

### **2.3.5 Localization studies of CLU**

The existence of different CLU isoforms and their different subcellular localization in a cell possibly attribute to its varied cellular functions. Several studies have shown that CLU is localized either in the cytoplasm, nucleus, or perinuclear aggregates [85,128]. Overexpression of CLU has shown its localization in the endoplasmic reticulum and golgi, the secretory pathway components [129]. Recently a new non-glycosylated 45 kDa mitoCLU form has been identified in human brain neurons and astrocytes which is localized to the mitochondrial matrix, however, the function of mitoCLU is still unknown [130]. Another study in the myoblast cell line has shown differential localization of  $\alpha$  and  $\beta$  chains of CLU showing differential lipid metabolism properties [131].

### **2.4 Nucleolus: structural organization and associated functions**

The nucleolus is one of the most prominent membrane-less sub-compartments in the nucleus involved in ribosome biogenesis [132]. Mammalian nuclei typically contain one to four nucleoli. It acts as a ‘cellular stress sensor’, where any alteration in nucleolar morphology or protein content indicates alterations in cell growth and proliferation, cell cycle deregulation, or senescence.

Different cell types show differences in nucleolar appearance. The ultrastructure of nucleolus revealed by electron microscopy showed three components: the central fibrillar centre (FC) surrounded by dense fibrillar centre (DFC), and granular centre (GC) region in which FC and DFC are embedded (Figure 4 A and B). The ribosomal DNA transcription and

processing occur in FC and DFC compartments respectively followed by maturation and ribosome assembly in the GC compartment [133].

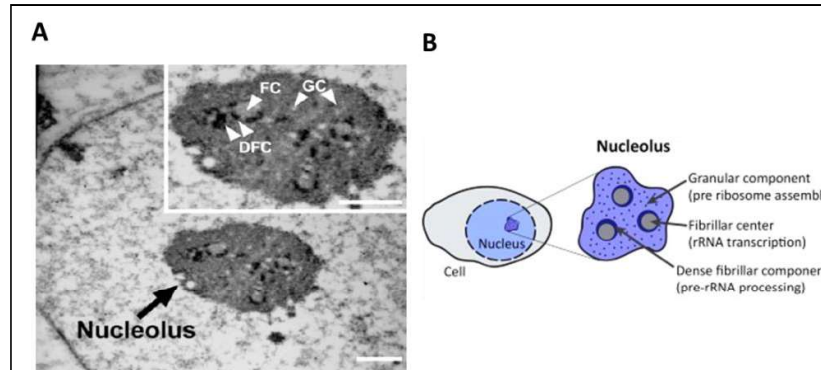


**Figure 4: Different sub-compartments of the nucleolus. (A) Electron micrograph of nucleolus showing FC, DFC and GC regions. (B) Schematic representation of nucleolus showing different sub-compartments where ribogenesis take place. (Adopted from Tiku et al., 2018) [134].**

#### 2.4.1 Nucleolar proteins

Apart from ribogenesis, nucleolus has been shown to be involved in other cellular processes like cell cycle regulation, proliferation, and centrosome maintenance [135]. Mass spectrometry based quantitative proteome analysis of human nucleoli in response to different stress stimuli showed flux of different proteins in the nucleolus which mainly include proteins involved in DNA repair, replication, cell cycle regulation, ribonucleolar proteins and chaperones [136]. Figure 5 represents the categorization of different nucleolar proteins identified using mass spectrometry, based on their functions.

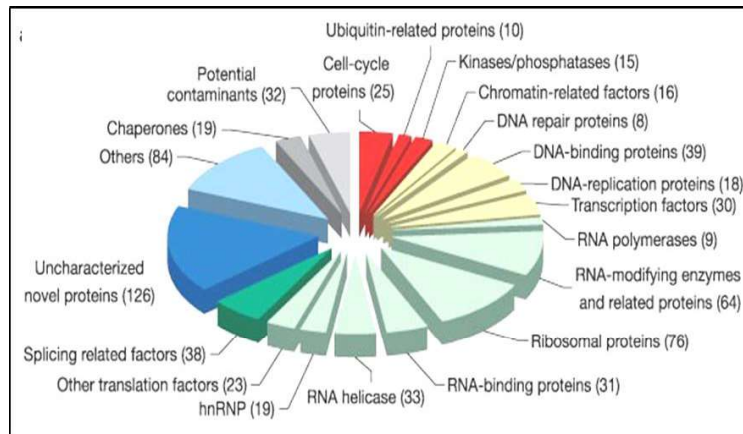


**Figure 5: Classification of nucleolar proteins involved in various cellular functions identified by quantitative proteome analysis.** The numbers in bracket indicate identified protein in each category. (Adopted from Andersen et al., 2005 ) [136].

- **Upstream binding factor (UBF)**

UBF is found in the FC and the DFC compartments of the nucleolus. It is an essential component of the RNA polymerase I pre-initiation complex which along with the SL-1 transcription factor carry out transcription of 5.8S, 18S, and 28S rRNAs [137]. It contains nucleic acid binding domains termed as high-mobility group (HMG) boxes due to its similarity with HMG chromosomal proteins. No consensus binding sequence has been recognized for UBF and it is suggested to recognize the structural features of DNA [138].

- **Fibrillarin**

Fibrillarin is one of the well-studied and highly conserved nucleolar proteins. It is a constituent of the nucleolar U3 snoRNP complex that is involved in 2'-O-methylation of pre-rRNA [139]. It is localized in the DFC compartment of the nucleolus and involved in pre-rRNA processing and ribosome assembly. N-terminal glycine and arginine rich (GAR) domain has been shown to be involved in the nucleolar accumulation of Fibrillarin, although the exact mechanism is not known. It has been postulated that positively charged nucleolar

localization sequence promote nucleolar accumulation due to electrostatic interaction with nucleolar components [140].

- **Nucleophosmin 1 (NPM1)/B23**

NPM1/ B23 is found in the GC compartment of the nucleolus and is involved in pre-rRNA processing [141]. It is an extensively studied nucleolar protein implicated in different cellular functions like ribosome biogenesis, DNA repair, mRNA processing, chromatin remodeling, apoptosis regulation, and embryogenesis. It was identified as a phosphoprotein having chaperonic functions as it prevents thermal denaturation, misfolding, and aggregation of proteins [142]. NPM1 is a nucleocytoplasmic shuttling protein that can bind to NLS containing peptides thereby acting as shuttle protein in nuclear/nucleolar import of proteins [143]. Heterozygous mutations in the exon 12 of the *NPM1* are most frequent in acute myeloid leukemia (AML) and it is overexpressed in most of the solid tumors [144].

- **Nucleolin (C23)**

Nucleolin is found in the GC compartment of the nucleolus and is involved in pre-rRNA processing [141]. It is a multifunctional phosphoprotein also present in the cytoplasm and nucleus of the cell. Nucleolin contains intrinsic nucleic acid dependent ATPase and helicase activities. Nucleolin can undergo auto-degradation via its DNA-dependent ATPase activity and plays a role in regulating cell growth and DNA replication [145]. It also has been suggested to have a chaperone-like role in facilitating interactions of ribonucleolar proteins and rRNA [146]. Nucleolin is a nuclear matrix-binding protein which is also involved in the regulation of cell differentiation, apoptosis, and remodeling of nucleosomes [147].

#### **2.4.2 Cajal body**

Cajal bodies (CBs) were first described as ‘nucleolar accessory body’ in neuronal cell nuclei by Ramon Y Cajal [148]. As the ultrastructure studies revealed ‘coiled thread-like structures’ within it, hence it was also called as a ‘coiled body’. CBs are evolutionarily highly conserved

and play an important role in small nucleolar ribonucleoprotein (snRNP) transport and maturation [149]. CBs are highly mobile structures that move throughout the nucleoplasm but are not found in cells of every tissue type [150]. CBs number and size both increases in response to increased snRNP production [151]. They are not usually associated with nucleoli (Figure 6), but can be induced to form a ‘nucleolar cap’ post nucleolar stress conditions such as reduced temperature or actinomycin D treatment.



*Figure 6: Immunofluorescence photograph showing SMN (survival of motor neuron protein), a cajal body marker. Cajal bodies are not associated with nucleolar marker protein Fibrillarlin. (Adopted from Pfister et al., 2019) [151].*

### 2.4.3 Nucleolar stress response

The nucleolus is a ‘Cellular stress sensor’, where any effect on ribosome biogenesis and cell growth induced by different types of cellular stress directly alters the nucleolar organization and composition [152]. Segregation of nucleolar components is induced by different stress conditions as mentioned in figure 7 like DNA damage induced by UV radiation or inhibition of topoisomerase II by Doxorubicin or etoposide, transcriptional inhibition by actinomycin D, serum deprivation, etc. [153].

Canonical (ribotoxic insults)	Non-canonical (wide range of cellular insults)
<u>1. rDNA damage</u> 1.1 UV, irradiation 1.2 Act.D (high dose) <u>2. Impaired rRNA transcription</u> 2.1 rRNA transcription inhibitor (Act.D (low dose) and other Pol I inhibitors) 2.2 rRNA elongation inhibitor 2.3 Transcription regulating protein defects <u>3. Impaired rRNA processing</u> 3.1 Inhibitors 3.2 Protein defects <u>4. Impaired ribosomal assembly</u> <u>5. Impaired ribonucleoprotein import or ribosome export</u>	<u>1. DNA damage:</u> 1.1 UV, irradiation 1.2 Genetoxic agents <u>2. Impaired RNA transcription:</u> RNA transcription inhibitor (Act.D (high dose) and other Pol II /III inhibitors) <u>3. Impaired protein translation</u> Inhibitors <u>4. Physiochemical perturbations</u> 4.1 Hypoxia 4.2 Oxidative stress 4.3 Heat shock, cold shock 4.4 Osmotic shock <u>5. Nutrient and serum starvation</u> <u>6. Metabolic stress</u>

**Figure 7: Different types of nucleolar stress inducers** (Adopted from Yang et al., 2018)

[153].

Nucleolar segregation is described by the condensation followed by separation of the FC and GC components, and the formation of ‘nucleolar caps’ surrounding the nucleolar remnant [154]. Upon inhibition of transcription or the presence of rDNA double strand breaks, FC and DFC compartments merge and form bipartite cap like structures at the nucleolar periphery. The DFC compartment remains in contact with the GC compartment whereas the FC projects into nucleoplasm (Figure 8) indicating that post nucleolar stress there is a reshuffling of nucleolar and nucleoplasmic proteins. Nucleolar proteome analysis has shown that several DNA damage related (DDR) proteins are detected at ‘nucleolar caps’, suggesting that these caps provide a platform for the recruitment of DDR proteins to repair rDNA damage in the nucleoli [155].

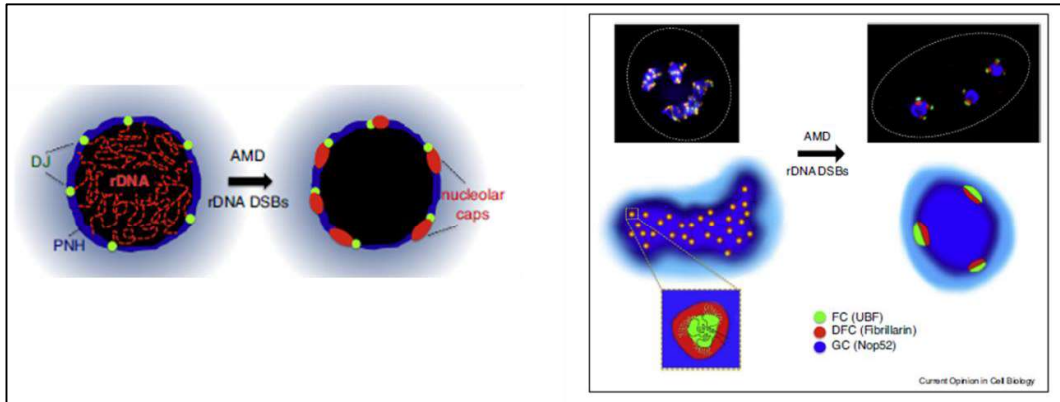


**Figure 8: Nucleolar segregation or cap formation in response to nucleolar stress**

*(Adopted from Mangan et al., 2017) [156]*

#### **2.4.3.1 p53 dependent nucleolar stress response:**

The MDM2-p53 feedback loop is activated in response to a variety of genotoxic and cytotoxic stress conditions and it also plays a central role in nucleolar or ribosomal stress response. The perturbation in any step of ribogenesis or rDNA double-strand breaks leads to nucleolar stress that leads to binding of ribonucleolar proteins to MDM2, thus inhibiting its E3 ubiquitin ligase activity thereby leading to p53 stabilization and activation. DNA damage caused by ultraviolet or ionizing radiation and genotoxic chemicals triggers the activation of the ATM-CHEK2 or ATR-CHEK1 cascade which leads to phosphorylation of MDM2 and thus leading to p53 stabilization. Different ribosomal proteins like RPL5, RPL11, and RPL23 have been shown to bind to MDM2 and stabilize p53 [157]. However, certain proteins like RPL26 binds to 5'-UTR region of p53 and increase the translational rate of p53 mRNA [158]. The activation of p53 leads to p21 activation leading to G1/S arrest or 14-3-3  $\sigma$  mediated G2/M arrest, thus leading to cell cycle arrest or apoptosis [153].

#### **2.4.3.2 p53 independent nucleolar stress response:**

The major non-p53 transcription factors that respond to nucleolar or ribosomal stress are c-Myc, E2Fs, and SP1. Most of the cancers show the presence of mutant p53 or are p53 null. In the case of HeLa cells, which lack functional p53, nucleolar stress induces cell cycle

arrest and/or apoptosis. Furthermore, it was found that RNA pol I inhibition in p53<sup>-/-</sup> cells caused a decrease in the E2F-1 transcription factor levels due to the release of RPL11, which in turn binds MDM2 thereby inactivating the E2F-1 stabilizing function of MDM2 [159]. This study showed the existence of a p53-independent, but RPL11-dependent nucleolar stress pathway that causes cell cycle arrest.

RPL11, apart from its role in the regulation of p53 and MDM2, also regulates c-myc at transcript and protein level [159]. During ribogenesis, RPL5 and RPL11 play an important role in the feedback signaling of c-Myc expression. These two proteins repress the c-myc and its target genes such as E2F and Nucleolin by blocking the recruitment of TRRAP cofactor (transformation/transcription domain-associated protein) at the promoter site. RPL11 binds to MBII domain of c-myc and recruit different miRNAs like miR-24 and miR-130a at 3'-UTR of c-myc mRNA [160].

Many nucleolar proteins can promote cell cycle arrest or apoptosis by bypassing the canonical p53 signaling. These p53-independent regulator proteins mainly include NPM1, ARF, and NuMA [161]. Although both NPM1 and ARF are well-recognized for their roles in p53 signaling, they are also involved in p53-independent signaling [162]. Under nucleolar stress conditions, NPM1 is transcriptionally induced and gets translocated from the nucleolus to the cytoplasm where it forms a complex with BAX. This NPM1-BAX interaction has been associated with cell resistance to death stimuli [162].

## **2.5 Ribosome biogenesis**

The human 80S ribosome is comprised of 40S and 60S subunit. The main function of the 40S subunit, comprising one strand of 18S ribosomal RNA (rRNA) and 33 different ribonucleoproteins (RPs), is to scan mRNAs by binding and unwinding it. Whereas, the 60S subunit is responsible for the formation of peptide bonds and the quality control of nascent peptides which consists of three strands of rRNA (5S, 5.8S, and 28S rRNA) and 47 RPs

[163]. The nucleolus is the main ribosome biosynthesis site and forms around nucleolar organizing regions (NORs) containing several hundred repetitions of the ribosomal DNA (rDNA) gene in human diploid cells. Interestingly, the number of rDNA repetitions that occur between human individuals varies, the physiological relevance of which is unknown [164]. The rDNA genes consist of 47S pre-rRNA transcriptional units containing 18S, 5.8S, and 28S rRNA sequences separated by intergenic spacers containing promoters, enhancers, and other regulatory sequences [165]. As depicted in figure 9, the ribosome biosynthesis involves following steps: (i) synthesis of components (pre-rRNAs, ribosomal proteins, assembly factors, and small nucleolar RNAs (snoRNAs) (ii) processing of pre-rRNAs (cleavage) (iii) covalent modification of pre-RNAs and assembly (iv) maturation and export of pre-ribosomes to the cytoplasm. 47S pre-rRNA transcript is synthesized by RNA Pol I and mature rRNAs are embedded within the Pol I–transcribed precursors, in noncoding spacer sequences i.e. internal transcribed spacers 1 and 2 (ITS1 and ITS2) and 5' and 3' external transcribed spacers (5' and 3' ETSs). Processing of pre-rRNA involves removal of these noncoding spacers using endo- and exoribonucleases, thereby generating the mature 5' and 3' termini of rRNAs. In the end, pre-40S and pre-60S subunits are exported to the cytoplasm, where they become part of the translation machinery after their final maturation process [165].

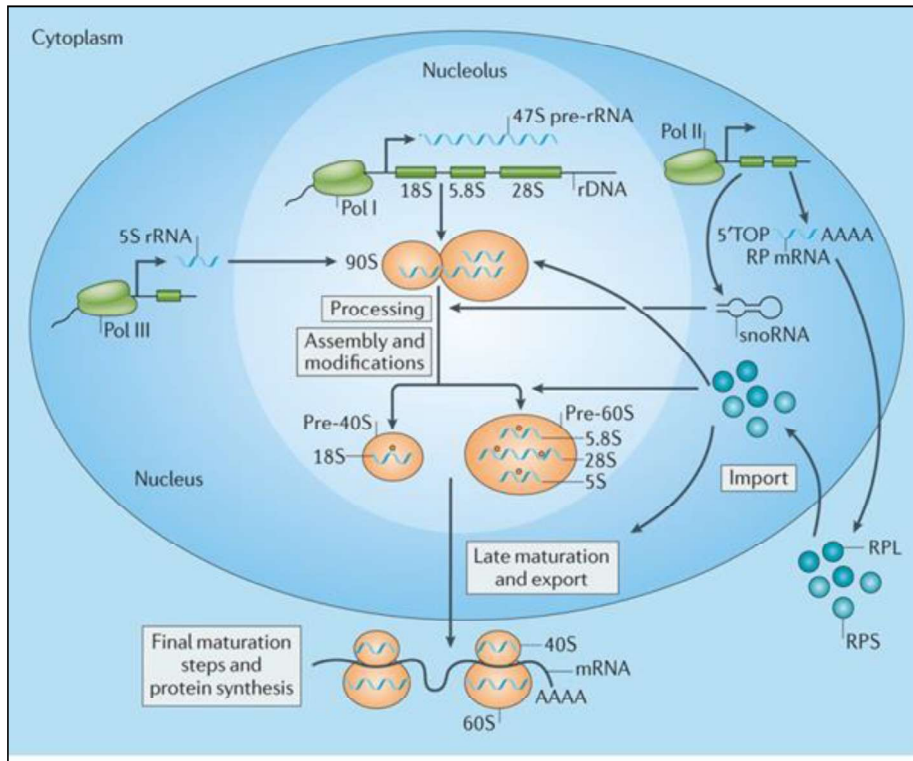


**Figure 9: Eukaryotic ribosome biosynthesis** (Adopted from Lafontaine et al., 2015) [165].

# *Chapter 3*

## *Aims and*

### *Objectives*

In light of the current information available about CLU from the literature, there are no studies available about the isoform specific expression and role of CLU in oral cancers. Earlier studies in the lab to evaluate the alterations in the expression of inhibitors of apoptosis (IAPs) family proteins using ribonuclease protection assay identified CLU as one of the downregulated transcripts. The role of CLU as an oncoprotein and its downstream signaling to promote tumorigenesis is very well studied in other cancers. Hence, downregulation of CLU seen in oral cancer cells prompted us to further investigate the isoform-specific expression, intracellular localization, and its tumor-suppressor like functions in oral cancer cells if any.

**Hypothesis:** CLU acts as a tumor suppressor protein in oral cancer cells.

**Aim of the study:** To understand the role of CLU in human oral cancer cells.

**Objectives:**

1. To identify differentially expressed CLU variants in OSCC vs. normal cells and in stressed vs. unstressed conditions
2. To overexpress or downregulate CLU variants to understand its functional relevance in OSCC

*Chapter 4*  
*Materials and*  
*methods*

## 4.1 Materials

The following reagents/chemicals/enzymes/kits were obtained from:

### **Sigma:**

**1. Chemicals:** Acrylamide, Ammonium persulfate (APS), N-N'-Methylenebisacrylamide, Boric acid, Bovine Serum Albumin (BSA), Bromophenol Blue,  $\beta$ -mercaptoethanol (BME), Coomassie brilliant blue (CBB), Diethyl Pyrocarbonate (DEPC), Dimethyl Sulfoxide (DMSO), Ethylenediaminetetraacetic acid (EDTA), Ethidium Bromide (EtBr), 4',6-diamidino-2-phenylindole (DAPI), 3,3'-Diaminobenzidine (DAB), Dithio Thritol (DTT), Fast green stain, Hydrocortisone, Glycine, Nonylphenyl Polyethylene Glycol (NP-40), Paraformaldehyde (PFA), Sodium Orthovanadate ( $\text{Na}_3\text{VO}_4$ ), Sodium Dodecyl Sulphate (SDS), Tris, Triton X-100, N,N,N',N'-Tetramethylethylenediamine (TEMED), Tween-20, Trichloroacetic acid, Lithium chloride (LiCl), CLU shRNA: MISSION® shRNA Plasmid DNA (SHCLND-NM\_203339).

**2. Drugs/Inhibitors:** Actinomycin D, Cycloheximide, Doxorubicin, 5-Fluorouridine, Tunicamycin, Swainsonine.

**Qualigens:** Acetone, Disodium hydrogen phosphate, DPX mountant, Glacial acetic acid, Magnesium chloride ( $\text{MgCl}_2$ ), NaOH, Sodium dihydrogen orthophosphate, Xylene.

**SISCO Research Laboratories:** Isopropanol, Methanol, Molecular biology grade alcohol, Sodium chloride (NaCl), sodium acetate.

**Calbiochem:** MG132

**Applied Biosystems:** High Capacity cDNA Reverse Transcription Kit (4374966), 2X PowerUp SYBR Green mastermix (A25742), MicroAmp Optical Adhesive Film Kit (Part No. 4360954), 384 well plate for real time PCR (AB1384).

**Invitrogen:** Low melting point (LMP) Agarose, Trypsin, L-Glutamine, Lipofectamine 3000.

**DSS Takara:** RNAiso Plus Total RNA extraction reagent, dNTPs, Taq Polymerase.

**Lucigen:** Masterpure DNA and RNA Purification Kit (#MC85200).

**Macherey-Nagel:** Nucleospin Plasmid DNA Isolation kit (#740588.50).

**Thermo Scientific:** RNA extraction kit, Protease inhibitor cocktail

**Gibco:** Cell culture media including Dulbecco's Modified Eagle Medium (DMEM), Iscove's Modified Dulbecco's Medium (IMDM), Dulbecco's Modified Eagle (DME) and Ham's F12 Medium (DMEM-F12).

**Hi-Media laboratories:** Fetal Bovine serum (FBS), 100X antibiotic solution.

**Dharmacon (GE Life sciences):** ON TARGET Plus Human CLU (Gene ID:1191) siRNA SMART pool, siGlo (to check transfection efficiency), 5X siRNA resuspension buffer.

**Nunc, BD-Falcon and Techno Plastic Products (TPP):** Tissue culture plates and flasks.

**Axygen and Tarson:** Nuclease free disposable tips and eppendorf tubes.

**Merck Millipore:** PVDF Membrane.

**Puregene:** 10-250 kDa prestained protein ladder.

**Advansta:** WesternBright ECL HRP Substrate (#K-12045-D20).

**Kodak:** X-ray films

**Vector labs (USA):** VectaStain ABC kit for IHC, Vectashield (Fluorescence anti-quench mounting medium).

**Plasmid constructs:** pEGFP-C1-Fibrillarin and pEGFP-C1-CLU plasmid constructs were procured from Dr. Dibyendu Bhattacharya (TMC-ACTREC) and Dr. Kristel Slegers (VIB, Belgium).

**Water:** All Lab reagents were prepared in ultrapure water (with Resistivity = 18 M $\Omega$  cm) obtained from Milli-Q water plant (Millipore).

**Primers:** All the primers (3 O.D. and 5 O.D.) used in the study were obtained from Eurofins in lyophilized form and were reconstituted in nuclease free water.

**Antibodies:** List of different primary and secondary antibodies used for western blotting and immunofluorescence localization studies is given in table 1:

**Table 1: Primary and secondary antibodies used in the study**

<b>Antibody name</b>	<b>Catalogue number</b>	<b>Company</b>
Clusterin (H-330)	sc-8354	Santacruz Biotechnology
Clusterin (A-9)	sc-166907	Santacruz Biotechnology
Nucleophosmin 1/B23 (E-3)	sc-271737	Santacruz Biotechnology
Fibrillarin (G-8)	sc-374022	Santacruz Biotechnology
Vinculin	ab-129002	Abcam
Nucleolin	M019-3	MBL Life Sciences
Upstream Binding factor (UBF)	sc-13125	Santacruz Biotechnology
Coilin	sc-55594	Santacruz Biotechnology
$\alpha$ -Tubulin	ab-7291	Abacam
BrdU	ab-6326	Abacam
anti-mouse IgG-HRP	314030	Thermo Scientific
anti-rabbit IgG-HRP	31460	Thermo Scientific
Goat anti-rabbit Alexa fluor 568	A-11011	Invitrogen
Goat anti-mouse Alexa fluor 488	A-11001	Invitrogen
Goat anti-rabbit Alexa fluor 488	A-11008	Invitrogen
Goat anti-mouse Alexa fluor 633	A-21126	Invitrogen

**Instruments:** List of instruments used in the study is given below in table 2.

**Table 2: Instruments used in the study**

<b>Instrument</b>	<b>Model</b>	<b>Company</b>
SDS-PAGE vertical electrophoresis apparatus	Mini-PROTEAN Tetra cell	Biorad, USA
Electroblotting	Mini Trans-Blot	Biorad, USA
Power packs for electrophoresis	PowerPac™ Basic Power Supply	Biorad, USA
pH meter	Orion™ 3-Star benchtop pH meter	Thermo Scientific
Microfuge	G-fuge	Genetix Biotech, India
Table top microcentrifuge	MIKRO 120	Hettich, Germany
Refrigerated centrifuge	Heraeus 75004413	Thermo Scientific
Inverted microscope	Axiovert-200M	Zeiss, Germany
Upright microscope	Axio Imager Z1	Zeiss, Germany
Real Time PCR machine	Quant Studio 12K Flex	Applied Biosystems, USA
ELISA reader	Epoch	Biotek, USA
Confocal microscope	LSM 780 Meta	Zeiss, Germany
CO <sub>2</sub> incubator	Heraeus®	Thermo Scientific, USA
Cryotome	CM1950	Leica, Germany
Spectrophotometer	NanoDrop 1000	Thermo Scientific, USA

## 4.2 Methods

### 4.2.1 Mammalian cell culture

**Cryopreservation of cells:** Freezing of cells was done when reached 80-90% confluency. Cells were washed with PBS and trypsinized. Once cells were detached from the culture plate, an appropriate quantity of complete media was added (depending on the size of the culture dish) and cells were collected in a centrifuge tube. Further, cells were centrifuged at 1250 rpm for 5 min and the pellet was resuspended in a freezing mixture composed of 90% fetal bovine serum and 10% DMSO. Cells were frozen in liquid nitrogen in a stepwise cooling manner.

**Revival of cells:** Frozen vials were thawed at 37<sup>0</sup>C in a water bath. Complete media (i.e. media containing serum) was added to the thawed mixture and centrifuged at 1250 rpm for 5 min. The pellet was resuspended in 1ml complete media and then cells were seeded in a suitable culture dish. The cells were passaged for at least two passages (as described below) before using it for experimental purposes.

**Passaging of cells:** Cells were passaged once reached 80-90% confluency. First, cells were washed twice with PBS and then trypsinized using 0.25% trypsin-EDTA. Once detached, complete media was added and then harvested cells were collected in a centrifuge tube. Cells were centrifuged at 1250 rpm for 5 min and resuspended in 1ml of complete medium. For counting, 10µl of cell suspension was mixed with 10µl 0.4% Erythrosin B or Trypan blue and then loaded onto hemocytometer (Neubauer chamber). The dead cells retained the stain whereas live cells were unstained. Cells in four WBC chambers were counted and the cell count was determined using the following formula:

$$\text{Total number of cells/ml} = \text{the average cell count per square} \times \text{dilution factor} \times 10^4$$

The cells were plated further as per the experimental requirement in a suitable culture dish.

**Table 3: List of different cancer cell lines used in the study**

Cell line	Origin	Culture media	Reference
HaCaT	Human Skin Keratinocyte	DMEM+HEPES+FBS	[166]
DOK	Dysplastic Oral Keratinocyte	DMEM+HEPES+FBS+ 0.4µg/ml Hydrocortisone	[167]
AW8507	Tongue squamous cell carcinoma	IMDM+FBS	[168]
SCC29B	Buccal mucosa squamous cell carcinoma	DMEM+HEPES+FBS	[169]
SCC40	Tongue squamous cell carcinoma	DMEM+HEPES+FBS	[169]
SCC15	Tongue squamous cell carcinoma	MEM+FBS+L- Glutamine+ non-essential amino acids+ Gentamycin	[170]
SCC25	Tongue squamous cell carcinoma	DMEM+HEPES+FBS	
SCC09	Tongue squamous cell carcinoma	DMEM-F12+ FBS+0.4µg/ml Hydrocortisone	

#### 4.2.2 Oral tissue sample collection and processing

**Ethics approval:** Hundred and twenty three (123) paired oral tumor tissue samples collected in the period 2011-2015, were obtained from ACTREC-TMC tissue repository (TTR), after the approval from Institutional Ethical Committee III (IEC-III) (Project no.: 900532). Following inclusion and exclusion criteria was considered for the selection of oral tumor tissue samples from patients in this study.

**Inclusion criteria:**

1. Age 18-75 years (both inclusive)

2. Patients with histologically proven squamous cell carcinoma
3. Patients with no prior history of malignancy and treatment

**Exclusion criteria:**

1. Patients with second primary neoplasm
2. Patients with HIV/ blood borne hepatitis

The tissue samples obtained from TTR were snap-frozen and stored at  $-80^{\circ}\text{C}$  until further processing. H & E analysis was carried out to determine the pathology of the paired tumor-normal samples and only those tissues with  $\geq 70\%$  tumor content were included in the study. 9 normal oral mucosa samples (Age group 18-75) were collected from patients who do not have clinically detectable lesions and who were undergoing minor dental surgical procedures from Nair Dental College, Mumbai. These samples were used as controls in this study as normal adjacent oral tissues often exhibit molecular alterations due to effects of 'field cancerization'. A part of the tissue sample was formalin fixed and paraffin-embedded at the histology facility in TMC-ACTREC for immunohistochemical studies. The clinicopathological characteristics of the patients samples used in the study are listed below in table 4.

**Table 4: Clinicopathological characteristics of the oral cancer patient samples used for immunohistochemistry study**

<b>Characteristic</b>	<b>Number (%)</b>
<b>Mean age of the patients</b>	49.7 years
<b>Sex</b>	
Male	24/123 (19.5)
Female	99/123 (80.5)
<b>Site of lesion</b>	
Alveolus	11/123 (8.94)
Buccal mucosa	72/123 (58.54)
Tongue	40/123 (32.52)
<b>Tumor (T) state</b>	
I/II	28/123 (22.76)
III/IV	92/123 (74.80)
missing	3/123 (2.44)
<b>Nodal (N) status</b>	
N0-N1	45/123 (36.59)
N2-N3	75/123 (60.97)
missing	3/123 (2.44)
<b>Differentiation status</b>	
Poorly differentiated	39/123 (31.70)
Moderately differentiated	67/123 (54.47)
Well differentiated	11/123 (8.94)
missing	6/123 (4.88)

#### **4.2.3 RNA extraction from cell lines using RNAiso Plus reagent**

The cell pellet was washed with 1X PBS and centrifuged at 2500 rpm. Further, the cell pellet was resuspended in RNAiso Plus (total RNA extraction reagent). After homogenization, 0.2 ml of chloroform was added per 1 ml of RNAiso Plus and then incubated for 5 min at room

temperature. This solution was further centrifuged at 12,000 g for 10 min at 4<sup>0</sup>C. The top layer containing RNA was collected in a separate centrifuge tube without touching the middle layer and 0.5-1 ml of isopropanol was added per 1 ml of RNAiso Plus used for homogenization. The mixture was incubated at -80<sup>0</sup>C overnight. The next day, after the mixture was thawed, it was centrifuged at 12,000 g for 10 min to precipitate the RNA. The supernatant was removed without disturbing the pellet and ~200-500 µl of 75% ethanol (prepared in DEPC water) was added. The mixture was centrifuged at 7500 g at 4<sup>0</sup>C for 5 min. This step was repeated twice. The supernatant was discarded carefully and the RNA pellet was dried at room temperature and then resuspended in 20µl of DEPC or nuclease-free water. The extracted RNA quantity and purity were assessed by using a spectrophotometer and stored at -80<sup>0</sup>C till further use.

#### **4.2.4 RNA extraction from tissues using RNA extraction kit (GeneJET RNA purification kit)**

RNA was extracted from tissue samples using a GeneJET RNA purification kit (Thermo Scientific) as per the manufacturer's instructions. In brief, approximately thirty to fifty 10µm sections of frozen tissues were obtained using cryotome and were collected in 300 µl lysis buffer supplemented with β-mercaptoethanol. The solution was vortexed for 10 s to mix thoroughly and then 600 µl of diluted Proteinase K (10 µl of the included Proteinase K diluted in 590 µl of TE buffer) was added. The solution was vortexed and incubated at room temperature for 10 min. The mixture was centrifuged at 12000 g for 5 min and the supernatant was transferred to a new RNase-free microcentrifuge tube. To this collected supernatant 450 µl of ethanol (95-100%) was added and mixed by pipetting. 700 µl of lysate was transferred to the GeneJET RNA purification column inserted in a collection tube. This was centrifuged at 12000 g for 1 min. The flow-through was discarded and the column was placed back in the collection tube. The column was washed with wash buffer 1 and 2. In the

end, 50-100  $\mu$ l of nuclease-free water was added to the center of the GeneJET RNA purification column membrane and centrifuged at 12000 g for 1 min to elute RNA. The extracted RNA was quantified using a spectrophotometer and stored at  $-80^{\circ}\text{C}$  till further use.

#### 4.2.5 cDNA synthesis

cDNA was synthesized using high capacity cDNA synthesis kit. 500-1000 ng of RNA was used for the cDNA synthesis. The 2X RT PCR master mix was prepared as described below in table 5.

**Table 5: Preparation of 2X RT mastermix for cDNA synthesis**

<i>Component</i>	<i>Volume (<math>\mu</math>l)</i>
<i>10X RT buffer</i>	<i>2</i>
<i>25X dNTPs</i>	<i>0.8</i>
<i>10X Random hexamer primers</i>	<i>2</i>
<i>Multiscribe reverse transcriptase enzyme</i>	<i>1</i>
<i>DEPC/Nuclease free water</i>	<i>4.2</i>

An equal volume of diluted RNA (10  $\mu$ l) was added to the master mix. Tubes were centrifuged briefly to spin down the contents in the tube and then placed in a thermocycler.

The PCR program for cDNA conversion is given below in table 6.

**Table 6: Thermal cycler conditions for the cDNA synthesis using High Capacity cDNA Synthesis Kit**

	<b>Step 1</b>	<b>Step 2</b>	<b>Step 3</b>	<b>Step 4</b>
<b>Temperature (<math>^{\circ}\text{C}</math>)</b>	25	37	85	4
<b>Time (min)</b>	10	120	5	$\infty$

#### 4.2.6 Quantitative real time PCR (qRT-PCR)

Quantitative real time PCR was performed using PowerUp SYBR green master mix. The primers used for the detection of CLU isoforms and rRNA transcripts are listed in table 7. The real time PCR reaction was put in 384 well plate in duplicate format and then run on Quant Studio 12K Flex system. The 5 $\mu$ l reactions were set up as described below in table 8. GAPDH was used as a housekeeping control. The real time data analysis was done using the dC<sub>t</sub> method as described by Livak *et al.*, 2001 [171].

**Table 7: The list of primers used for quantitative real time PCR**

Name of the primer	Primer Sequence (5'-3')	Reference
sCLU Forward	ACAGGGTGCCGCTGACC	[9]
sCLU Reverse	CAGCAGAGTCTTCATCATGCC	
nCLU Forward	GGGTGCCGCTGACCGAAAT	
nCLU Reverse	GAGTCTTTATCTGTTTCACCCCG	
GAPDH Forward	GCATCTTCTTTTGCCTCG	
GAPDH Reverse	TGTAAACCATGTAGTTGAGGT	
45S rRNA Forward	GAACGGTGGTGTGTCGTT	[172]
45S rRNA Forward	GCGTCTCGTCTCGTCTCACT	
28S rRNA Forward	AGAGGTAAACGGGTGGGGTC	
28S rRNA Reverse	GGGGTCGGGAGGAACGG	
18S rRNA Forward	GATGGTAGTCGCCGTGCC	
18S rRNA Reverse	GCCTGCTGCCTTCCTTGG	

**Table 8: Reaction set up for Real Time PCR using SYBR Green Chemistry**

<b>Component</b>	<b>Volume (<math>\mu</math>l)</b>
5X SYBR Green Mix	2.5
Forward Primer	0.25
Reverse Primer	0.25
cDNA (5ng/ $\mu$ l)	2

#### **4.2.7 Immunohistochemistry (IHC)**

The tissues were fixed in 10% buffered formalin (prepared in PBS) overnight followed by preparation of paraffin blocks. The 10  $\mu$ m tissue sections were obtained from paraffin embedded blocks on silane coated slides. The tissues were subjected to dehydration by passing through several grades of xylene and alcohol followed by blocking of endogenous peroxidase by methanol and hydrogen peroxide in dark for 30 min at room temperature. The tissue sections were washed with PBS and then subjected to antigen retrieval in citrate buffer (10mM, pH 6.0) in a microwave for 5 min. Then, slides were allowed to cool and were washed with PBS. Normal horse serum was used for blocking [for CLU antibody (sc-166907) raised in mouse]. The slides were incubated in a blocking agent for 1 hour at room temperature in a humidified chamber. The blocking agent was removed by dabbing it on the tissue paper without allowing it to dry and then primary antibody was added and incubated overnight at 4<sup>0</sup>C in a humidified chamber. Negative controls were kept for each section. The next day, slides were washed with 0.1% PBST and PBS for 10 min each. Then, tissue sections were incubated with biotin- conjugated secondary antibody for 1 hour at room temperature. The slides were washed with 0.1% PBST and PBS for 10 min each and then were incubated with avidin-biotin complex (ABC) for 1 hour at room temperature in a humidified chamber. Following washes with PBS, sections were stained with freshly prepared 3,3'-Diaminobenzidine (DAB) and H<sub>2</sub>O<sub>2</sub> for 3-5min. The slides were washed with deionized water and then counterstained with Hematoxyline (1:1 diluted in deionized water)

for 1-2 min followed by dipping it in tap water. In the end, tissue sections were dehydrated by serial washes with alcohol and xylene and then mounted with DPX mountant. The immunostaining of CLU was evaluated for both epithelial and stromal compartments of the tissue. To assess the CLU expression, percent positivity and intensity scores were assigned to both of these compartments. The immunostaining was scored by counting the percentage of cells expressing CLU in at least 10–15 different fields. The staining intensity was scored using a three-point semi-quantitative scale as: 0-negative, 1-mild, 2-moderate, and 3-intense. The resulting combined H-score on a scale of 0-300 was calculated as the sum of the percentage of stained cells multiplied by the intensity scores.

#### **4.2.8 Immunofluorescence microscopy**

Cells were grown on coverslips (22mm X 22mm) to 70-80% confluency. Cells were washed twice with 1X PBS and then fixed with 4% paraformaldehyde for 15-20 min at room temperature. Following PBS wash, cells were permeabilized with 0.3% Triton X-100 for 10 min at room temperature and washed with PBS twice. Further, cells were blocked with a 5% BSA blocking agent (prepared in PBS) for 1 hour at room temperature in a humidified chamber. After blocking, the primary antibody was added at appropriate dilution (diluted in PBS) and incubated either overnight at 4<sup>0</sup>C or at room temperature for 1 hour in a humid chamber. For dual staining, if two antibodies in use are from different species, two primary antibodies were mixed at respective dilutions and incubated at 4<sup>0</sup>C overnight. After primary antibody incubation, cells were washed with PBS twice and then incubated with fluorophore conjugated secondary antibody in dark for 1 hour at room temperature in a humid chamber followed by PBS washes. Cell nuclei were stained with DAPI followed by mounting of coverslips upside down on glass slides using Vectashield fluorescence anti-quenching mounting solution. Coverslips were sealed from all slides using a nail polish and dried

properly and kept at  $-20^{\circ}\text{C}$  until image acquisition under the confocal microscope. Images were acquired on a fluorescence confocal microscope LSM780.

For nuclease treatment related experiment, cells were first permeabilized and fixed with methanol (as methanol acts as both permeabilizer and fixer) and then further treated with DNase I or RNase A at  $37^{\circ}\text{C}$  for 20 min in a humidified chamber. Then further blocking step onward it was processed as described above.

#### **4.2.9 siRNA and shRNA transfection**

For CLU knockdown, cells were either transfected with ON TARGET Plus Human CLU siRNA (transient knockdown) or pLKO.shCLU construct (stable knockdown). One day prior transfection, cells were seeded at 60-70% confluency in a complete media. Next day, for transfection, complete media without antibiotic solution was added to cells. Briefly, siRNA or pLKO.shRNA and transfection reagent Lipofectamine 3000 were diluted in an incomplete medium in separate tubes as per the manufacturer's instructions. Both diluted contents were mixed and incubated further for 30 min at room temperature to allow the lipid-DNA complexes to form and then these complexes were added on to the cells in a drop wise manner. Cells were incubated with these complexes for 24-48 hours at  $37^{\circ}\text{C}$  and then further harvested for analysis purpose. siGLO Green transfection indicator was used to check the transfection efficiency of the reagent. The efficiency of target gene knockdown was assessed by evaluating the transcript or protein levels by real-time PCR or western blotting.

For shRNA mediated stable knockdown, after 48 hours of transfection, cells were harvested and plated in 100mm culture dish. After 24 hours, the selection agent puromycin was added and cells were maintained under selective pressure till visible individual clones were seen. The individual clones were spot trypsinized and harvested in either 12-well or 24-well plate and maintained in puromycin selection pressure. Once reached to 90% confluency, cells were harvested (and small proportion of these cells were plated back to culture further

and prepare freeze downs) and checked for the target gene knockdown by real time PCR and western blotting.

#### **4.2.10 5-Fluorouridine incorporation assay**

To assess the effect of CLU knockdown on ribogenesis, cells were first transfected with siCLU for 48 hrs. After completion of 48 hrs, cells were washed with ice-cold PBS and then incubated with 4 mM 5-FUrd in an incomplete medium for 20 min at 37<sup>0</sup>C. Further, cells were washed with PBS and processed for immunofluorescence based detection of incorporation of 5-FUrd using monoclonal anti-BrdU antibody.

#### **4.2.11 Protein extraction and western blotting**

##### **A. Protein extraction**

For protein extraction from oral tumor tissue samples, 5 micrometer frozen tissue sections were obtained using cryotome and were homogenized in an appropriate volume of NP-40 lysis buffer containing protease inhibitor cocktail. The homogenized samples were incubated on ice for 30 min at 4<sup>0</sup>C and further centrifuged at 12000 rpm for 20 min at 4<sup>0</sup>C. The supernatant was collected in fresh tubes as a whole cell lysate and quantified using Folin-Lowey protein estimation assay.

Similarly for protein extraction using cell lines, cultured cells were washed with PBS and trypsinized with 0.25% Trypsin-EDTA for 5 min at 37<sup>0</sup>C. Cells were harvested in a 1.5ml eppendorf tube and centrifuged at 2500 rpm for 5 min. The pellets were resuspended in an appropriate volume of NP-40 lysis buffer containing protease inhibitor cocktail and incubated on ice for 30 min. Cells were centrifuged at 12000 rpm for 20 min at 4<sup>0</sup>C. The supernatant was collected in a fresh tube as a whole cell lysate and pellet was discarded. The cell lysates were quantified using Bradford protein estimation assay and stored at -80<sup>0</sup>C till further use.

### **B (I) Protein estimation using Folin-Lowry method**

BSA standards were prepared from 1mg/ml BSA stock as described in table 9 below and unknown protein lysates were diluted such that its concentration falls within the standard protein concentration range. 1ml of CTC working reagent was added to the different BSA standards and unknown protein samples (cell line/ tissue lysate) and tubes were incubated in dark at R.T. for 10 min. Further, 500 µl of Folin-Ciocalteu reagent was added and incubated at R.T. for 30 min in dark. The absorbance was measured at 750 nm using spectrophotometer. The standard curve was plotted and R<sup>2</sup> value was measured. The unknown protein concentration was determined using the standard curve equation.

**Table 9: Folin-Lowry protein estimation assay**

<b>BSA concentration (mg/ml)</b>	<b>D/W (µl)</b>	<b>CTC working reagent (µl)</b>		<b>Folin-Ciocalteu reagent (µl)</b>	
Blank	1000	1000	<i>Incubate at R.T. for 10 min in dark</i>	500	<i>Incubate at R.T. for 30 min in dark and then take at O.D. at 750nm</i>
5	995	1000		500	
10	990	1000		500	
15	985	1000		500	
20	980	1000		500	
25	975	1000		500	
30	970	1000		500	

### **B (II) Protein estimation using Bradford method**

This assay is performed in 96-well microtitre plate. BSA standards were prepared from 1 mg/ml BSA (serial dilution method) as described in table 10 and 5 µl of each standards were added in triplicate in 96 well plate along with blank. 1 µl of the cell lysate was added in each well in triplicate. 100 µl of Bradford reagent was added in each well and absorbance was measured at 595 nm. The standard curve was plotted and the unknown concentration was extrapolated using standard curve equation.

**Table 10: Bradford protein estimation assay**

<b>BSA concentration (mg/ml)</b>	<i>Add 5 <math>\mu</math>l of each diluted BSA standards in triplicate in 96 well plate</i>	<b>Total amount of protein (<math>\mu</math>g)</b>	<i>Add 100 <math>\mu</math>l Bradford's reagent and incubate for 5 min at R.T. and take absorbance at 595nm.</i>
1		5	
0.5		2.5	
0.25		1.25	
0.125		0.0625	
0.0625		0.3125	

### **C. Nucleolar protein fractionation**

Nucleoli isolation was carried out as described by Li and Lam, 2015 [173]. Briefly, oral cancer cells were grown to >90% confluency in a 100mm dish. Cells were washed with cold sucrose-containing solution I (0.5 M sucrose, 3 mM MgCl<sub>2</sub> with Cocktail protease inhibitor, Roche), harvested by scraping into 3 ml solution I and sonicated on ice in a BioRuptor at 50% amplitude for 10 cycles (15 sec ON/15 sec OFF). Disruption of cellular and nuclear membranes was verified by phase contrast microscopy. The suspension was then underlaid with an equal volume of solution II (1 M sucrose, 3 mM MgCl<sub>2</sub> with Cocktail protease inhibitor) and centrifuged at 1800 g for 10 min at 4<sup>0</sup>C. The 0.5 M sucrose phase was collected as the cytosolic plus nuclear protein fraction. To purify nucleoli further, the nucleoli-containing pellet was resuspended in 1 ml solution I, underlaid with an equal volume of solution II, centrifuged and the pellet resuspended in 500  $\mu$ l solution I as the nucleolar fraction. Equal amounts of the two fractions were boiled in 1x Laemmli sample buffer and used for immunoblot analysis. Appropriate Cyto-nuclear and nucleolar markers were used to assess the purity of each fraction.

## D. Western blotting

### i. Sample preparation for western blotting

For sample preparation, the required amount of protein lysate (for 25 $\mu$ g of protein) is mixed with 6X Laemmli buffer and the total volume is adjusted using 1X Laemmli buffer to 20  $\mu$ l. The samples were boiled at 100<sup>0</sup>C for 5 min before loading on SDS-PAGE gel.

### ii. SDS-Polyacrylamide gel electrophoresis (SDS-PAGE)

SDS-PAGE is an analytical method to resolve proteins based on their molecular weight. The polymerized matrix is formed by cross-linking of acrylamide and N, N'-methylene Bis-Acrylamide. The pore size is determined by the ratio of acrylamide to bis-acrylamide and by the concentration of acrylamide used. The increased concentration of acrylamide results in smaller pore size. Hence, for different molecular weight proteins, resolving gels of different percentage (8% to 15%) were used as per the requirement. The composition of resolving and stacking gels are given in the table 11 below. The boiled protein samples were loaded on the wells of stacking gel along with a pre-stained protein ladder (to evaluate the mobility of proteins in electrophoresis) and electrophoresed at 25mA for 2 to 3 hours at R.T.

**Table 11: Composition of resolving and stacking gel for SDS-PAGE**

Components	12% resolving gel	5% stacking gel
De-ionized water	3.3 ml	6.8 ml
30% Acrylamide solution	4ml	1.7 ml
1.5 M Tris (pH 8.8)	2.5 ml	-
1.0 M Tris (pH 6.8)	-	1.25 ml
SDS (10%)	0.1 ml	0.1 ml
APS (10%)	0.1 ml	0.1 ml
TEMED	0.008 ml	0.008 ml

### **iii. Electroblothing**

Proteins separated on a SDS-PAGE gel were electroblotted on a Polyvinylidene difluoride (PVDF) membrane to allow the binding of antibodies for the detection of specific protein of interest. Wet electroblotting was carried out at 80 V for 3 hours at 4°C or 18 V for 16 hours at R.T. Transfer of proteins on PVDF membrane was evaluated by staining the membrane with Fast green or Ponceau S solution and destained by washing with distilled water and destainer. Further, membrane was blocked with blocking solution (5% BSA prepared in Tris buffered saline with added 0.1% tween-20 or 5% non-fat dry milk (NFDM) in Tris buffered saline) for 1 hour or overnight (as per the standardization done for individual antibody). Subsequently, blots were incubated with primary antibody solution (diluted at an appropriate concentration in 2.5% BSA or 2.5% non-fat dry milk) for overnight at 4°C or 2 hours at R.T. depending on the standardized protocol for respective antibody. Then the blots were washed thrice with TBST for 20 min each followed by incubation with HRP-conjugated secondary antibodies for 1 hour at R.T. The blots were then washed three times with TBST for 20 min each. The blots were visualized using WesternBright ECL HRP substrate in ChemiDoc imaging system (Biorad) as per the manufacturer's instructions.

#### **4.2.12 Cycloheximide chase assay**

To determine the half-life of CLU, Cycloheximide chase assay was performed. In brief, cells were grown to 70-80% confluency and then treated with 100µg/ml Cycloheximide and were harvested at different time points. The protein extraction was done as described in the above section and the level of CLU was determined relative to Vinculin which was used as a housekeeping control. Mcl-1 was used as a positive control in the assay.

#### **4.2.13 Cell proliferation assay (MTT assay)**

1000 to 2000 cells were seeded in 96 well culture plate in triplicates and allowed to grow overnight. Next day, 20µl of MTT reagent (from 5mg/ml stock) was added in each well and

incubated for 4 hours at 37<sup>0</sup>C. The formazan crystals formed by the metabolism of MTT by cells were dissolved by the addition of 100µl 10% acidified SDS. The absorbance was measured at 540 nm with a 690 nm reference wavelength on a microplate ELISA reader. The absorbance of the cells was measured at different time points (0, 24, 48 and 72 hours) and then growth curve was plotted using three independent experiments, to determine the cell proliferation.

#### **4.2.14 Loss of heterozygosity detection using Sequenom MassARRAY iPLEX Platform**

##### **A. DNA extraction**

DNA was extracted from 10 matched paired oral tumor samples using MasterPure DNA extraction kit. In brief, 10 µm tissue sections were obtained from frozen tissue using cryotome and were collected in a 300µl of Tissue and Cell Lysis Solution containing the Proteinase K. The tissue was homogenized properly and incubated at 65<sup>0</sup>C for 15 min with intermittent vortexing every 5 min. The samples were incubated on ice for 3-5 min and then 150 µl of MPC Protein Precipitation Reagent was added. The mixture was vortexed vigorously for 10 s followed by centrifugation at 10000 g for 10 min at 4<sup>0</sup>C. The supernatant was collected in a separate eppendorf tube and 500 µl of isopropanol was added. The mixture was mixed by gently inverting the tubes 30-40 times followed by centrifugation at 10000 g for 10 min at 4<sup>0</sup>C. The supernatant was discarded and the pellet was washed twice with 70% ethanol (prepared in DEPC water) followed by centrifugation step. At the end, supernatant is discarded and the pellet is air dried at R.T. and resuspended in 20-30 µl TE buffer. The obtained DNA was quantified using spectrophotometer and A260/280 ratio was noted to check the purity of DNA.

##### **B. MassEXTEND genotyping**

The DNA extracted from 10 paired oral tumor samples were used for genotyping using Sequenom MassEXTEND genotyping assay. This assay is based on the mass variance of

allele-specific primer extension products. For loss of heterozygosity analysis at chromosome 8p21 location (the region where CLU is located), the single nucleotide polymorphisms (SNPs) in this region were selected from dbSNP and COSMIC database based on their minor allele frequency (MAF). Only SNPs with  $MAF \geq 1\%$  were used in the study. First, a standard PCR was run to obtain a 110 bp amplicon product. The primers used for amplification create 10bp long tag at their 5' end. The PCR product was treated with shrimp alkaline phosphatase (SAP) to remove the unincorporated dNTPs and it was further heat inactivated at 80°C for 5 min. Then extension primer was added which matches to the sequence adjacent of target SNP. The locus specific primer extension reaction (iPLEX assay) is mainly comprised of extension primer, enzyme, buffer and mass-modified nucleotides. The resulting reactions were treated with a cation exchange resin to remove extraneous salts that may interfere with the mass spectrometry based analysis. Subsequently, the iPLEX reaction product was loaded onto 384-well spectroCHIP pads and subjected to MALDI-TOF MS analysis. The obtained peaks were visualized and analyzed using Sequenom's MassARRAY RT software.

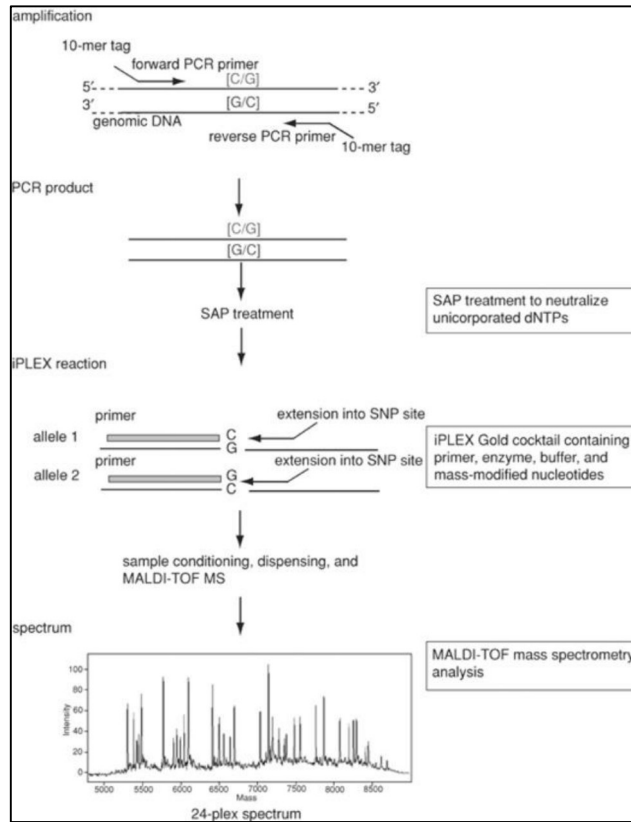


**Figure 10: The Schematic of MassEXTEND iPLEX reaction** (Adopted from Gabriel et al., 2009) [174].

### C. DNA sequencing

Additionally to confirm the loss of heterozygosity at specified position, the PCR products were subjected to DNA sequencing analysis. The PCR products were purified using QIAquick PCR Purification Kit (Qiagen) as per the manufacturer's instructions to remove the enzymes, unbound nucleotides and buffer component. The 2µl (50 ng) of the PCR product and 1 µl of 1.6pmoles/ µl primer (forward/reverse) were subjected to sequencing on an automated sequencer. The sequence (chromatogram) was read using Chromas Lite 2.1 software (technelysium.com.au).

#### 4.2.15 Methylation specific PCR (MSP)

Genomic DNA was extracted using Masterpure DNA extraction Kit from oral tumor samples. Prostate cancer cell line PC3 was used as a positive control for methylation of CLU promoter. Bisulfite conversion was performed on 500 ng of genomic DNA using the EZ DNA Methylation- Gold™ Kit (Zymoresearch, Irvine, CA) according to the manufacturer's instruction. The efficiency of conversion was routinely examined by PCR before using the bisulfite-treated DNA for MSP amplification. The primers used for MSP assay were designed by using the MethPrimer software which are listed below in table 12. PCR amplification was carried out with HotStart Taq DNA Polymerase.

**Table 12: Primers used for MSP assay**

Name of the primer	Sequence (5'-3')
CLU methylated forward	TTGGGATAGATAGTCGGGTTAATC
CLU methylated reverse	CTCCAAAAAAAAACCTAAAATACG
CLU unmethylated forward	TTGGGATAGATAGTTGGGTTAATTG
CLU unmethylated reverse	AACTCCAAAAAAAAACCCTAAAATACA

#### 4.2.16 miRNA expression analysis oral tumor samples

The total RNA was extracted from tissue samples using RNAiso Plus reagent as described in earlier section. The extracted RNA was quantified using spectrophotometer and 250-500ng of RNA was used further for cDNA synthesis. Next, using high capacity cDNA synthesis kit, total RNA was converted into cDNA using miRNA specific stem-loop reverse transcription primers (SLRT) as described by Chen et al.,2005 [175]. This miRNA specific cDNA was used as a template for the quantitation using real-time PCR using SYBR green master mix as described in the earlier section. The details of the primers used in this study are given below in table 13.

**Table 13: Primers used for miRNA specific cDNA synthesis and real-time PCR**

Name of the primer	Primer sequence (5'-3')
miR-15a SLRT	GTCGTATCCAGTGCAGGGTCCGAGGTATTCGCACTGGATACGACCACAAA
miR-15a Forward	CACACGTAGCAGCACATAATGG
miR-21 SLRT	GTCGTATCCAGTGCAGGGTCCGAGGTATTCGCACTGGATACGACTCAACA
miR-21 Forward	GGCACGCACACGTAGCTTATCAGA
miR-17-3p SLRT	GTCGTATCCAGTGCAGGGTCCGAGGTATTCGCACTGGATACGACCTACAA
miR-17-3p Forward	CACGCTCAGACTGCAGTGAA
miR-374b SLRT	GTCGTATCCAGTGCAGGGTCCGAGGTATTCGCACTGGATACGACCTGGTT
miR-374b Forward	CACGCACACGCAATATAATACAACCTG
RNU44 SLRT	GTCGTATCCAGTGCAGGGTCCGAGGTATTCGCACTGGATACGACAGTCAG
RNU44 Forward	CACGCACACCCTGGATGATGA
Universal reverse primer	CCAGTGCAGGGTCCGAGGTA

#### **4.2.17 Analysis of CLU amino acid sequence for the detection of nuclear and nucleolar localization sequence:**

##### ***Nuclear localization signal analysis:***

The presence of nuclear localization signal (NLS) in sCLU sequence was determined using the open source software cNLS Mapper [176]. This tool predicts the NLSs specific to the importin  $\alpha\beta$  pathway. An NLS score of 8, 9, or 10 indicates an exclusive nuclear localization; a score of 7 or 8 indicates a partial nuclear localization; a score of 3, 4, or 5 indicates nucleus/cytoplasm localization and a score of 1 or 2 an exclusively cytoplasmic localization.

##### ***Nucleolar localization signal analysis:***

The presence of Nucleolar Localization Signal (NoLS) in CLU amino acid sequence (1-449) was determined using an online tool nucleolar localization sequence detector (NoD) [177]. The output page of NoD shows an amino acid sequence highlighted in 'red' as putative NoLS and a graph showing the average NoLS prediction score for every 20 amino acids in the protein. The NoLS is predicted if the average output score of eight consecutive amino acid residues calculated by the artificial neural network (ANN) is at least 0.8. The putative NoLS of protein with a score above 0.8 is highlighted in the pink region of the graph.

#### **4.2.18 Analysis of CLU amino acid sequence for the detection RNA binding motif**

##### ***RNA binding motif analysis using RNABindR and PPRInt:***

The online web-based servers RNABindR [178] and PPRInt [179] were used to predict the presence of putative RNA-interacting residues in sCLU sequence (residues 1–449). The output for RNA interacting residues were obtained in the following format: 1. For RNABindR: 0 (non-interacting) and 1 (interacting). 2. For PPRInt: red (interacting) and blue (non-interacting). For better understanding the results obtained from these servers were aligned in the format '+' (for interacting) and '-' (for non-interacting) with color code of red for PPRInt and blue for RNABindR.

#### **4.2.19 In silico analysis of CLU**

##### ***Clusterin structure prediction:***

There are no solved crystal structures of sCLU or its homologous proteins. Therefore, sCLU structure prediction was done using trRosetta, a de novo structure prediction software [180]. The top-scoring model was selected and energy minimized in YASARA which was used for further docking studies [181]. The sequence conservation of CLU across different species was assessed by aligning the protein sequences of sCLU from humans and other species using PRALINE multiple sequence alignment tool [182].

##### ***Docking with interacting partners:***

The energy minimized model of CLU was individually subjected to blind docking with the HMG5 box of UBF (HMG5 PDB ID: 2HDZ), NPM1 (PDB ID: 2VXD), RBD domain of Nucleolin (PDB ID: 2KRR) and Fibrillarin (PDB ID: IPX) using Z-dock [183] and the top scoring model was chosen for interaction analysis.

#### **4.2.20 Statistical analysis**

Statistical analysis was performed using GraphPad Prism 7 (GraphPad, San Diego, CA) and SPSS 21.0 (SPSS Inc., Chicago, IL, USA). A statistical difference among two groups was determined by two-tailed student's t-test. A p-value < 0.05 was considered statistically significant. Normality distribution was checked using the Shapiro Wilk test. The CLU expression analysis in paired oral tumor samples was performed using Wilcoxon signed rank test. One-way ANOVA was used to compare the differences in the expression of CLU transcripts among different cell lines. Percent positivity for the CLU expression in the tumor epithelium and stroma was used to categorize the cohort into low/high expressors to be used for following analysis. Associations of CLU expression with clinicopathological parameters were tested using Chi-square tests. Univariate analysis of CLU expression with Overall Survival and Recurrence-Free Survival was analyzed using Kaplan-Meier curves.

#### ***4.2.21 Molecular cloning methods:***

**Host strain:** *E. coli* DH5 $\alpha$

***Luria-Bertani (LB) medium preparation:*** 20 g of LB broth powder was dissolved in 800 ml distilled water (D/W) and then final volume was adjusted to 1 litre. The media was sterilized by autoclaving. For making LB-agar plates, 35 g Luria agar powder was added into 1 liter D/W and sterilized by autoclaving and poured in 90 mm sterile plates.

#### ***Preparation of ultra-competent cells:***

From the glycerol stock, cells were streaked on a freshly made LB agar plate and incubated at 37<sup>0</sup>C overnight. A single colony was inoculated next day in a 5 ml LB broth and incubated overnight on a shaker incubator at 37<sup>0</sup>C for 8 hours till O.D<sub>600</sub> reaches 1.5 to 2.0. The 10 ml of starter culture was added to 100 ml of SOB media and incubated at 37<sup>0</sup>C for 1 hour and then transferred at 18<sup>0</sup>C at 80 rpm for 12-16 hours till O.D<sub>600</sub> reaches 0.4 (approximately after 16-18 hours). The cells were centrifuged at 4000 rpm for 10 minutes at 4<sup>0</sup>C. The supernatant was discarded and the pellet was resuspended in 40 ml of ice-cold transfer buffer and placed on ice for 10 minutes. Later it was centrifuged at 4000 rpm for 10 minutes at 4<sup>0</sup>C and the pellet was resuspended in 10ml of ice-cold transfer buffer. 700 $\mu$ l of DMSO was added in it and placed on ice for 10 minutes. 100 $\mu$ l of cells were transferred in pre-chilled eppendorf tubes and snap frozen. The transformation efficiency of these cells was checked before use.

#### ***Transformation:***

Competent cells were mixed with either 50-100 ng of plasmid DNA or with ligation mixture, tapped and incubated for 30 min on ice. A heat shock at 42<sup>0</sup>C was given for 90 s and transferred on ice for 2 min. 1 ml of LB broth was added to it and incubated further at 37<sup>0</sup>C for 45 min. The mixture was centrifuged for 5 min at 5000 rpm and supernatant was discarded leaving 100  $\mu$ l behind. The pellet was mixed and spread on LB plate (with appropriate antibiotic for selection of positive clones) and incubated at 37<sup>0</sup>C for overnight.

***Plasmid DNA extraction using TELT method:***

TELT method is a easy, quick and cost-effective method for isolating plasmid DNA.

In this method, a single isolated bacterial colony of *E. coli* was inoculated into 1.5ml LB broth containing appropriate antibiotic and incubated further at 37<sup>0</sup>C for 16 hr at 200 rpm. The bacterial culture was then centrifuged at 14000 rpm at 4<sup>0</sup>C for 1 min. The supernatant was discarded and the cell pellet was resuspended in 150µl TELT buffer and vortexed briefly. Next, 5 µl lysozyme (Stock 50mg/ml) was added to the mixture and mixed well. The tube was incubated on ice for 1 min and then put in a boiling water bath for 1 min. After that the tube was immediately placed on ice for 10 min. Next, the tube was centrifuged at 15000 rpm at 4<sup>0</sup>C for 10 min. After centrifugation, the supernatant was collected in a new tube and then 330µl ice chilled absolute alcohol was added to it and incubated it at -20<sup>0</sup>C for 30 min. After that tube was centrifuged at 15000 rpm at 4<sup>0</sup>C for 10 min. In the next step, 200 µl chilled 70% ethanol was added to the DNA pellet and again centrifuged at 15000 rpm at 4<sup>0</sup>C for 5min. The pellet was dried completely by removing all the traces of alcohol and re-suspended in 20µl TE buffer.

***Restriction enzyme digestion***

Restriction enzyme digestion of CLU CDS and pEGFP-N1 plasmid using Bam HI and Hind III was performed as described below in table 14.

***Table 14: Restriction enzyme digestion of pEGFP-N1 plasmid and CLU CDS***

<b>Components</b>	<b>Volume (µl)</b>
2 µg pEGFP-N1	Add as per the concentration of the plasmid DNA
10X Fast digest buffer	5
Hind III	1
Bam HI	1
NFW	As required
Total reaction volume	50

Components	Volume (μl)
PCR amplified CLU CDS (1.0-1.5 μg)	Add as per the concentration of the extracted DNA
10X Fast digest buffer	5
Hind III	0.5
Bam HI	0.5
Nuclease free water	As required
Total reaction volume	50

**Ligation:**

After restriction enzyme digestion, the digested products were run on a agarose gel and gel purified. The concentration of purified vector and insert DNA was measured before setting up the ligation reaction. The typical ratio of vector: insert used in ligation reaction was 1:3 which may vary depending upon the size of the vector and insert. The amount of vector and insert fragment required to achieve 1:3 molar ratio was calculated as per the formula mentioned below:

*Molecular weight of the insert or plasmid DNA: size in base pairs X 650*

*Moles of DNA required= (2 X Concentration of DNA)/molecular weight*

The ligation reaction was set up as mentioned below in table 15.

**Table 15: Ligation reaction**

Components	Volume (μl)
Vector	Add vector and insert as per the 1:3 molar ratio
Insert	
T4 DNA ligase buffer (10X)	1
T4 DNA ligase enzyme	0.4
Nuclease free water	As required to make up the total volume to 10 μl
Incubate the ligation mixture at 16 <sup>0</sup> C overnight.	

# *Chapter 5*

## *Results*

## 5.1 To assess the expression of CLU in oral tumor samples

### 5.1.1 Evaluation of different CLU transcripts in oral tumor samples using isoform specific quantitative real-time PCR (qRT-PCR)

To investigate the biogenesis of different transcript variants of CLU in oral tumor samples, isoform specific qRT-PCR was carried out using primers specific to each transcript variant. The samples included in the study were obtained from different oral subsites like buccal mucosa, tongue, and alveolus. The secretory isoform of CLU (sCLU) was the predominant isoform detected in all paired oral tumor tissue samples whereas the other variants of CLU including nuclear CLU ( $\Delta$ Exon 2), NR\_038335.1, and NR\_045494.1 were not detected in any samples. Several studies in oral cancers have shown that the entire oral cavity is exposed to the carcinogen, which may result in molecular alterations in the adjacent tissue [184,185]. Hence, we also included 9 normal oral tissues from healthy individuals in our study. Figure 11 shows that the sCLU transcripts were significantly downregulated ( $P < 0.0001$ ) in oral tumor tissues compared to their adjacent normal tissue ( $n=50$ ) and tissues obtained from healthy volunteers.

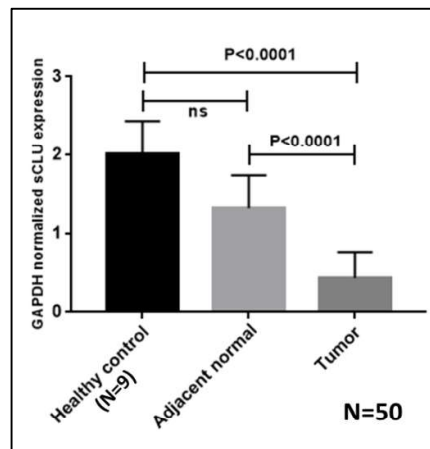
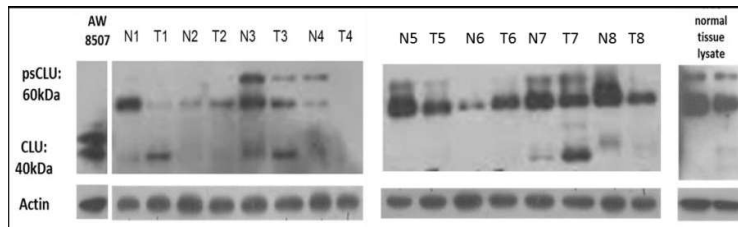


**Figure 11:** qRT-PCR analysis for the expression of sCLU in paired oral tumor samples. Quantitative real-time PCR showing significant downregulation of sCLU transcripts in oral

tumor samples compared to their adjacent normal tissues and healthy control tissues ( $P < 0.0001$ )

### 5.1.2 Evaluation of CLU protein expression in oral tumor samples using western blotting and immunohistochemistry

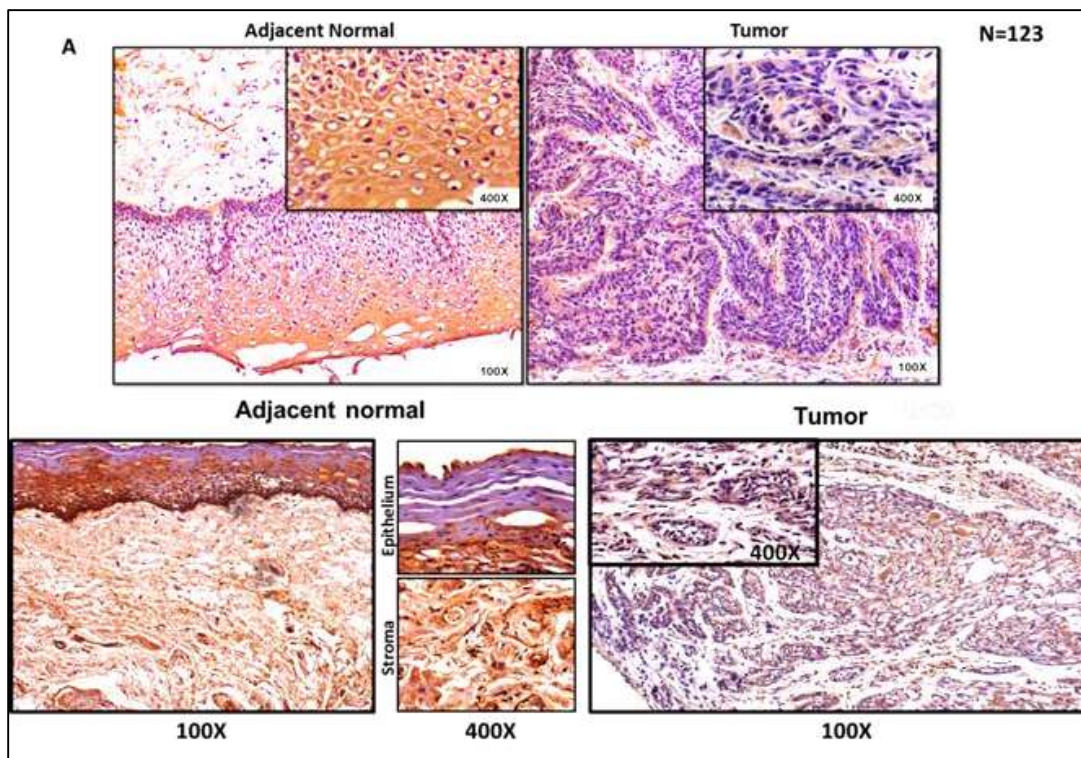
The expression levels of CLU protein in paired oral tumor samples were studied using western blot and immunohistochemical analysis. We observed downregulation of pre-secretory form of CLU (psCLU: 60kDa) in 16 out of 25 oral tumor samples compared to their adjacent normal. The representative western blot images of select paired tissue samples are shown in figure 12. The mature form of CLU (40kDa) was detected in few oral tumor samples. The healthy control lysate predominantly showed the presence of psCLU (60kDa) and a faint band of mature CLU (40kDa). These observations confirm the presence of secretory form (sCLU) as the predominant form in oral tumors.



**Figure 12: Expression of sCLU protein in oral tumor samples.** Western blot analysis showing downregulation of psCLU (60 kDa) in tumor samples compared to their adjacent normal tissues. The healthy control tissue lysate also shows the presence of psCLU form whereas AW8507 tongue cancer cell line shows the presence of mature 40 kDa sCLU.

Additionally, to evaluate the expression and localization of CLU in oral tumor samples immunohistochemistry was performed (n=123). We observed cytoplasmic expression of CLU in both epithelium and stromal compartments of a tumor and adjacent normal tissues (Figure 13 A). The scoring was done independently for stromal and epithelial

compartments. The CLU staining in different stromal components mainly included fibroblast, endothelial cells, skeletal muscle cells, neutrophils, macrophages, etc. We observed significant downregulation of CLU expression in tumor cells and associated stromal cells. We observed a significant decrease in percent positivity and intensity of CLU in both of these compartments of tumors compared to its adjacent normal tissues also indicated by low H-score in tumor samples (Figure 13 B).



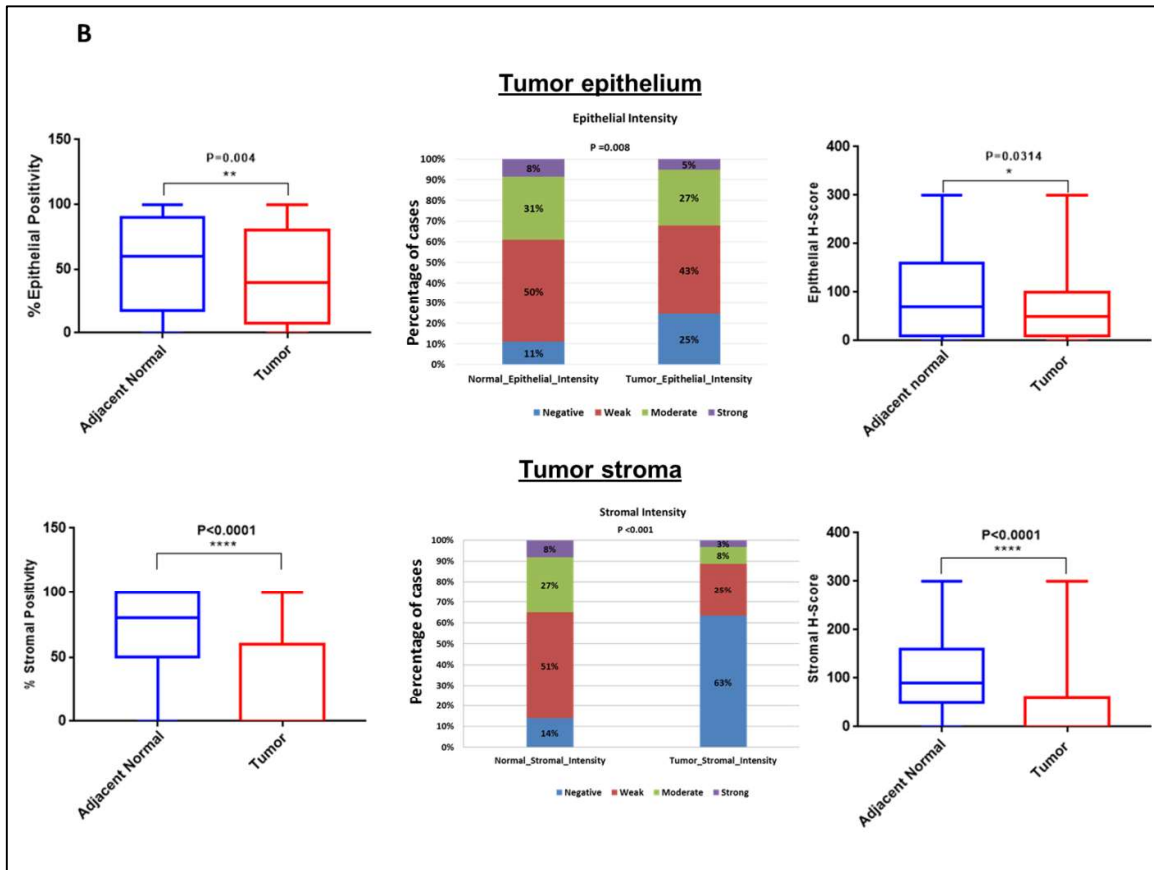


**Figure 13: Immunohistochemical analysis of CLU expression in oral tumor samples. (A)** Immunohistochemical staining for sCLU showing downregulation of sCLU in oral tumors compared to adjacent normal tissues. **(B)** % positivity, intensity, and H-score calculated for the epithelial and stromal expression of sCLU in paired oral tumor-normal samples.

However, no significant association was seen between tumor epithelial or stromal staining of CLU and gender, age at diagnosis, habits, TNM status, or tumor differentiation status (Table 16). Out of 123 samples included in the study, follow-up data was available for only 74 patients. The median follow-up period was 98.5 months (95%CI, 91 months-105 months) and the median survival time was not reached i.e. more than 50% of patients survived. Figure 14 shows the results of the univariate analysis related to patient prognosis.

Interestingly, it was observed that low percent positivity in an epithelial compartment is associated with poor overall survival (OS) (P=0.11) and recurrence-free survival (RFS) (P=0.075), contrarily high percent positivity in the stromal compartment is associated with poor OS (P=0.35) and RFS (P=0.26). In summary, transcript and protein expression analysis of CLU in oral tumors showed downregulation of sCLU compared to their adjacent normal tissues, indicative of its possible tumor suppressor like role.

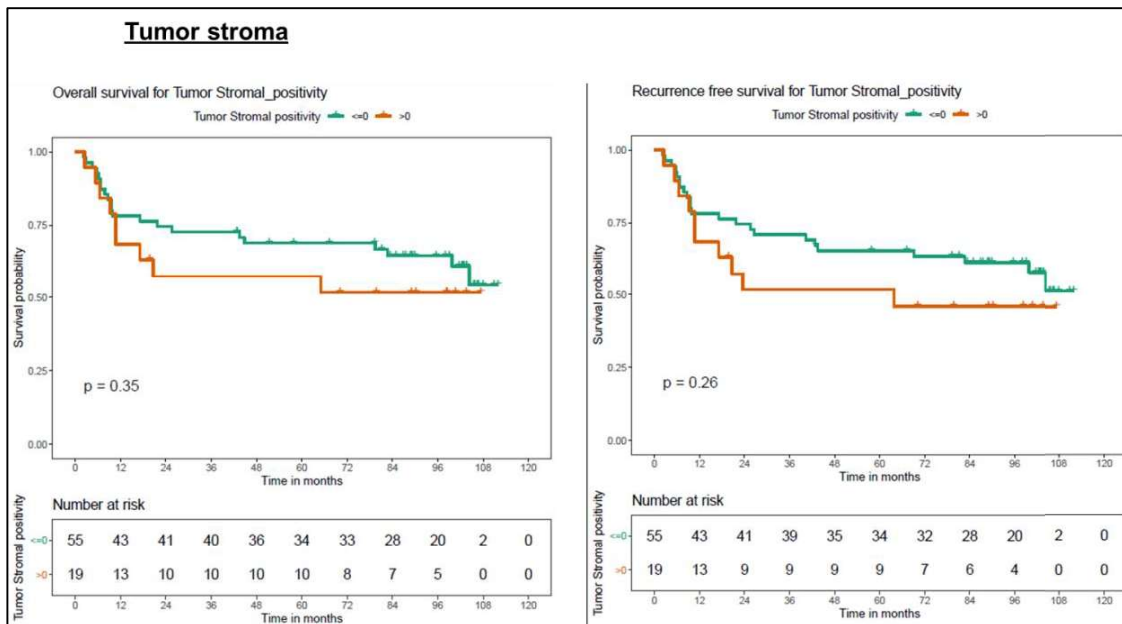
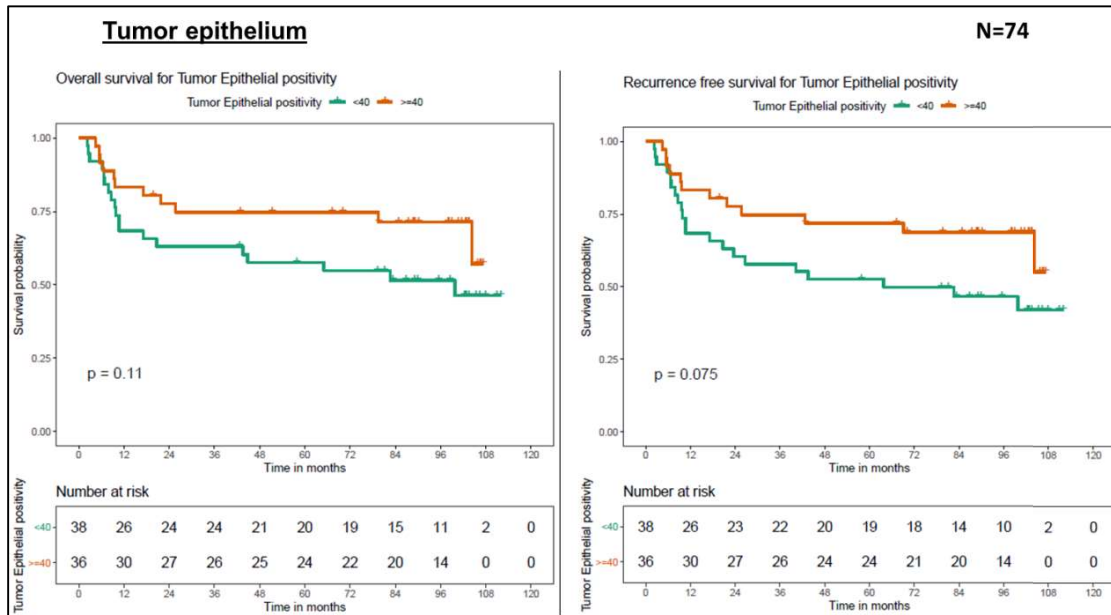
		Tumor Epithelial % positivity			Tumor Epithelial Intensity			Tumor Epithelial Hscore			
Variable	Level	Total (n=123)	<=40 (n=67)	>40 (n=56)	p-value	Low (n=29)	High (n=94)	p-value	<=50 (n=66)	>50 (n=57)	p-value
Age	mean (sd)	49.7 (12.3)	51 (12.4)	48.1 (12.1)	0.2094	48.8 (13.8)	50 (11.8)	0.6577	50 (12.3)	49.3 (12.3)	0.7794
	missing	2	1	1		0	2		1	1	
Sex	Female	24 (19.5)	12 (17.9)	12 (21.4)		7 (24.1)	17 (18.1)		14 (21.2)	10 (17.5)	
	Male	99 (80.5)	55 (82.1)	44 (78.6)	0.7934	22 (75.9)	77 (81.9)	0.652	52 (78.8)	47 (82.5)	0.7766
T status	I / II	28 (23.3)	14 (21.2)	14 (25.9)		6 (20.7)	22 (24.2)		13 (20.0)	15 (27.3)	
	III / IV	92 (76.7)	52 (78.8)	40 (74.1)	0.6962	23 (79.3)	69 (75.8)	0.893	52 (80.0)	40 (72.7)	0.4703
	missing	3	1	2		0	3		1	2	
N status	No	45 (37.5)	26 (39.4)	19 (35.2)		11 (37.9)	34 (37.4)		25 (38.5)	20 (36.4)	
	N+	75 (62.5)	40 (60.6)	35 (64.8)	0.7762	18 (62.1)	57 (62.6)	1	40 (61.5)	35 (63.6)	0.9623
	missing	3	1	2		0	3		1	2	
Differentiation status	Poor	39 (33.3)	20 (31.7)	19 (35.2)		12 (41.4)	27 (30.7)		20 (32.3)	19 (34.5)	
	Moderate	67 (57.3)	39 (61.9)	28 (51.9)		15 (51.7)	52 (59.1)		36 (58.1)	31 (56.4)	
	Well	11 (9.4)	4 (6.3)	7 (13.0)	0.3736	2 (6.9)	9 (10.2)	0.5453	6 (9.7)	5 (9.1)	0.9651
	missing	6	4	2		0	6		4	2	
Tobacco habit	No	3 (3.3)	2 (4.0)	1 (2.4)		2 (10.0)	1 (1.4)		2 (4.0)	1 (2.4)	
	Yes	89 (96.7)	48 (96.0)	41 (97.6)	1	18 (90.0)	71 (98.6)	0.2276	48 (96.0)	41 (97.6)	1
	missing	31	17	14		9	22		16	15	
Alcohol habit	No	78 (84.8)	43 (86.0)	35 (83.3)		19 (95.0)	59 (81.9)		44 (88.0)	34 (81.0)	
	Yes	14 (15.2)	7 (14.0)	7 (16.7)	0.9495	1 (5.0)	13 (18.1)	0.2774	6 (12.0)	8 (19.0)	0.5182
	missing	31	17	14		9	22		16	15	

		Tumor Stromal % positivity			Tumor Stromal Intensity			Tumor Stromal Hscore			
Variable	Level	Total (n=123)	<=0 (n=77)	>0 (n=46)	p-value	Low (n=78)	High (n=45)	p-value	<=0 (n=78)	>0 (n=45)	p-value
Age	mean (sd)	49.7 (12.3)	49.3 (12.1)	50.4 (12.7)	0.6416	49.5 (12.2)	50.1 (12.7)	0.7924	49.5 (12.2)	50.1 (12.7)	0.7924
	missing	2	1	1		1	1		1	1	
Sex	Female	24 (19.5)	18 (23.4)	6 (13.0)		18 (23.1)	6 (13.3)		18 (23.1)	6 (13.3)	
	Male	99 (80.5)	59 (76.6)	40 (87.0)	0.2444	60 (76.9)	39 (86.7)	0.2814	60 (76.9)	39 (86.7)	0.2814
T status	I / II	28 (23.3)	17 (22.7)	11 (24.4)		17 (22.4)	11 (25.0)		17 (22.4)	11 (25.0)	
	III / IV	92 (76.7)	58 (77.3)	34 (75.6)	1	59 (77.6)	33 (75.0)	0.9168	59 (77.6)	33 (75.0)	0.9168
	missing	3	2	1		2	1		2	1	
N status	No	45 (37.5)	30 (40.0)	15 (33.3)		30 (39.5)	15 (34.1)		30 (39.5)	15 (34.1)	
	N+	75 (62.5)	45 (60.0)	30 (66.7)	0.5923	46 (60.5)	29 (65.9)	0.6956	46 (60.5)	29 (65.9)	0.6956
	missing	3	2	1		2	1		2	1	
Differentiation status	Poor	39 (33.3)	22 (29.7)	17 (39.5)		23 (30.7)	16 (38.1)		23 (30.7)	16 (38.1)	
	Moderate	67 (57.3)	44 (59.5)	23 (53.5)		44 (58.7)	23 (54.8)		44 (58.7)	23 (54.8)	
	Well	11 (9.4)	8 (10.8)	3 (7.0)	0.5018	8 (10.7)	3 (7.1)	0.6463	8 (10.7)	3 (7.1)	0.6463
	missing	6	3	3		3	3		3	3	
Tobacco habit	No	3 (3.3)	3 (4.8)	0 (0.0)		3 (4.8)	0 (0.0)		3 (4.8)	0 (0.0)	
	Yes	89 (96.7)	59 (95.2)	30 (100.0)	0.5493	60 (95.2)	29 (100.0)	0.5734	60 (95.2)	29 (100.0)	0.5734
	missing	31	15	16		15	16		15	16	
Alcohol habit	No	78 (84.8)	55 (88.7)	23 (76.7)		56 (88.9)	22 (75.9)		56 (88.9)	22 (75.9)	
	Yes	14 (15.2)	7 (11.3)	7 (23.3)	0.2309	7 (11.1)	7 (24.1)	0.1923	7 (11.1)	7 (24.1)	0.1923
	missing	31	15	16		15	16		15	16	

Categorical variable presented as counts (percentage) and compared using chi square test  
Continuous variable presented as mean (sd) and compared using independent T test.

**Table 16: Association of sCLU with clinopathological parameters in oral tumors (n=123).**



**Figure 14: Kaplan-Meier curves of OS and RFS for CLU expression in tumor epithelial and stromal compartment.** Kaplan-Meier curves of OS and RFS show that low CLU expression in the tumor epithelium and high in the stroma is associated with poor OS and RFS of the oral cancer patients.

## **5.2 Understanding the possible mechanisms of CLU downregulation in oral tumor samples**

To explore different regulatory mechanisms like methylation of CLU promoter, loss of heterozygosity (LOH) at chromosome 8p21 location, or miRNA mediated post-transcriptional gene silencing which may contribute to CLU downregulation, we carried out methylation-specific PCR, LOH analysis using massSequenom array and miRNA profiling in 10 oral tumor samples.

### **5.2.1 Detecting methylation of CLU promoter using methylation specific PCR (MSP)**

CLU gene promoter region was retrieved from the UCSC genome browser. The prediction of CpG islands and bisulfite primers designing was carried out using a MethPrimer, an online primer designing tool (<http://www.urogene.org/methprimer/>) (Figure 15 A). Since in the case of oral cancers, adjacent normal tissue may also show genetic and molecular alterations due to exposure to different carcinogens (called ‘field cancerization’), in this study we used buccal scrapings from healthy volunteers as ‘normal’ control. Prostate cancer cell line PC3 was used as a control where CLU promoter is earlier reported to be methylated [186]. Figure 15 B shows representative gel images of methylation specific PCR of tumor samples and control samples (i.e. samples obtained from healthy volunteers). Both healthy controls and tumors showed the presence of methylated and unmethylated alleles with no difference in their methylation pattern. PC3 cells showed the presence of both methylated and unmethylated forms. The sample size used for MSP in this study is less (n=10), hence this needs to be repeated in a larger sample cohort to confirm the role of methylation in CLU gene regulation.

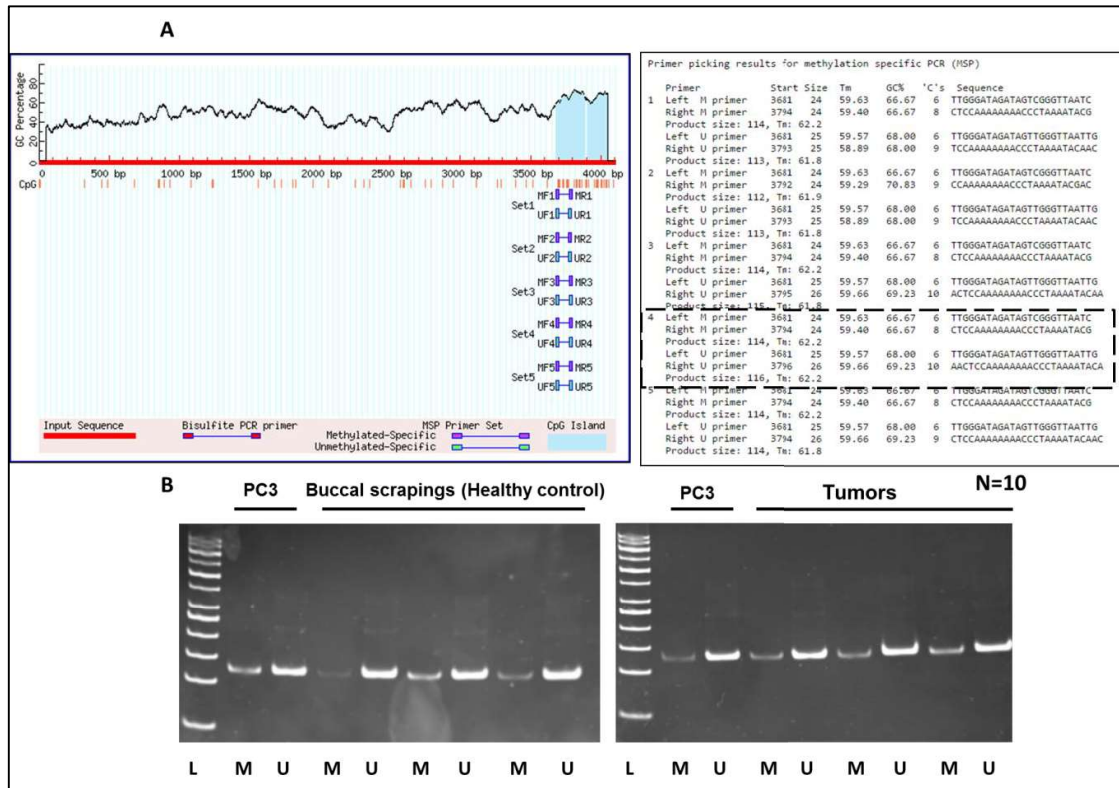


**Figure 15: Methylation specific PCR in oral tumor samples. (A)** *CLU* promoter analysis using MethPrimer online tool showing the prediction of CpG islands and primer designing. The primer sets in the square box were used for MSP. **(B)** Representative gel image of methylation specific PCR for oral tumors and healthy controls. PC3 prostate cancer cell line was used as a positive control for MSP assay. Both healthy controls and tumors showed the presence of methylated and unmethylated alleles.

### 5.2.2 Detecting loss of heterozygosity at *CLU* locus chromosome 8p21 using Sequenom Mass ARRAY system

The LOH analysis was performed in 10 paired oral tumor samples using Sequenom MassEXTEND genotyping assay. For this analysis, 41 germline and 33 somatic mutations with minor allele frequency  $\geq 1\%$  were selected using dbSNP and COSMIC databases. As illustrated in figure 16 A, for a given normal/tumor pair, each SNP can be defined as “LOH”

(heterozygous in normal and LOH in tumor), “retention” (both normal and tumor are heterozygous), and “non-informative” (homozygous in normal). Representative spectra are shown in figure 16 B. We observed the presence of homozygous alleles in all the normal samples for all the SNP markers selected for the analysis. This suggests the output of this preliminary LOH study as ‘non-informative’. The computerized analysis of the spectra was done by Sequenom’s MassARRAY RT software. Based on this preliminary finding, LOH may not be contributing to the downregulation of CLU although this study further needs to be extended in a larger sample set to confirm this observation.

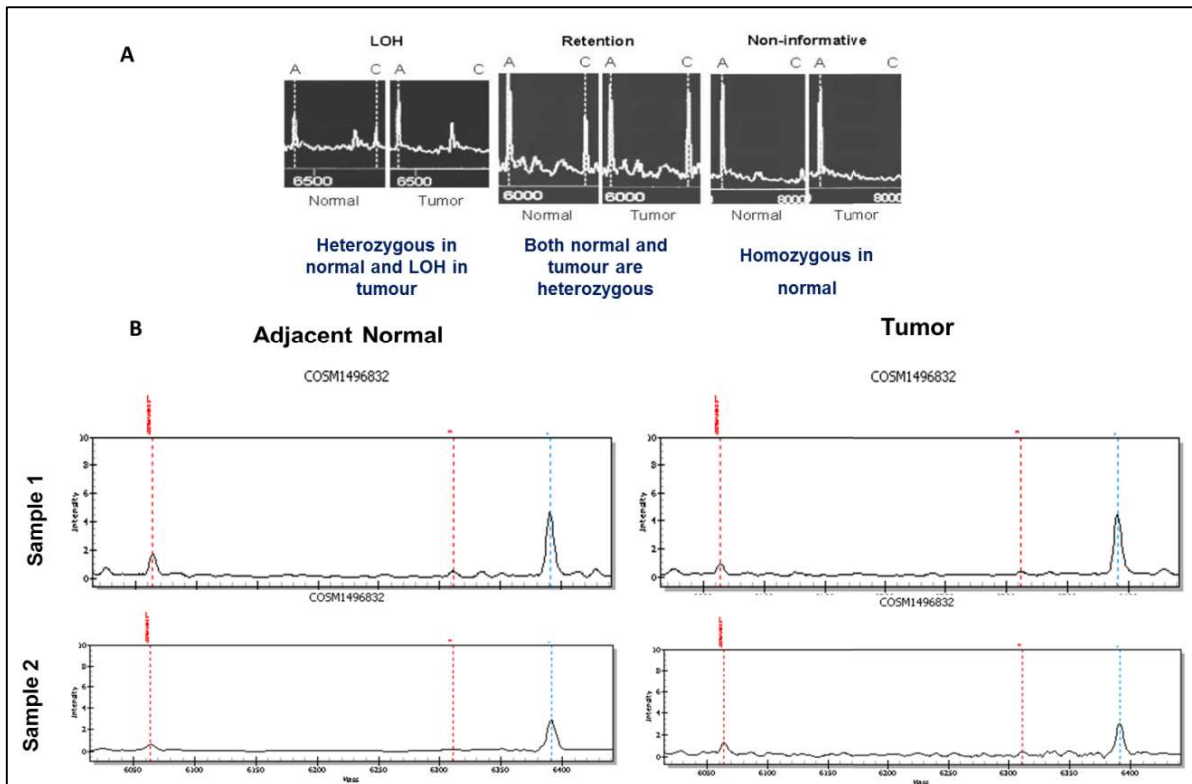


**Figure 16: Study of LOH in oral tumor samples using Sequenom MassEXTEND genotyping assay. (A) Representative illustrations of LOH, retention, and Noninformative SNPs detected by MassEXTEND genotyping assay. (B) Representative spectra showing the presence of homozygous allele in adjacent normal tissue samples, as a result of which the output is ‘Noninformative’.**

### **5.2.3 Expression profiling of miRNA predicted to target CLU in oral tumors samples**

Apart from LOH and methylation of the gene promoter, miRNA-mediated post-transcriptional gene silencing can also contribute to the downregulation of sCLU in oral tumors. In the case of HNSCC and neuroblastoma, the role of miR-21 and miR-17-92 cluster in the regulation of CLU is reported [13,96]. Hence, to explore the role of miRNAs in the downregulation of CLU in oral tumor samples, we first searched for miRNAs that are predicted to target CLU using different online prediction tools like PicTar, TragetScan, and MiRanda. The list of different miRNAs predicted to target CLU by these different tools is given in figure 17 A. Further, based on literature information, the miRNAs which are overexpressed in oral tumors and also predicted to target the CLU were shortlisted for miRNA expression analysis. This includes miR-15a, miR-17-3p, miR-21, and miR-374b. The miRNA expression analysis was performed in 10 paired tumor samples using SYBR green based real-time PCR. Figure 17 B shows that there is a significant increase in miR-15a and miR-21 expression in oral tumors compared to their adjacent normal tissues. We also observed an increase in miR-17-3p levels in oral tumors although not statistically significant, whereas miR-374 b levels were downregulated in oral tumors compared to adjacent normal. This suggests possible role of miR-15a and miR-21 in the regulation of CLU. However, this study further needs to be performed in more number of samples and further experimental validation like luciferase assay to confirm the binding of miRNA to CLU 3'-UTR region is warranted in the future.

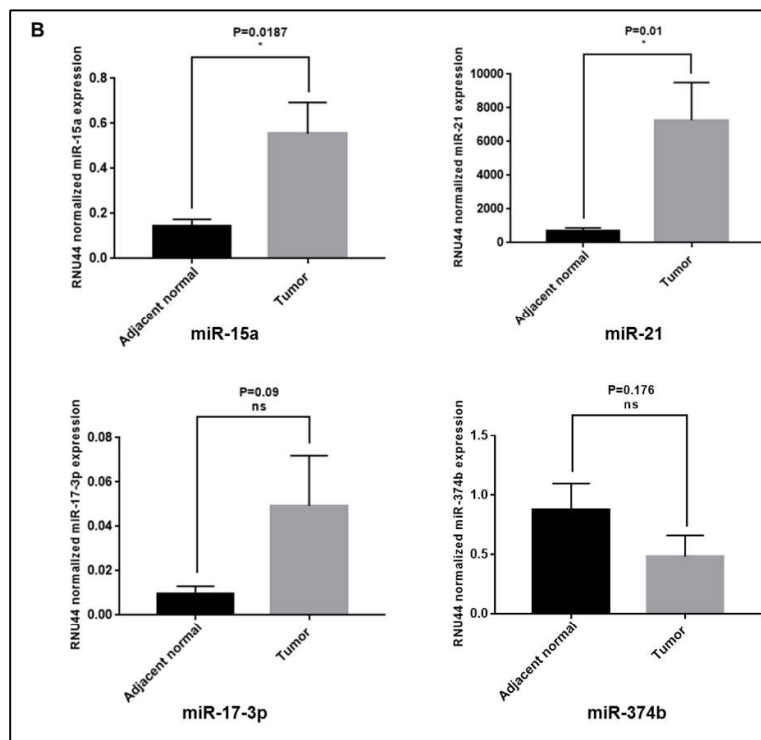
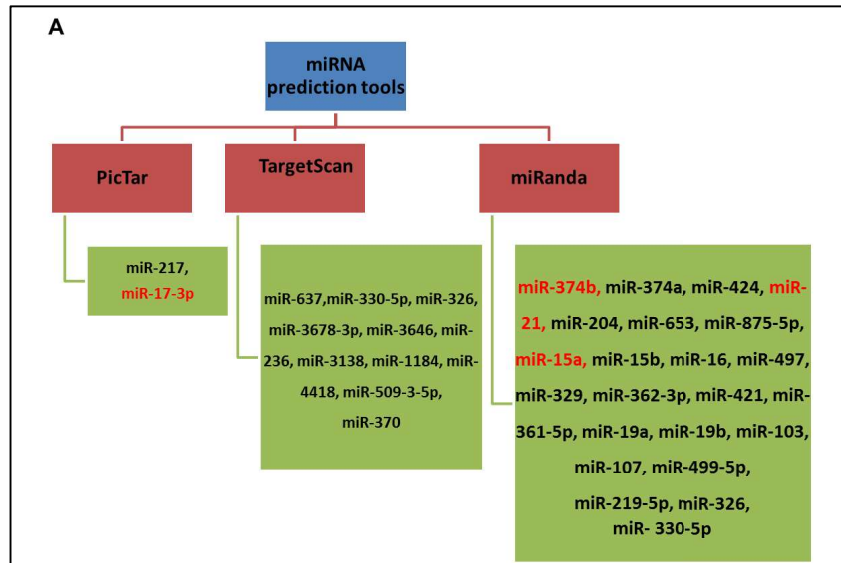


**Figure 17: miRNA expression profiling in oral tumor samples. (A)** List of miRNAs predicted to target *CLU* by different prediction tools like PicTar, TargetScan, and miRanda. The miRNAs highlighted in red text are overexpressed in oral tumors. **(B)** Expression profiling of miR-15a, miR-21, miR-17-3p, and miR-374b in paired oral tumor samples ( $n=10$ ).

### 5.3 To assess the expression of CLU in oral cancer cell lines

#### 5.3.1 To check the expression of different CLU variants in oral cancer cell lines using isoform specific qRT-PCR

As explained in section 5.1, we carried out isoform-specific qRT-PCR analysis in human oral dysplastic keratinocyte (DOK) and oral cancer cell lines of different origin (i.e buccal mucosa and tongue). We also included HaCaT, an immortalized skin keratinocyte cell line as a control. We observed sCLU as the predominant isoform in HaCaT and oral cancer cell lines. We observed decreased expression of sCLU transcripts (Figure 18), whereas nCLU transcript levels were very low or undetectable.

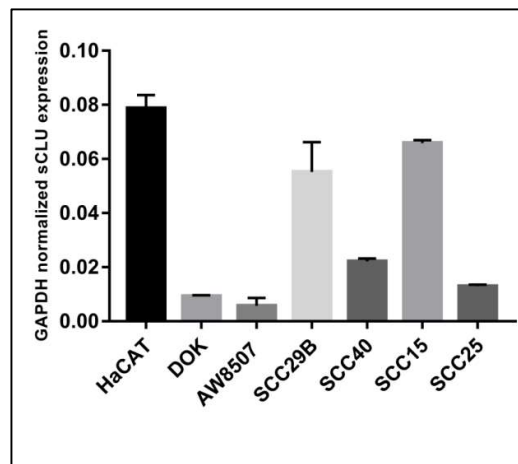


*Figure 18: Expression of sCLU transcripts in oral cancer cell lines. qRT-PCR showing downregulation of sCLU transcripts in DOK and oral cancer cell lines compared to HaCaT, a skin keratinocyte cell line used as a control.*

#### 5.3.2 Evaluating the expression of CLU protein in different oral cancer cell lines

Unlike the 60kDa psCLU form detected in oral tumor samples; all oral cancer cell lines and DOK showed the presence of 40kDa mature sCLU (Figure 19 A). We did not observe the presence of 49 kDa nCLU form in any of the cell lines. Since sCLU is a secretory protein, we

also detected its presence in the culture supernatant of different oral cancer cell lines using TCA precipitation which detected 40kDa mature sCLU (Figure 19 B).

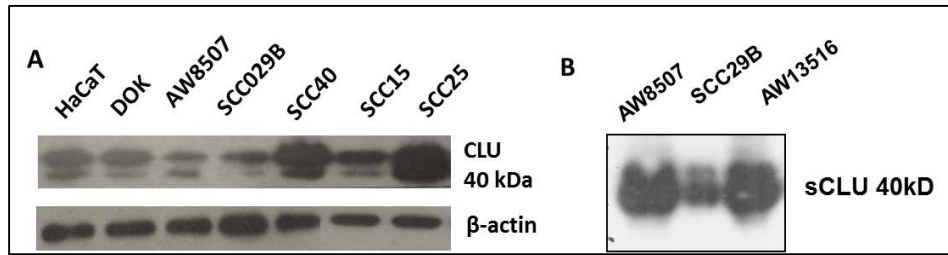


**Figure 19: Expression of sCLU protein in oral cancer cell lines. (A) Expression of sCLU in HaCaT and oral cancer cell lines. (B) Detection of sCLU in culture supernatant of oral cancer cell lines using TCA precipitation.**

### 5.3.3 Assessing the CLU protein stability and possible mechanisms associated with the stability

#### 5.3.3.1 Cycloheximide (CHX) chase assay to determine the CLU protein stability

Though we observed downregulation of sCLU transcripts, all oral cancer cell lines showed the presence of abundant protein expression, suggesting that CLU protein is stabilized in case of oral cancer cells. Hence, to determine the stability of CLU we performed Cycloheximide chase assay in AW8507 tongue cancer cell line. Mcl-1 was used as a control for the assay. As shown in figure 20 A, we observed that CLU levels were unaltered after 24 hr treatment with 100µg/ml CHX, indicating that CLU is stable up to 24 hrs. On the other hand, Mcl-1 levels were diminished by 6 hrs after CHX treatment (Figure 20 B).

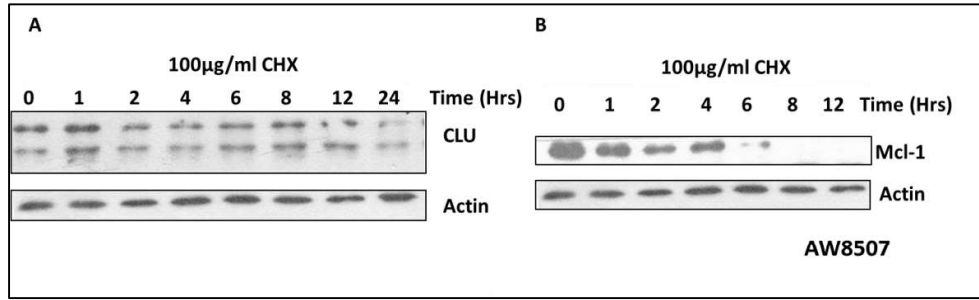


**Figure 20: Cycloheximide chase assay to assess the CLU stability.** (A) CHX chase assay to check the stability of CLU in AW8507 tongue cancer cell line. (B) Mcl-1 which was used as a control for the assay showing diminished levels post 6 hr treatment with CHX.

### 5.3.3.2 Mechanisms of CLU degradation in oral cancer cells

To determine the proteolytic pathway involved in the regulation of CLU, we assessed the effect of inhibition of proteasome and lysosomal degradation pathways on CLU expression in oral cancer cells. We treated oral cancer cells with proteasome inhibitor MG132 (5µM, 24 hr) and lysosome pathway inhibitor chloroquine (50 µM, 16 hr), and its effect on the expression of sCLU was assessed. We observed accumulation of sCLU post-treatment with both MG132 and chloroquine (Figure 21) suggesting the involvement of both these pathways in the degradation of sCLU.

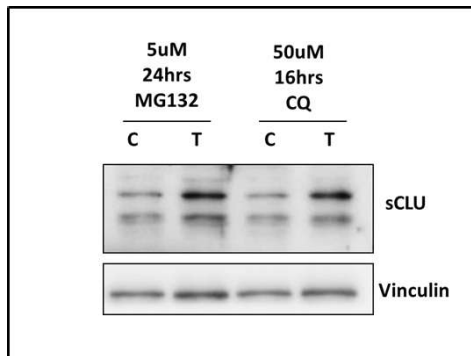


**Figure 21: Effect of inhibition of proteasome and lysosomal degradation pathways on CLU levels.** Treatment of AW8507 cells with MG132 and Chloroquine showed accumulation of sCLU.

### 5.3.3.3 Understanding the role of glycosylation in the stability of CLU in oral cancer cells

CLU is a heavily glycosylated molecule and there are several reports which suggest glycosylation can contribute to the stability of a protein [187–189], hence we wanted to determine the effect of glycosylation inhibitors on CLU expression. Oral cancer cells were treated with N-linked glycosylation inhibitors Tunicamycin and Swainsonine which inhibit glycosylation at different stages. Tunicamycin inhibits the first step of glycosylation by blocking the transfer of N-acetylglucosamine-1-phosphate (GlcNAc-1-P) from UDP-GlcNAc to dolichol. Swainsonine acts at later stages of glycosylation by inhibiting  $\alpha$ -mannosidase II that leads to the accumulation of paucimannose oligosaccharides like Man4GlcNAc2 and Man5GlcNAc2 [190]. Interestingly, post treatment with tunicamycin (5 $\mu$ g/ml for 24 hr), we observed a decrease in sCLU expression levels whereas Swainsonine (2 $\mu$ g/ml for 24 hr) treatment had no effects on CLU expression levels, suggesting that the deglycosylation of CLU (using Tunicamycin) may affect its stability (Figure 22 A). L-PHA lectin was used as a positive control for Tunicamycin (Figure 22 B). Additionally, cells were treated with tunicamycin in combination with MG132, which resulted in the accumulation of CLU (Figure 22 C). These observations suggest the possible role of glycosylation in CLU stability in oral cancer cells.

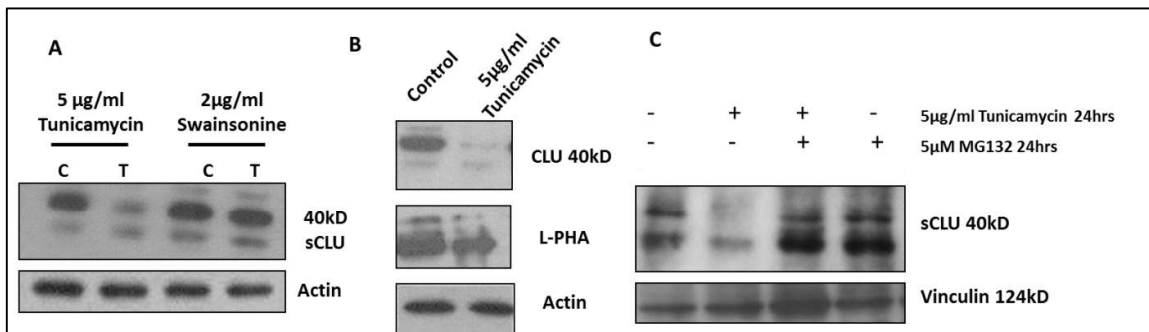
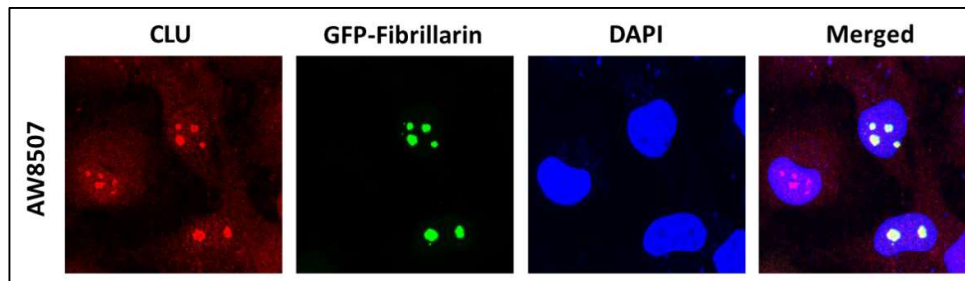


**Figure 22: Effect of N-linked glycosylation inhibitors on CLU expression.** (A) Effect of Tunicamycin and Swainsonine on sCLU expression (C: Control, T: Treated with drug). (B)

*Effect of Tunicamycin on L-PHA lectin (positive control for the assay). (C) Effect of tunicamycin in combination with MG132 on sCLU expression levels.*

#### **5.4 To study the localization of CLU in oral cancer cell lines**

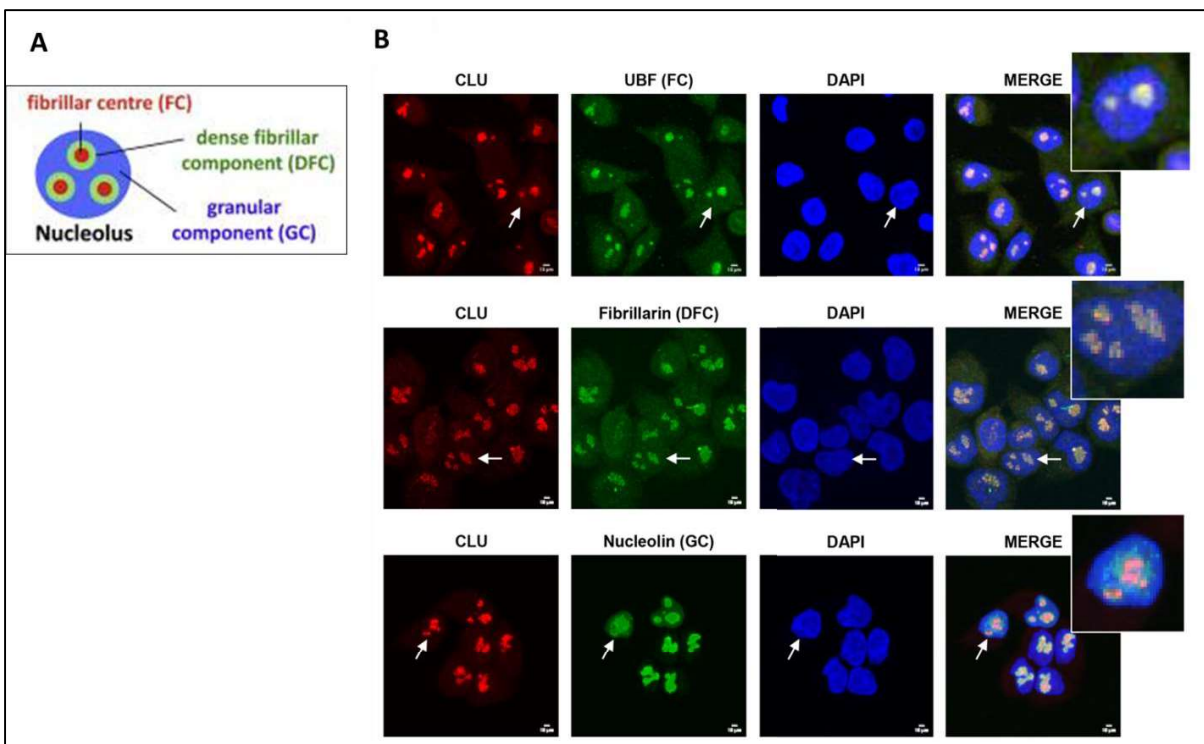
Since we observed predominant expression of a secretory form of CLU in oral cancer cell lines, to determine its intracellular localization we carried out immunofluorescence analysis. To our surprise, we observed CLU be more prominently localized in the nucleolus and also in the cytoplasm and nucleus. To confirm its nucleolar localization we did co-localization studies by overexpressing pEGFP-C1-Fibrillarin construct (Fibrillarin, a DFC region nucleolar marker) in oral cancer cells AW8507, and indeed we observed co-localization of CLU with GFP-Fibrillarin as clearly seen in the merge panel of figure 23.



**Figure 23: Immunofluorescence based localization study of CLU in oral cancer cell line AW8507. Immunofluorescence staining showing co-localization of CLU (red) with pEGFP-C1-Fibrillarin (green) in AW8507 cell line.**

The electron microscopy studies have shown that nucleolus is divided into different sub-compartments which include FC, DFC, and GC regions where different processes of ribosome biosynthesis take place. Figure 24 A shows a schematic representation of different sub-compartments of the nucleolus. We have demonstrated the co-localization of CLU with FC and DFC region markers UBF and Fibrillarin respectively and partial co-localization with GC region marker Nucleolin (Figure 24 B). The above-mentioned localization studies were

carried out using paraformaldehyde (PFA) as a fixative, hence further to ensure that the nucleolar localization of CLU observed is not a fixation artifact, we used methanol which acts as a permeabilizer and fixative both in immunofluorescence study. We observed nucleolar localization of CLU after using methanol instead of paraformaldehyde, although the cytoplasmic staining of CLU is more prominent with methanol fixation compared to PFA (Figure 24 C), this confirms that nucleolar localization of CLU is not a fixation artifact.



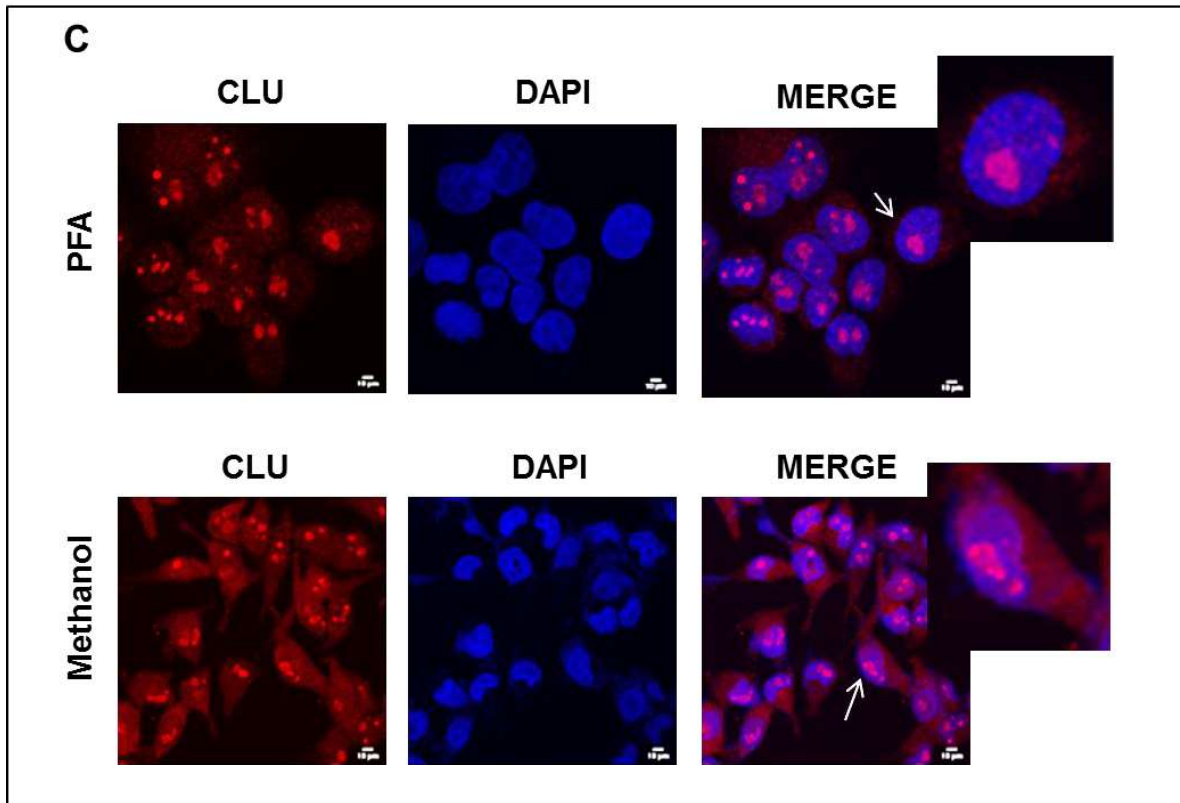


**Figure 24: Co-localization of CLU with different nucleolar markers.** (A) Schematic representation of different components of the nucleolus. (B) Co-localization of CLU with different nucleolar markers UBF (FC), Fibrillarin (DFC), and Nucleolin (GC). (C) Localization of CLU in the nucleolus with different fixation-permeabilization techniques.

Further to ensure the specificity of the CLU antibody (sc-8354 rabbit polyclonal antibody), we performed CLU silencing using CLU siRNA. The downregulation of CLU was confirmed by using western blotting and immunofluorescence. Western blot analysis showed downregulation of CLU protein (40kDa) post-treatment with CLU siRNA (Figure 25 A) and concomitantly loss of nucleolar localized CLU was also seen by immunofluorescence analysis (Figure 25 B). This confirmed the specificity of the CLU antibody used for western blotting and immunofluorescence related experiments reported in this study.

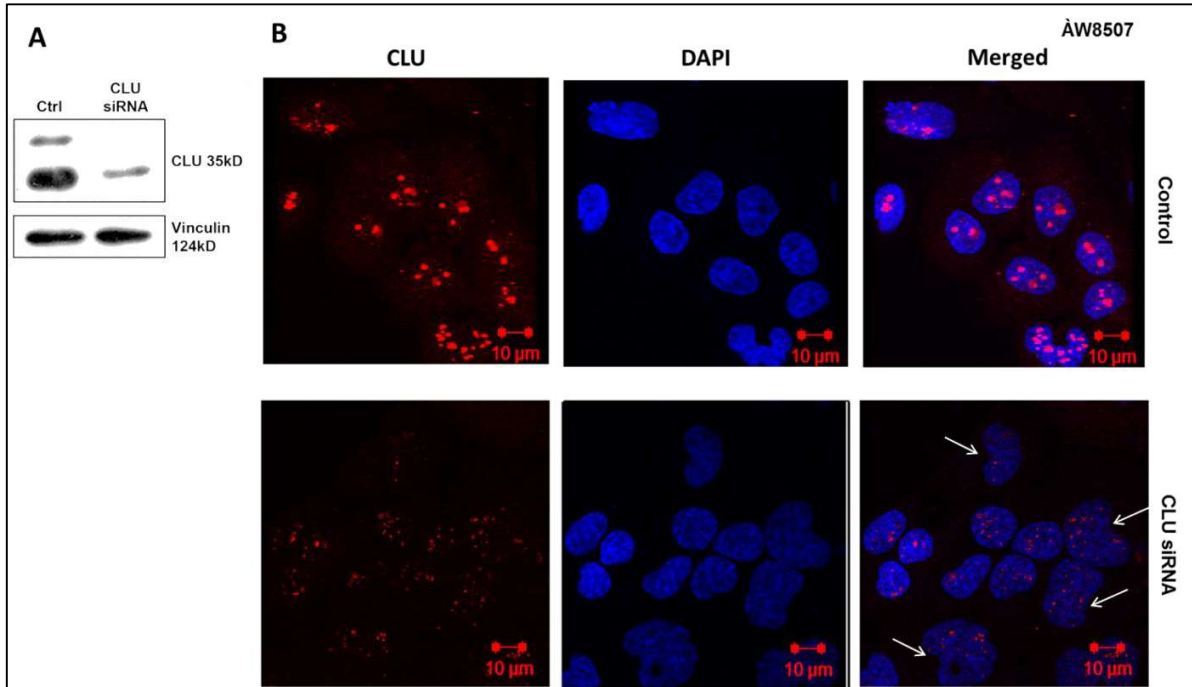


**Figure 25: Confirmation of CLU antibody used for western blotting and immunofluorescence.** *siRNA mediated knockdown of CLU confirmed by (A) western blotting and (B) immunofluorescence using CLU sc-8354 polyclonal antibody (scale bar: 10 μm).*

Additionally, nucleolar fractionation was carried out in AW8507 tongue cancer cell line. Figure 26 A shows a phase contrast microscopic image of isolated nucleoli. Western blot analysis of isolated nucleolar fraction showed the presence of sCLU in the nucleolar fraction along with other nucleolar marker proteins like Fibrillarin and Nucleolin (Figure 26 B). The absence of the cytoplasmic marker Vinculin in the nucleolar fraction confirmed the lack of cross-contamination from other cellular compartments. This study confirmed and highlighted the novel nucleolar localization of sCLU in the nucleolus of oral cancer cells.

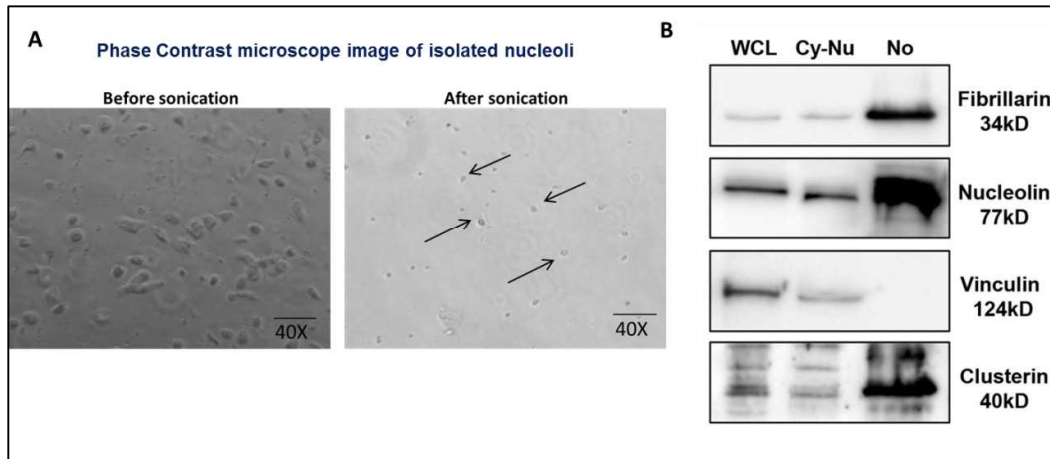


**Figure 26: Nucleolar fractionation studies in AW8507 oral cancer cell line. (A)** Phase contrast image of the isolated nucleoli after sonication. **(B)** Western blotting of isolated nucleolar and cyto-nuclear fractions showing the presence of sCLU (40 kDa) in the nucleolar fraction. Fibrillarin and Nucleolin were used to assess the purity of nucleolar fraction and Vinculin was used as cyto-nuclear fraction control.

## 5.5 Overexpression of GFP tagged CLU construct and its localization study in oral cancer cells

### 5.5.1 Molecular cloning of sCLU coding region (CDS) in pEGFP-N1 construct

In one of the approaches to confirm the nucleolar localization of CLU, we cloned CLU CDS in the pEGFP-N1 construct, where CLU will be at the N-terminus of EGFP. The cloning strategy for sCLU cloned in a mammalian expression construct pEGFP-N1 was simulated and recorded using SnapGene software (GSL Biotech, Chicago, IL, USA) as shown in figure 27 A. The pEGFP-N1-GFP construct was double digested with HindIII and BamHI restriction enzymes followed by gel elution and purification for further downstream cloning of CLU CDS (Figure 27 B). Further, full length CLU CDS (NM\_001831) was amplified using specific primers with flanking restriction sites HindIII and BamHI at the end. The gradient PCR reaction was set up for the amplification of CLU CDS as mentioned in

materials & methods and amplification was carried out at a gradient of 2<sup>0</sup>C at temperatures between 66<sup>0</sup>C to 74<sup>0</sup>C (Figure 27 C). The 1372 bp amplified product of CLU CDS was observed along with one non-specific band of lower size. We selected 68<sup>0</sup>C annealing temperature for further amplification of CLU CDS and the specific band at 1372 bp was gel eluted and purified using a gel extraction purification kit (Figure 27 D). This CLU CDS PCR amplified product was further digested with HindIII and BamHI and gel purified. Both double digested insert and vector were mixed in a 3:1 molar ratio for ligation reaction set up.

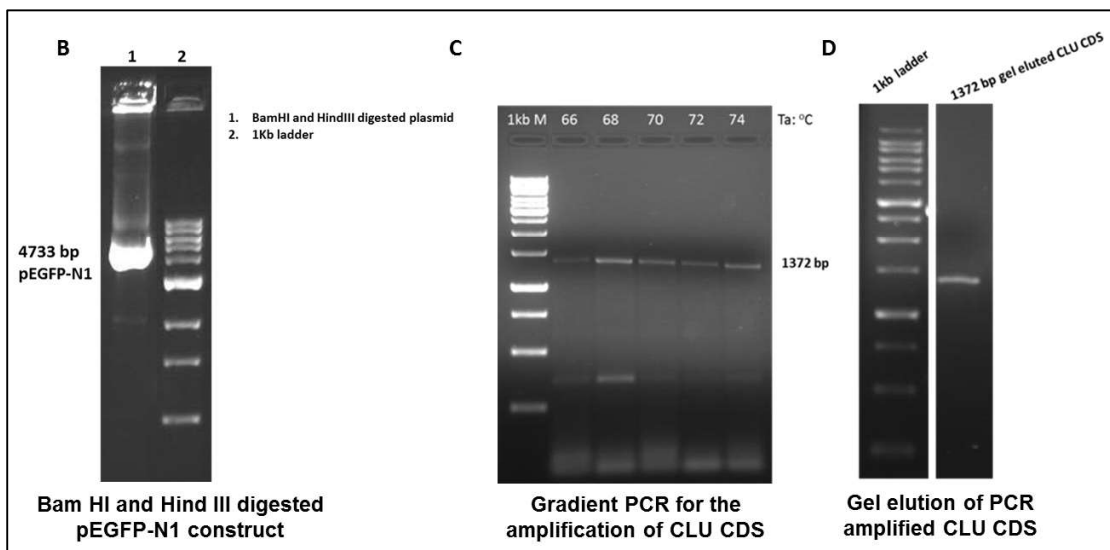
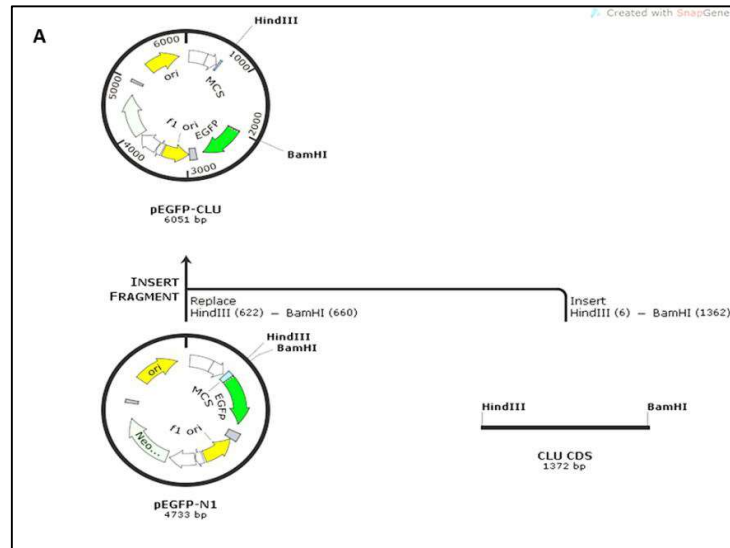


**Figure 27: Molecular cloning of CLU CDS in pEGFP-N1 mammalian expression construct. (A) Strategy for CLU CDS cloning in pEGFP-N1 construct. (B) Double digestion of pEGFP-N1-GFP construct using BamHI and HindIII. (C) Gradient PCR for the amplification of CLU CDS of 1372 bp. (D) Gel eluted PCR amplified product of CLU CDS.**

The ligation reaction mixture was transformed into *E. coli* DH5 $\alpha$  strain and obtained transformant colonies were screened for positive clones. Plasmids from these transformant colonies were extracted using TELT method and screened for positive clone by using a

strategy as explained in figure 28 A. We screened 19 clones for the presence of cloned CLU CDS by digesting their plasmids with BglII restriction enzyme. Since BglII has a single restriction site in the plasmid, the negative clone (without insert) did not give any release, on the other hand, CLU CDS also has one BglII restriction site, as a result of which the positive clone showed a release of 938 bp fragment. Figure 28 B shows that 13 out of 19 plasmids screened were positive. Further, two randomly selected positive clones (clone 1 and 13) were reconfirmed by PCR for the presence of CLU using CLU CDS specific primers (Figure 28 C). Also, some of the plasmids isolated were double digested with BamHI and HindIII to confirm the release of 1372bp CLU CDS (Figure 28 D). The CLU CDS cloned in the pEGFP-N1 construct was referred to as 'pFGFP-N1-sCLU' which was used for further overexpression studies.

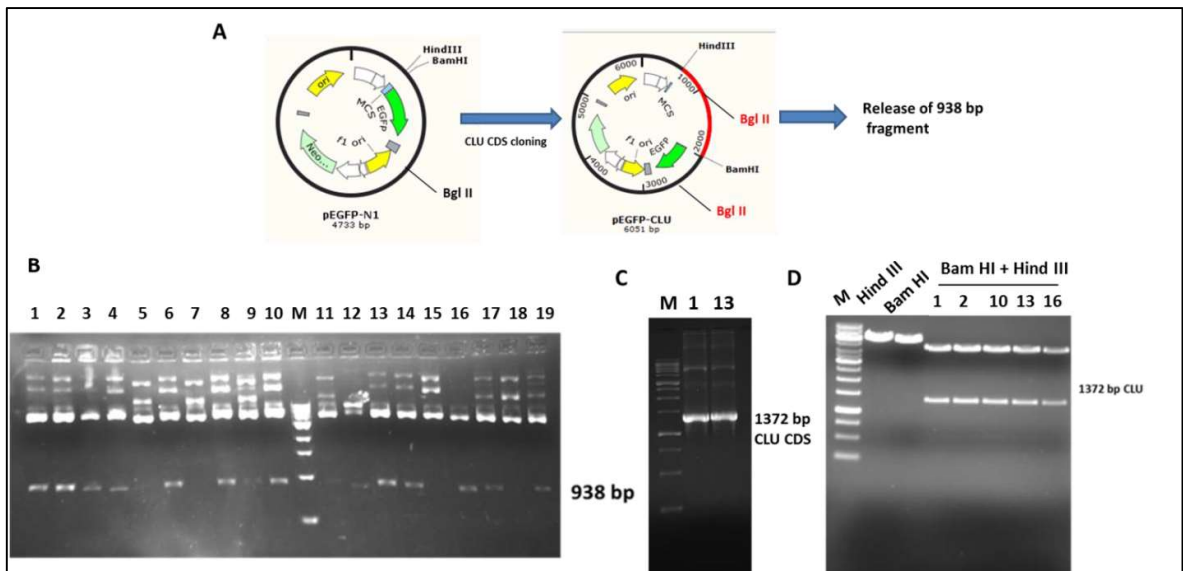


**Figure 28: Screening of positive clones for the presence of CLU CDS. (A)** Screening strategy used for the selection of positive clone (i.e with cloned CLU CDS). **(B)** 13 out of 19 clones screened showed the release of 938 bp fragment. **(C)** PCR amplification of plasmids obtained from clone 1 and 13 using CLU CDS specific primers. **(D)** Confirmation of positive

clones by double digestion with *Bam*HI and *Hind* III. All the plasmids (from clones 1, 2, 10, 13, and 16) double digested with *Bam*HI and *Hind* III showed release of 1372 bp *CLU* CDS.

### 5.5.2 Overexpression of pEGFP-N1-sCLU in oral cancer cell lines

The overexpression of pEGFP-N1-sCLU in AW8507 showed GFP tagged sCLU to be localized in the cytoplasm, nucleus, and also in the nucleolus (Figure 29). However, the nucleolar staining of GFP tagged CLU was not as prominent as seen for the endogenous CLU detected using CLU antibody. The nucleolar presence was confirmed by its co-localization with the nucleolar marker NPM1/B23.

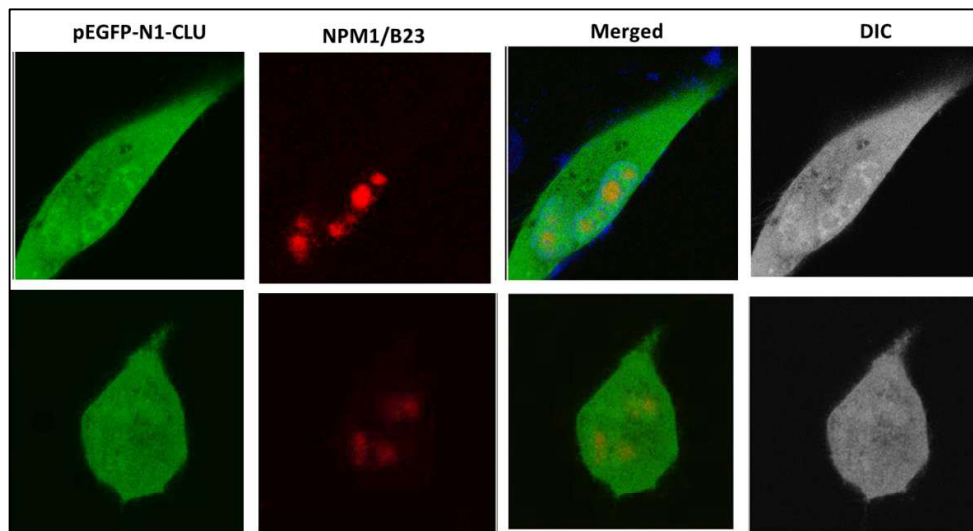


**Figure 29: Overexpression of pEGFP-N1-CLU construct in AW8507 cell line.** Overexpression of pEGFP-N1-CLU construct in AW8507 cell line showing its presence in the cytoplasm, nucleus, and nucleolus (scale bar: 5  $\mu$ m).

### 5.5.3 Overexpression of pFGFP-C1-sCLU in oral cancer cell lines

To rule out the possibility of the hindrance of C-terminally tagged GFP to enter the nucleolus, we overexpressed pEGFP-C1-sCLU (a kind gift from Dr. Kristel Slegers, Belgium) in oral cancer cells where the EGFP tag is at the N-terminus of cloned sCLU. Interestingly, the

overexpression of this construct showed the localization of N-terminally tagged GFP-sCLU in the cytoplasm and endoplasmic reticulum (ER) and golgi body, the components of the secretory pathway where the post-translational modification of sCLU takes place (Figure 30 A). This GFP-tagged CLU present in ER and golgi was also detected using CLU antibody. As shown in figure 30 B, CLU antibody detected GFP-sCLU present in the ER, golgi, and cytoplasm along with the endogenous CLU present in the nucleolus.

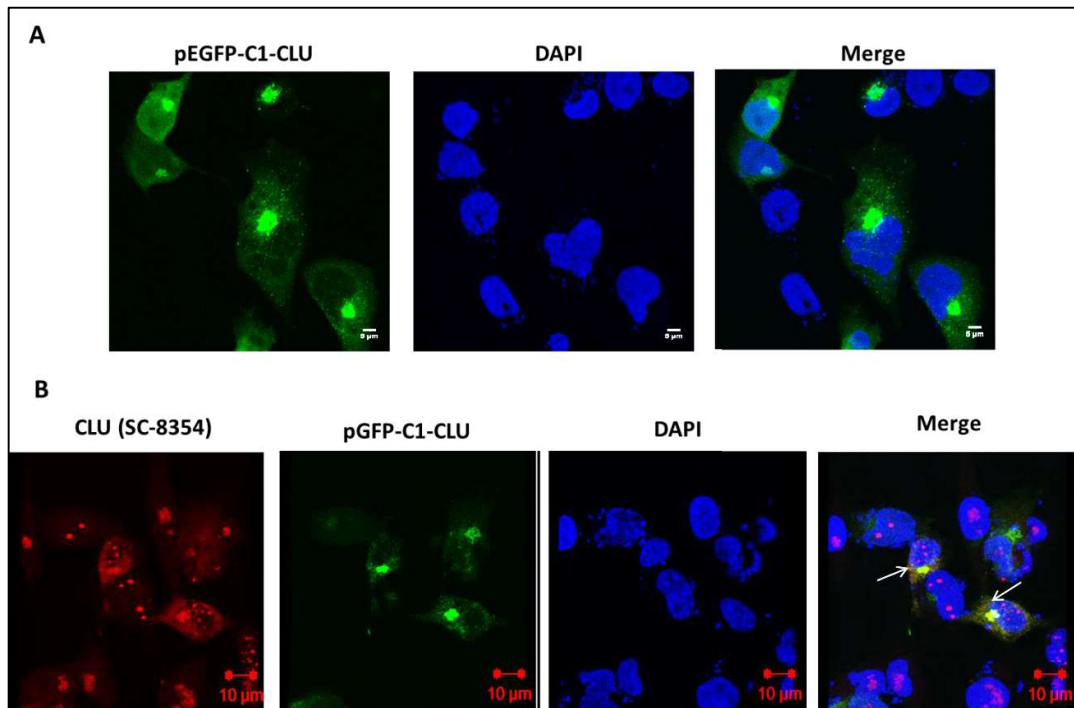


**Figure 30: Overexpression of pFGFP-C1-sCLU in AW8507 cells. (A)** Overexpression of pFGFP-C1-sCLU in AW8507 cells showing localization of CLU in ER and golgi (scale bar: 5 µm). **(B)** Detection of CLU in pFGFP-C1-sCLU transfected AW8507 cells using CLU antibody (sc-8354) showing localization of CLU in ER, golgi, and nucleolus (scale bar: 10 µm).

In summary, both N- and C- terminally GFP tagged CLU did not show its presence in the nucleolus as that was seen for the endogenous CLU in oral cancer cells. There could be two possible explanations for this observation: i) The nuclear localization sequence of CLU is

sterically hindered in GFP tagged sCLU, as a result of which importin- $\beta$  mediated nuclear import is blocked. ii) The endogenous sCLU present in the nucleolus may be tightly bound to RNA or protein, as a result of which there is a poor exchange with overexpressed tagged sCLU.

## **5.6 Identification of nucleolar and nuclear localization sequence of CLU using bioinformatics tools**

Since we observed nucleolar localization of sCLU, we determined the presence of nucleolar localization sequence in CLU protein using bioinformatics tool nucleolar localization sequence detector (NoD). Analysis of the full-length sCLU sequence (residues 1-449) using NoD did not predict the presence of any nucleolar localization sequence (NoLS) as shown in figure 31 A, suggesting that the presence of sCLU in nucleolus may be dependent on nuclear localization sequence (NLS).

Further, to determine the presence of bipartite nuclear localization sequence (NLS) in the sCLU protein structure (NCBI Reference Sequence: NP\_001822.3), sCLU amino acid sequence was analyzed using cNLS Mapper ([http://nlsmapper.iab.keio.ac.jp/cgi-bin/NLS\\_Mapper\\_form.cgi](http://nlsmapper.iab.keio.ac.jp/cgi-bin/NLS_Mapper_form.cgi)), an online bioinformatics tool which predicts importin  $\alpha$ -dependent nuclear localization sequences. It predicted a putative nuclear localization signal, identified by 30 amino acids (KQIKTLIEKTNEERKTLLSNLEEAKKKKED) in the amino acid region 54-83 (Figure 31 B). The NLS score of 5 suggested its localization in both nucleus and cytoplasm.

Additionally, Leskov et al., 2003 have also reported the presence of additional two NLS sequences at the C-terminal region of CLU [85]. The highlighted sequences represent the putative NLS sequences described by Leskov et al., 2003 in figure 31 C. However, there

is no experimental evidence to show whether sCLU localization to nucleus/nucleolus is NLS dependent.

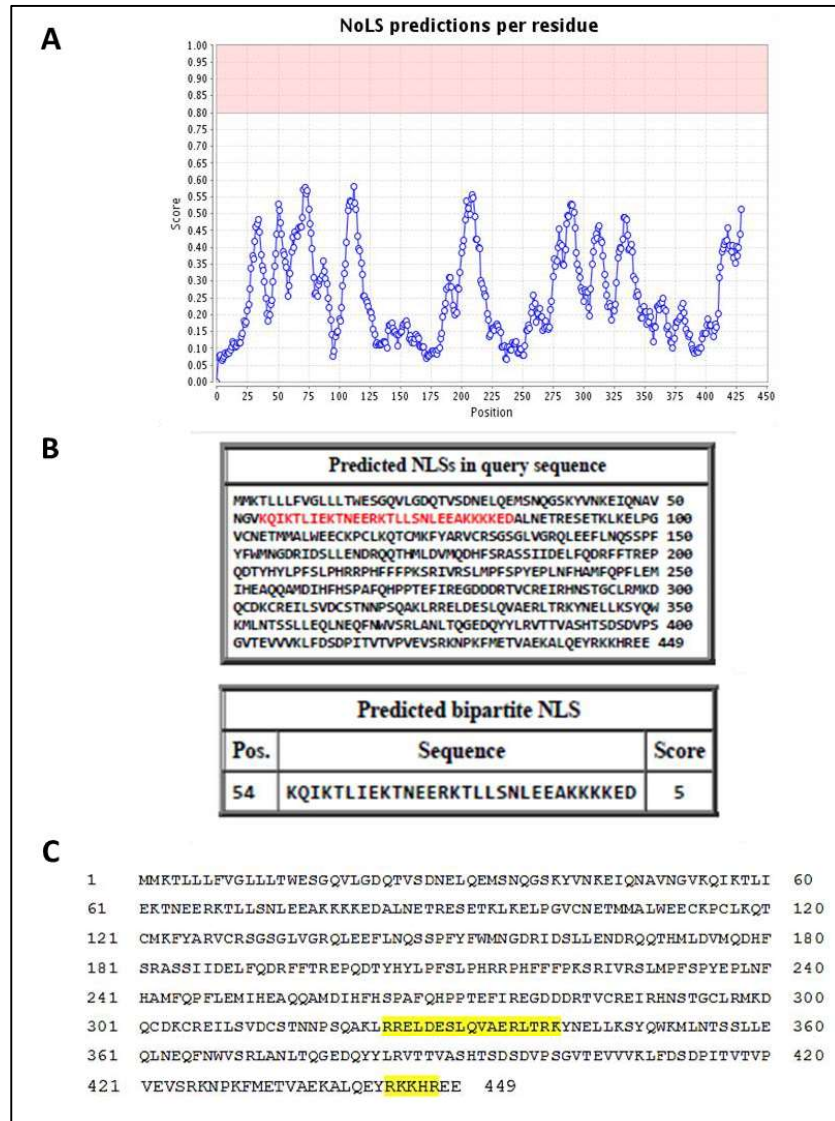


**Figure 31: Identification of Nucleolar and nuclear localization sequence in CLU amino acid sequence. (A) Detection of NoLS in CLU amino acid sequence using an online tool NoD. The pink region in the graph represents the NoLS candidate signal. In the case of CLU, no such NoLS was detected. (B) Prediction of NLS in CLU amino acid sequence using cNLS Mapper showing the presence of bipartite NLS with score 5. (C) NLS sequence predicted by Leskov et al., 2003 showing the presence of two NLSs at the C-terminus of CLU.**

### **5.7 Effect of nuclease treatment on nucleolar localization of CLU**

Since CLU is mainly localized at the FC/DFC interface of nucleolus where 47S pre-rRNA is transcribed from rDNA, and harbors proteins with the ability to interact with DNA and/or RNA. Hence in order to determine whether nucleolar localization of CLU is DNA or RNA dependent, AW8507 oral cancer cells were permeabilized and digested with 10 $\mu$ g/ml of DNase I or 100  $\mu$ g/ml of RNase A and then processed for immunofluorescence based detection. Post DNase-I treatment, we did not observe any change in nucleolar localization of CLU. RNase A treatment resulted in translocation of CLU from the nucleolus to nucleoplasm, whereas Nucleolin, an RNA dependent nucleolar marker used as an assay control disappeared completely post-treatment (Figure 32 A), suggesting that the nucleolar localization of CLU may be RNA dependent. We also investigated for the presence for RNA binding sequences in CLU protein using online RNA web-based servers PPRInt and RNABindR. Both servers commonly identified a continuous stretch of 7-11 amino acid residues at N and C terminal of CLU as potential RNA-interacting residues as indicated by the “+” sign (highlighted in green). The results obtained from RNABindR and PPRInt are highlighted in ‘blue’ and ‘red’ color code respectively (Figure 32 B). Taken together, localization of sCLU to nucleolus may be RNA dependent.

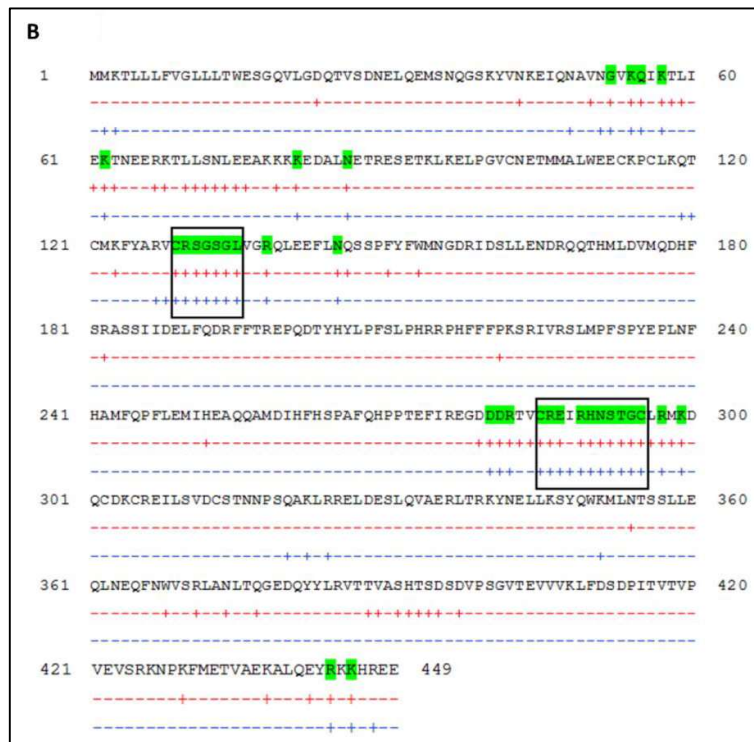
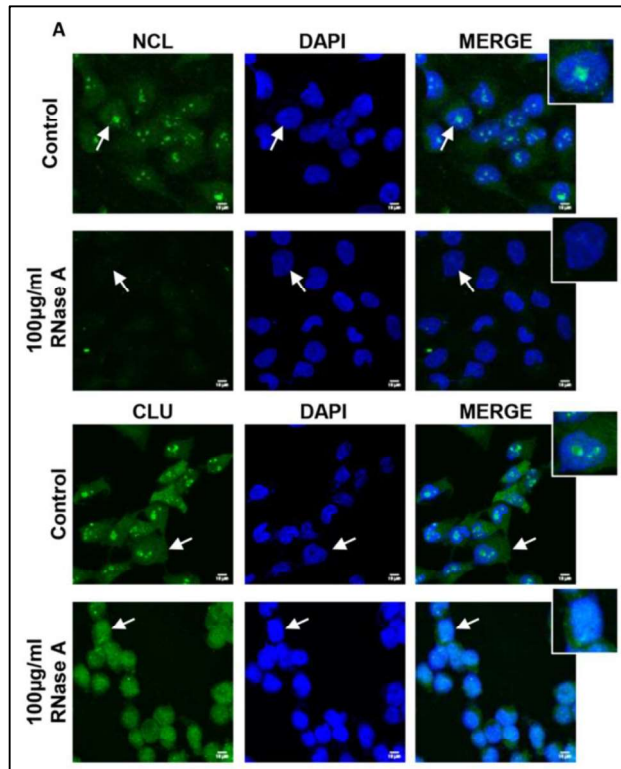


**Figure 32: Effect of RNase A treatment on localization of CLU. (A) Effect of RNase A treatment on nucleolar localization of CLU and Nucleolin (NCL). (B) Analysis of CLU amino**

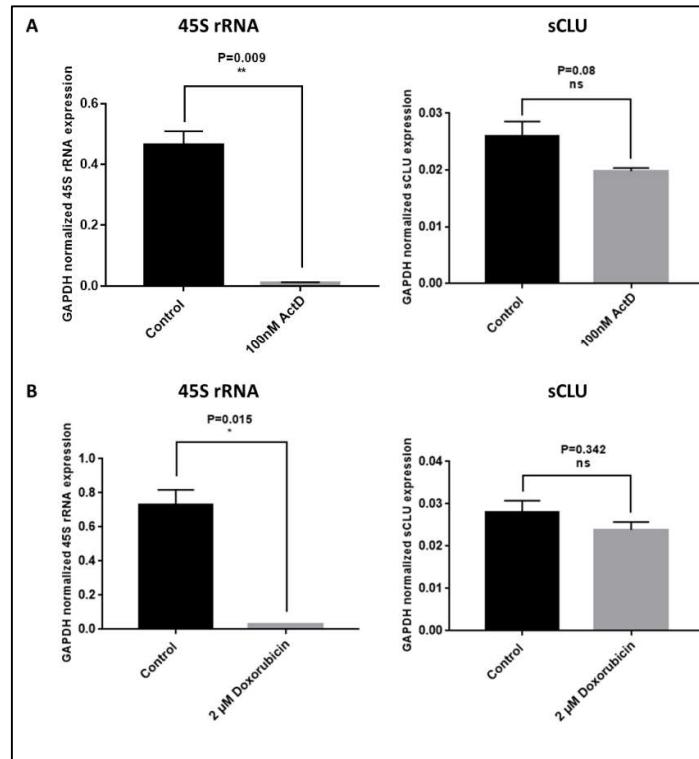
*acid sequence for the presence of RNA binding regions using RNABindR (blue) and PPRInt (red). The sequences highlighted in green are the putative RNA binding regions predicted by both these servers.*

## **5.8 Effect of stress on expression and nucleolar localization of sCLU**

sCLU is a stress-inducible chaperone molecule; hence the effect of different stress stimuli on its expression and localization was studied. The effect of nucleolar and metabolic stress was evaluated in this study.

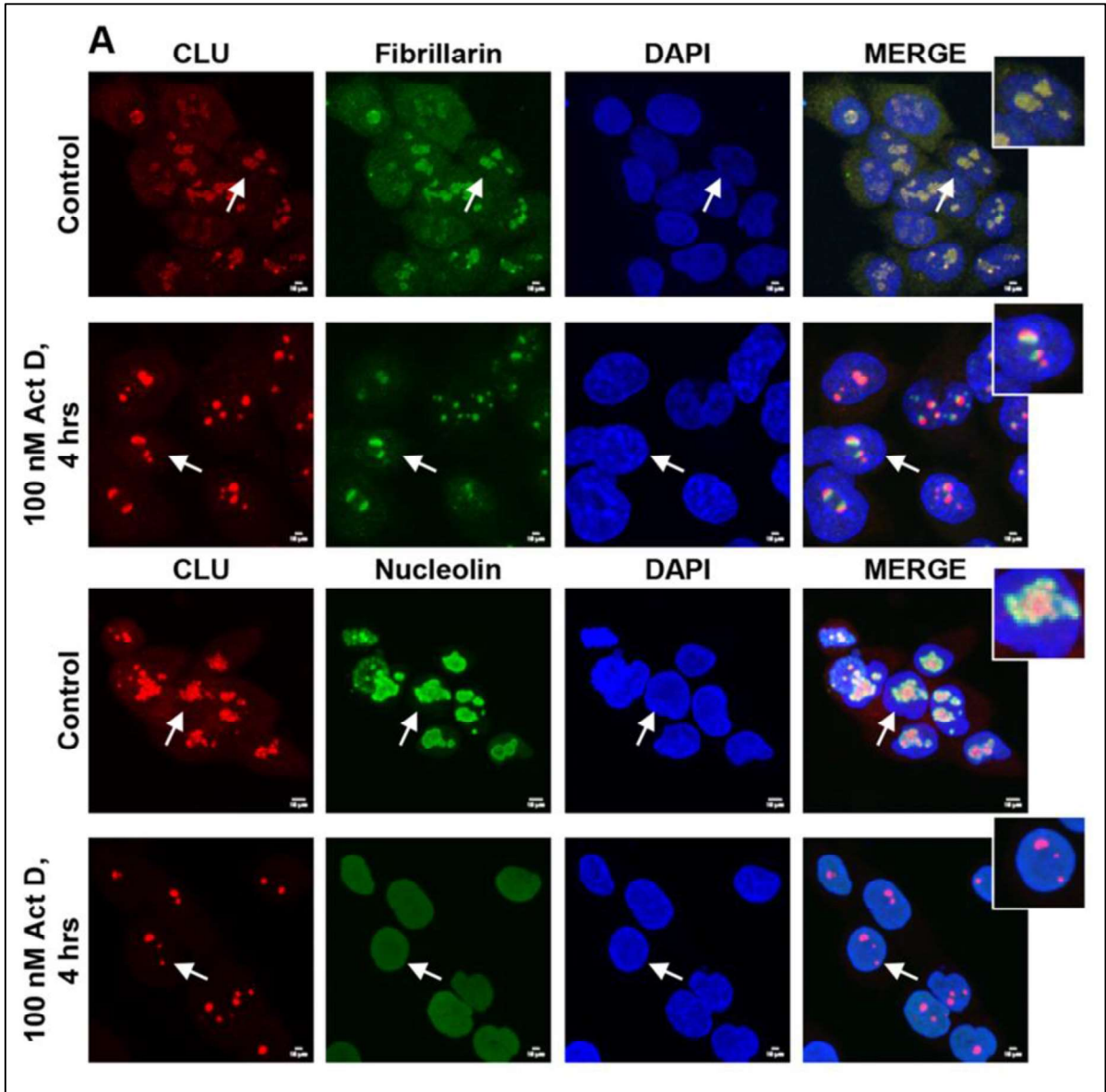
- **Effect of nucleolar stress on CLU expression and localization**

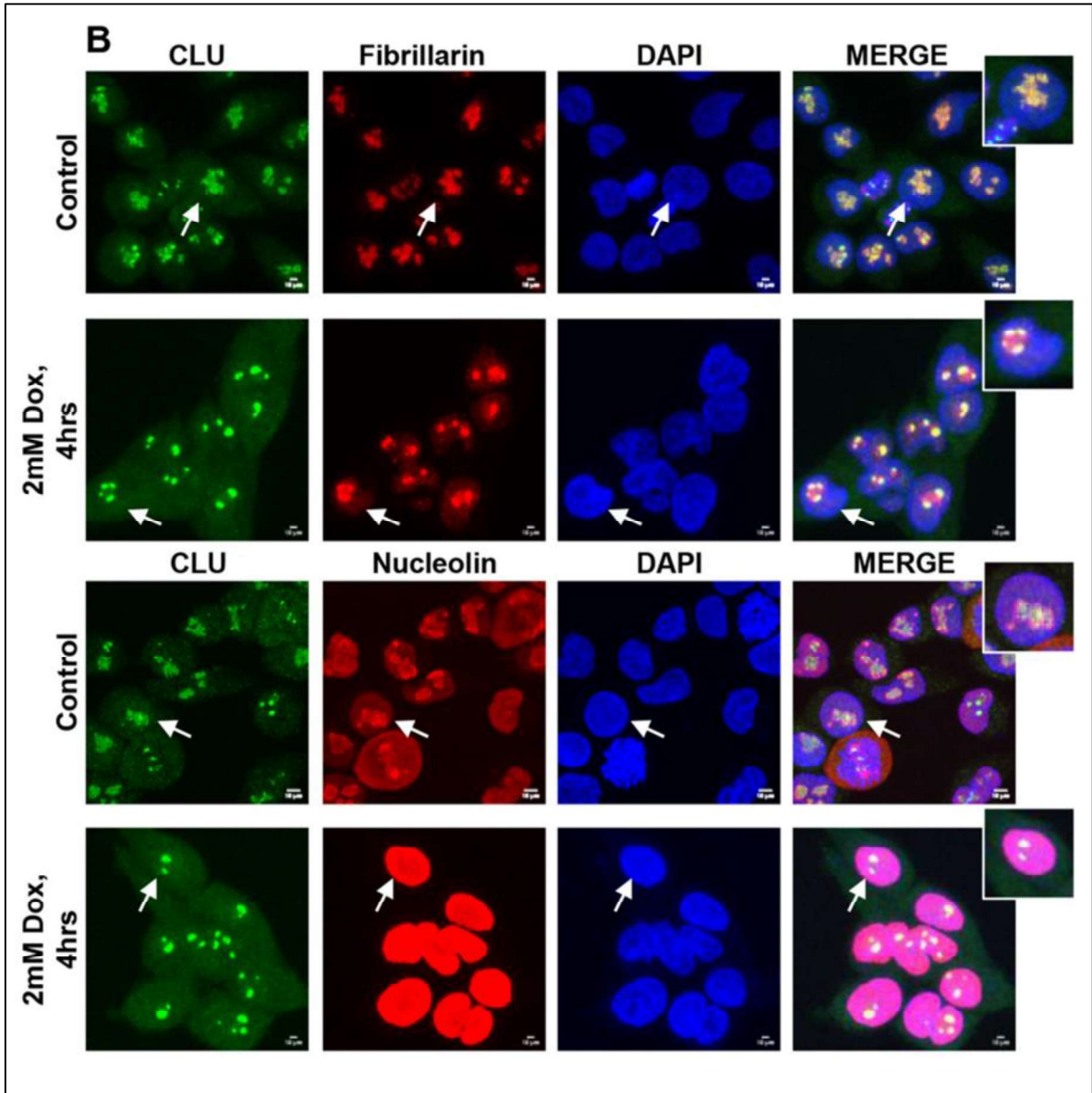
Actinomycin D, an anti-cancer drug inhibits RNA Pol I-dependent rDNA transcription by intercalating in GC-rich DNA sequence of 45S ribosomal gene, thereby inducing nucleolar stress. Similarly, doxorubicin acts as a DNA intercalator and inhibitor of topoisomerase II, thereby inhibiting ribogenesis and inducing nucleolar stress. To assess the effect of different nucleolar stress inducers on CLU expression and localization, AW8507 cells were treated with 100 nM actinomycin D and 2 mM doxorubicin for 4 hr. We observed a decrease in ribogenesis as indicated by the decrease in 45S rRNA transcripts post-treatment with actinomycin D and doxorubicin. However, no significant change in the levels of sCLU transcripts was observed (Figure 33 A and B).



**Figure 33: Effect of ribosome biogenesis inhibitors actinomycin D and doxorubicin on 45S rRNA and sCLU transcripts.** (A and B) Treatment of actinomycin and doxorubicin in AW8507 cells showed decrease in 45S rRNA transcripts but no change in sCLU transcripts was observed.

Immunofluorescence based localization studies showed segregation of CLU with other nucleolar proteins like Fibrillarin at the nucleolar periphery forming bipartite ‘nucleolar caps’ or ‘necklace-like’ pattern post actinomycin D and doxorubicin treatment. Interestingly, GC region marker protein Nucleolin translocated from the nucleolus to nucleoplasm post-treatment with both actinomycin D and doxorubicin (Figure 34 A and B). Additionally to assess the reversibility of actinomycin-D induced nucleolar disassembly, rescue experiment was performed. Cells were treated with 100 nM Actinomycin D for 4 hr followed by incubation in complete media without the drug for further 24 hr. This showed a decrease in the size of nuclei with no reversal of nucleolar segregation (Figure 34 C).





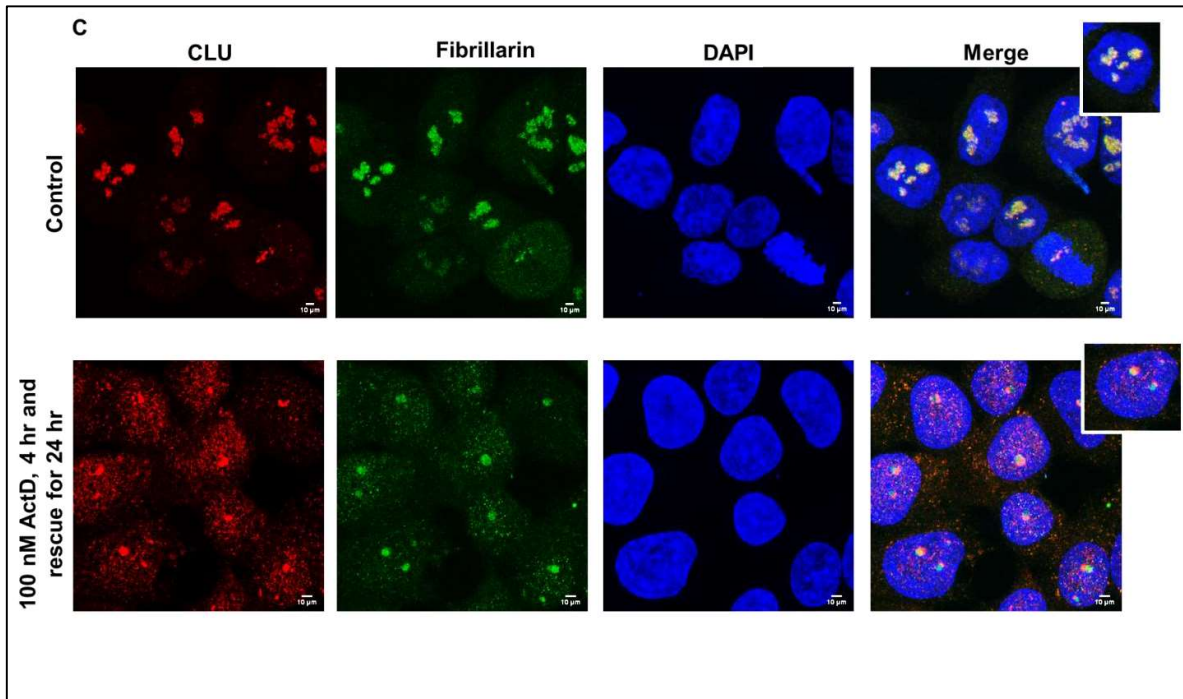


**Figure 34: Effect of Actinomycin D and Doxorubicin on nucleolar localization of CLU.**

*(A and B) Effect of Actinomycin D and Doxorubicin on nucleolar localization of CLU and nucleolar proteins like Fibrillarlin and Nucleolin. (C) Effect of removal of Actinomycin D from culture media (rescue) on localization of CLU and Fibrillarlin.*

Additionally, it is well known that Cajal bodies get recruited at nucleolar caps in response to nucleolar stress conditions [135]. Hence, we also evaluated the effect of nucleolar stress stimuli on Cajal bodies using Coilin as a marker for the Cajal body. Interestingly, we did observe the association of coilin with CLU at the nucleolar caps induced by actinomycin D treatment (Figure 35).

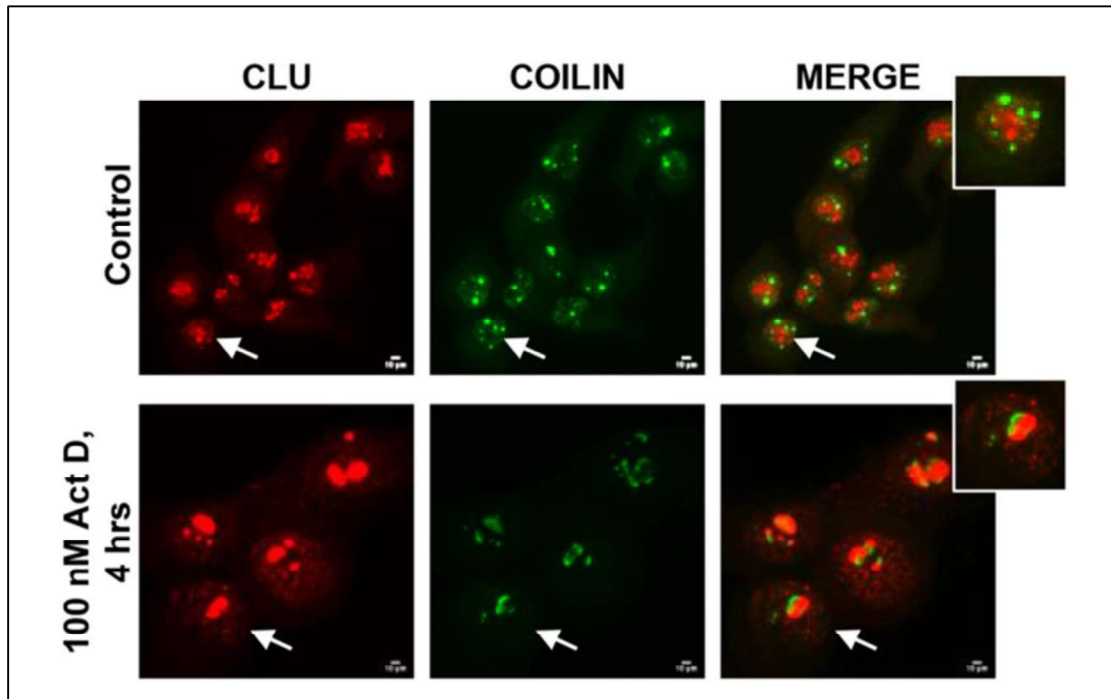


**Figure 35: Effect of Actinomycin D treatment on localization of CLU and Coilin.**

*Association of cajal bodies (Coilin) with CLU at the nucleolar caps formed post treatment with Actinomycin D.*

- **Effect of metabolic stress on CLU expression and localization**

Similar to nucleolar stress, we also evaluated the effect of metabolic stress conditions like radiation and hypoxia. Although sCLU is reported to get induced post radiation in different cancer cell lines, in case of oral cancer cell lines we did not find any alteration in sCLU transcript and protein levels as shown by qRT-PCR and western blotting (Figure 36 A and B). Also, there is no induction or change in the levels of nCLU transcripts post radiation treatment. Immunofluorescence based studies did not show any change in nucleolar localization of CLU or formation of ‘nucleolar caps’.

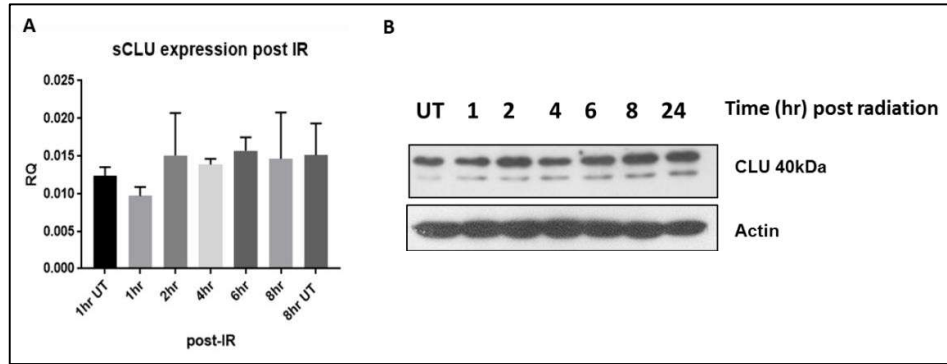


**Figure 36: Effect of radiation on sCLU expression. (A and B)** The effect of radiation on sCLU transcript and protein levels. No change in sCLU transcript and protein expression was seen post radiation treatment.

Further, we also evaluated the effect of hypoxia mediated metabolic stress on CLU expression and localization. In this study,  $\text{COCl}_2$  was used as chemical agent to induce hypoxia. Treatment of oral cancer cells with lower concentration of  $\text{COCl}_2$  (100  $\mu\text{M}$ , 24 hr) showed decrease in sCLU protein levels (Figure 37 A). Immunofluorescence studies showed congregation of CLU at the nucleolar periphery whereas NPM1 did not show any change in the localization (Figure 37 B). This pattern appeared like ‘budding yeast’ which is not typical as that of ‘nucleolar caps’ seen post nucleolar stress induction.

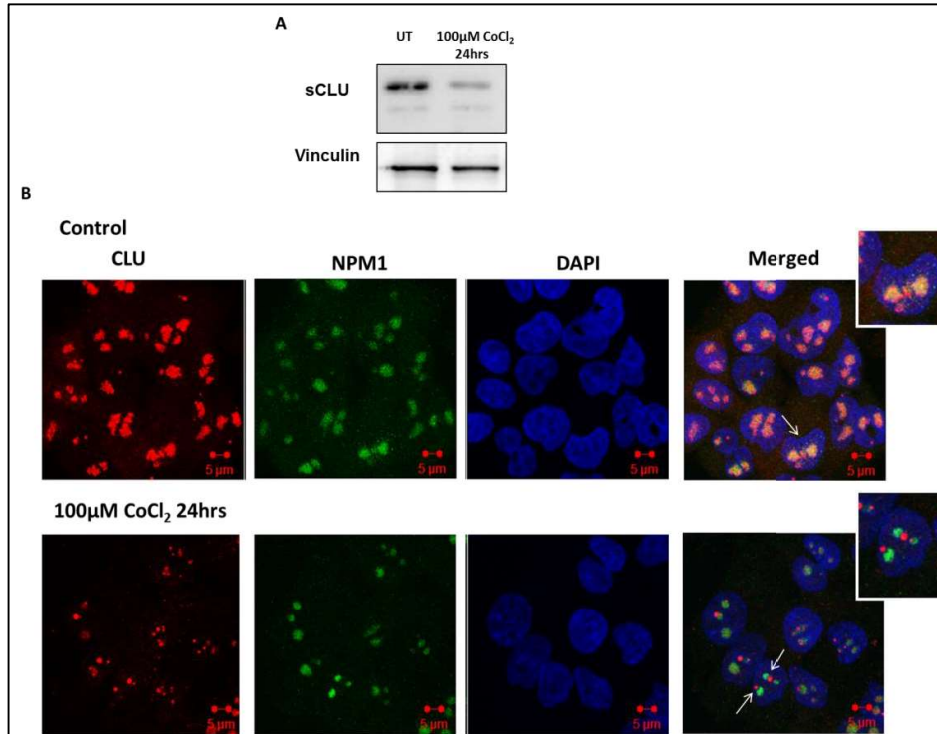


**Figure 37: Effect of hypoxia inducing agent  $COCl_2$  on  $CLU$  expression and localization.**

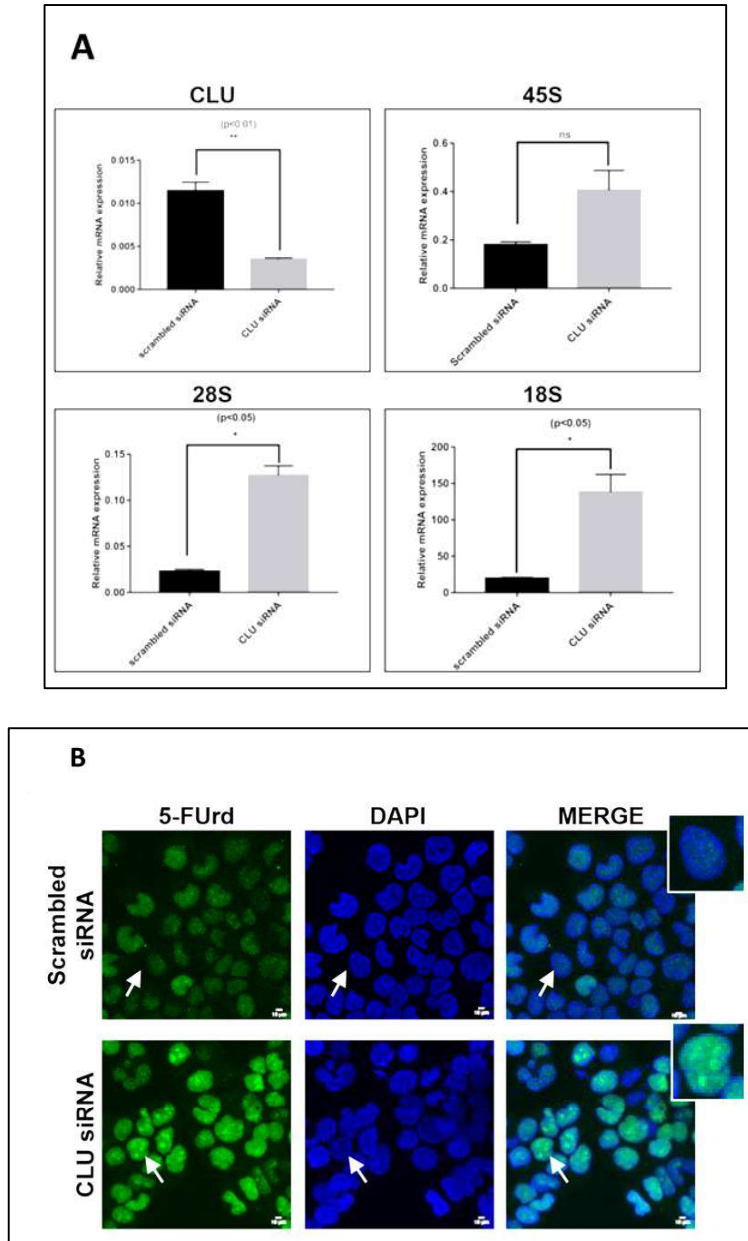
**(A)** Treatment of AW8507 cells with 100  $\mu M$   $COCl_2$  showing decrease in sCLU protein levels by western blotting. **(B)** Treatment of AW8507 cells with 100  $\mu M$   $COCl_2$  showing 'budding yeast' type of nucleolar segregation pattern of  $CLU$  and  $NPM1$ .

## 5.9 Effect of $CLU$ knockdown in oral cancer cell lines

### 5.9.1 Effect of $CLU$ knockdown on ribosome biogenesis

Since we observed  $CLU$  to be localized at the FC/DFC interface of the nucleolus, where rDNA transcription and processing of rRNA take place, we evaluated the effect of  $CLU$  knockdown on ribosome biosynthesis. We checked the transcript levels of rRNAs post knockdown of  $CLU$  using qRT-PCR. We observed an increase in the levels of 45S, 28S, and 18S rRNA transcripts post  $CLU$  knockdown, however, an increase in 45S rRNA was not statistically significant (Figure 38 A). An increase in 28S and 18S rRNAs suggests the possible role of  $CLU$  in rRNA processing. To further confirm this we also performed 5-

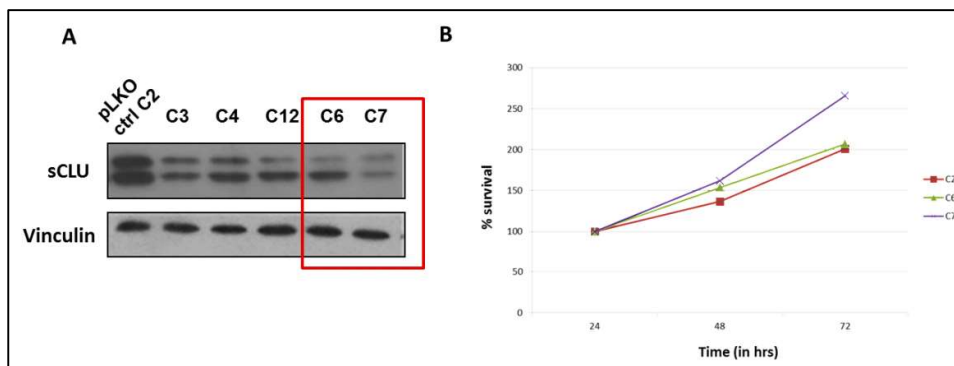
fluorouridine (5-FUrd) incorporation assay. Interestingly, post CLU knockdown we observed a pronounced increase in 5-FUrd uptake as shown in figure 38 B. This suggests the role of CLU in the negative regulation of ribosome biogenesis.



**Figure 38: Effect of CLU knockdown on ribosome biogenesis. (A) qRT-PCR showing effect of CLU knockdown on rRNA transcripts. (B) Effect of CLU knockdown on 5-FUrd incorporation in SCC09 cells.**

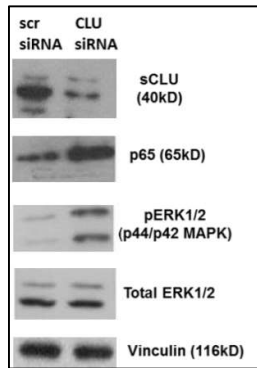
### 5.9.2 Effect of CLU knockdown on proliferation

To understand the effect of CLU knockdown on cell proliferation, we carried out MTT assay in shRNA mediated stable knockdown clones of sCLU. Figure 39 A shows levels of sCLU in different clones with different levels of sCLU knockdown in AW8507 cell line. Clone 6 and 7 showed >50% knockdown of sCLU which were further selected for proliferation experiment. MTT reduction assay showed a significant increase in the proliferation of C6 and C7 knockdown clones as compared to vector control cells (Figure 39 B).



**Figure 39: Effect of CLU knockdown on proliferation in oral cancer cells. (A)** Western blotting showing expression of sCLU in different in shCLU transfected AW8507 oral cancer cell line clones. C6 and C7 clones showed > 50% CLU knockdown. **(B)** MTT proliferation assay showing increased proliferation in CLU knockdown clones C6 and C7 compared to shControl C2 clone.

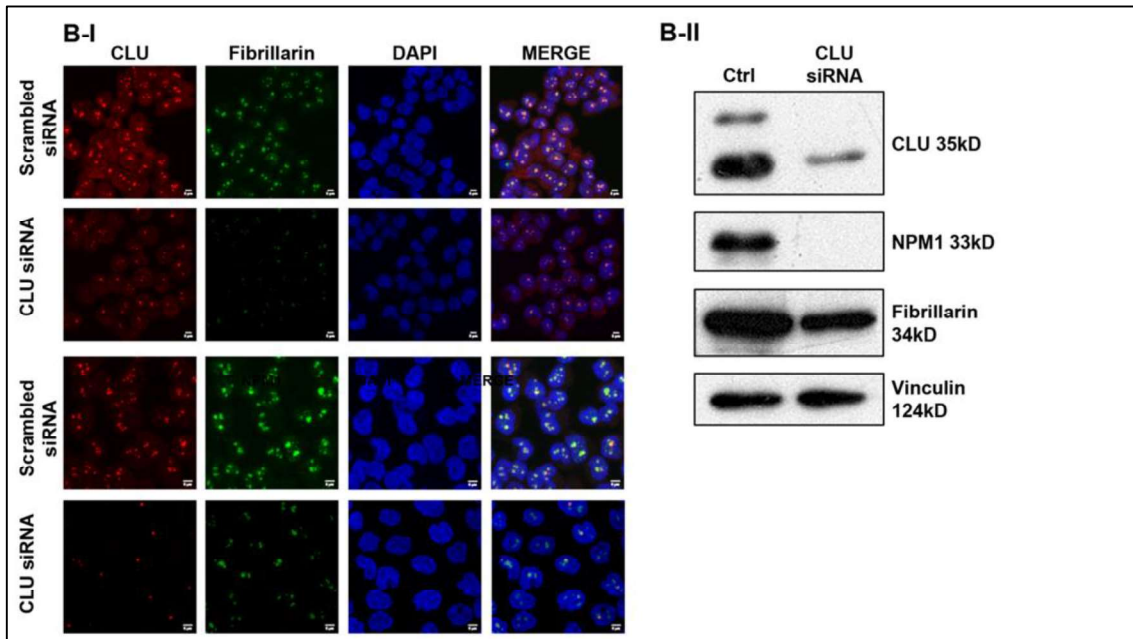
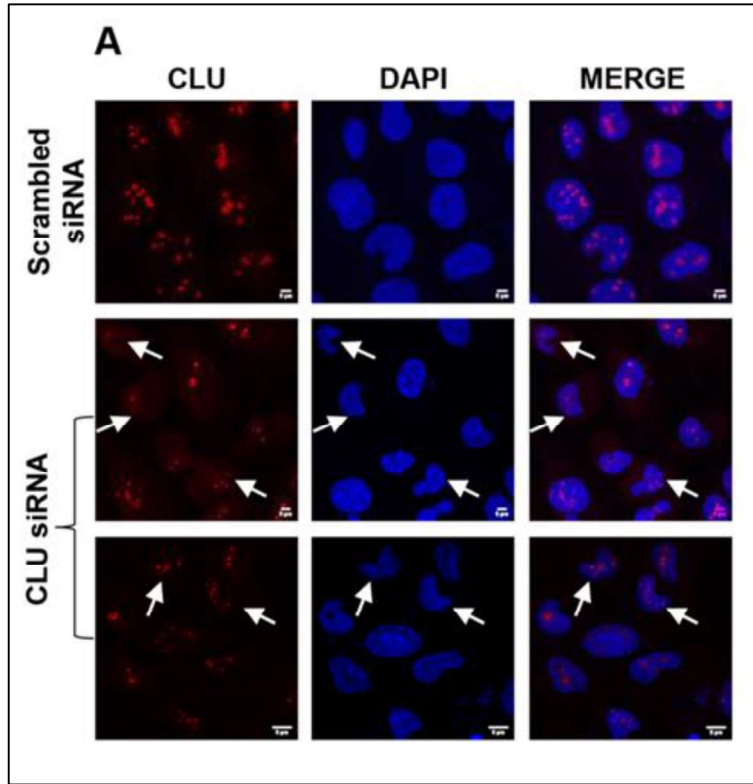
Interestingly, in support of this finding, we observed an increase in NF  $\kappa$ B-p65 and pERK1/2 levels after siRNA mediated CLU knockdown, which are known to regulate proliferation (Figure 40). Taken together, we observed an increase in ribogenesis and proliferation post knockdown of CLU, suggesting its possible tumor suppressor like role in oral cancer cells.



**Figure 40: Effect of CLU knockdown on downstream signaling components.** *siRNA mediated knockdown of CLU in AW8507 cells showing increase in p65 and pERK1/2 levels possibly contributing to increased proliferation seen post CLU knockdown.*

### 5.9.3 Effect of CLU knockdown on nuclear morphology

Immunofluorescence studies showed that knockdown of sCLU resulted in defects in nuclear shapes. Approximately 40-50% of the CLU downregulated cells showed aberrant nuclear shapes like irregular, lobulated, and ruffled (Figure 41 A). Interestingly, post knockdown of CLU, we observed a decrease in nucleolar proteins NPM1 and Fibrillarin levels as shown by western blotting and immunofluorescence (Figure 41 B I and II), which were earlier reported to regulate the nuclear shape [191,192]. Since it has been shown earlier that NPM1 and Fibrillarin regulate nuclear shape by maintaining the cytoskeletal structural proteins like tubulin and actin, we checked the effect of CLU knockdown on cytoskeletal protein tubulin (Figure 41 C). Surprisingly, we observed shrunk tubulin filaments post knockdown of CLU indicating that it regulates nuclear shapes by maintaining the cytoskeletal structure proteins either independently or in association with nucleolar proteins NPM1 and Fibrillarin.



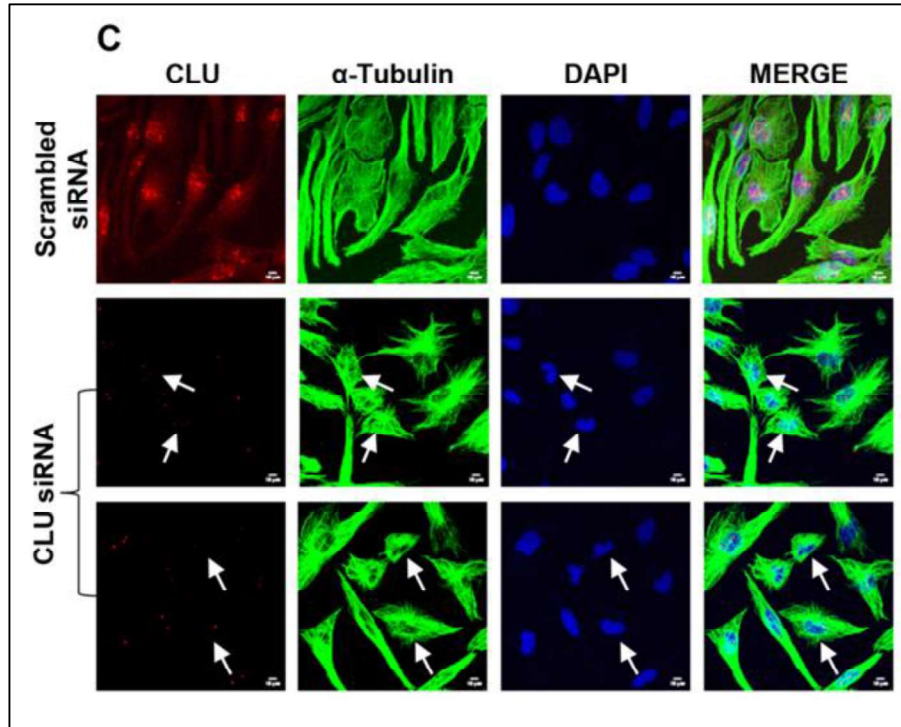


**Figure 41: Effect of CLU knockdown on nuclear morphology and nucleolar proteins in oral cancer cells. (A)** CLU knockdown cells showing aberrant nuclear shapes like irregular and lobulated shown by white arrowheads. **(B I and II)** CLU knockdown cells showing decrease in NPM1 and Fibrillarin levels as shown by immunofluorescence and western blotting. Scale bar: 5  $\mu$ m. **(C)** CLU knockdown cells showing shrunk tubulin filaments. Scale bar: 10  $\mu$ m.

### 5.10 *In silico* approach to predict the structure of CLU and its interaction with nucleolar proteins

Since we observed a decrease in nucleolar proteins NPM1 and Fibrillarin levels post sCLU knockdown, we hypothesized that sCLU may have chaperonic role in the stabilization of these proteins. To explore this possibility, we used an *in silico* approach to understand the possible mode of interaction of CLU with these proteins. There are no crystal or NMR structures of CLU available, probably due to its heavily glycosylated nature. Additionally, sCLU does not have any homologs or similar domain-containing proteins, therefore,

commonly used tools for structure prediction including i-TASSER and Robetta were not able to predict the structure of sCLU. Therefore, the structure of sCLU was predicted using trRosetta server, a *de novo* structure prediction software which utilizes transform-restrained Rosetta was used for structure prediction. The trRosetta server predicted 5 different models of sCLU, which were more or less similar in terms of the secondary fold, but differed in the alignment and direction of the alpha helices (Figure 42). The top scoring model 'A' was selected further for docking studies. The predicted model of sCLU was primarily alpha helical in nature, encompassing nine extended amphipathic  $\alpha$  helices and a single beta sheet of three  $\beta$ - strands at the C-terminal end. The N and C-terminus of sCLU lie close to each other. The ten cysteine residues involved in disulfide bond formation are arranged on alpha helices of beta and alpha chain of CLU and positioned in close proximity to engage in disulfide bond formation.

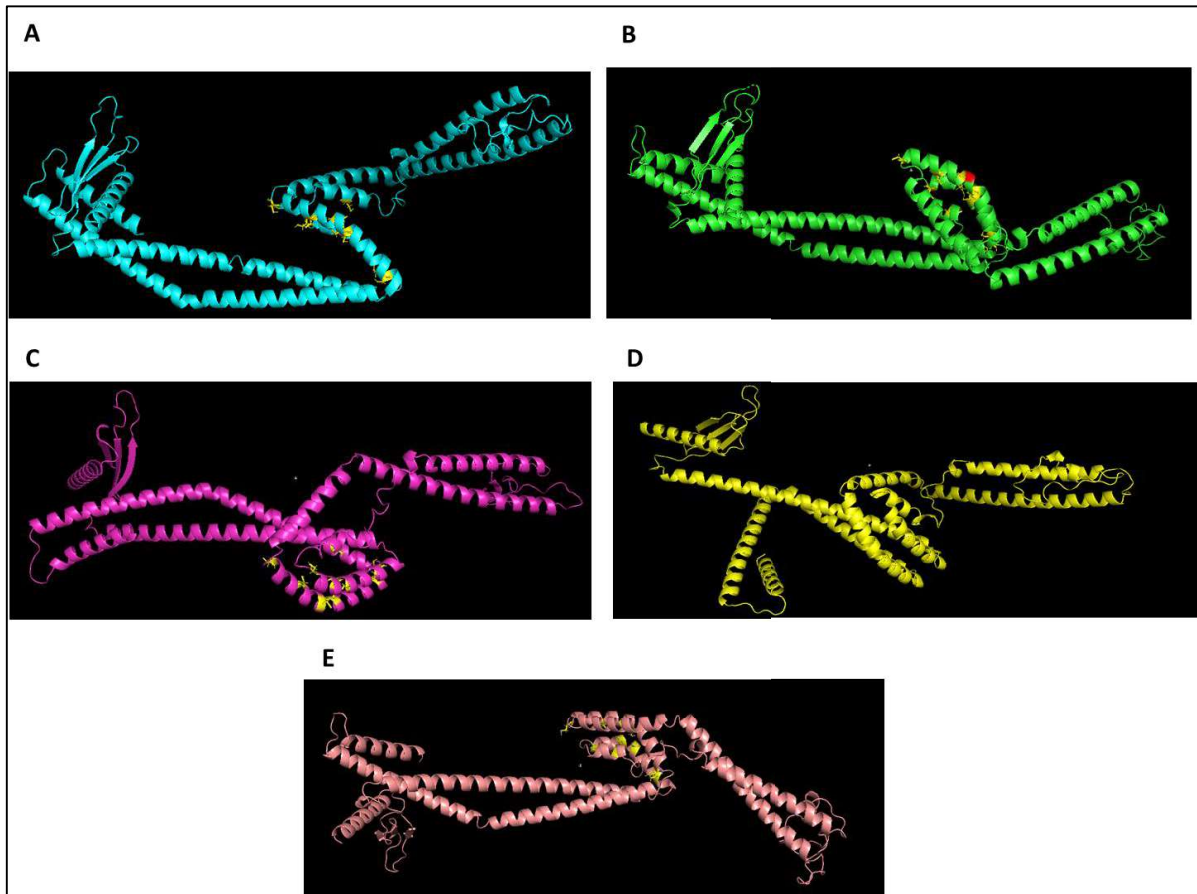


**Figure 42: Predicted structures of sCLU using trRosetta tool. (A to E) Different models of sCLU predicted using trRosetta tool.**

This predicted model of sCLU (model ‘A’) was energy minimized in YASARA server and subjected to blind docking with different nucleolar proteins like UBF, NPM1, Fibrillarin and Nucleolin using Z-DOCK, an online docking server. The top scoring model from the predicted docked structures was used further for analysis. Interestingly, in all the complexes the amino acid residues ranging between positions 140-155 of sCLU were predominantly involved in interaction with these client proteins. To test the sequence conservation in this stretch of residues across different species, we performed multiple sequence alignment of the protein sequences of sCLU using PRALINE tool, which showed

that this stretch of residues involved in interaction is highly conserved across different species (Figure 43).

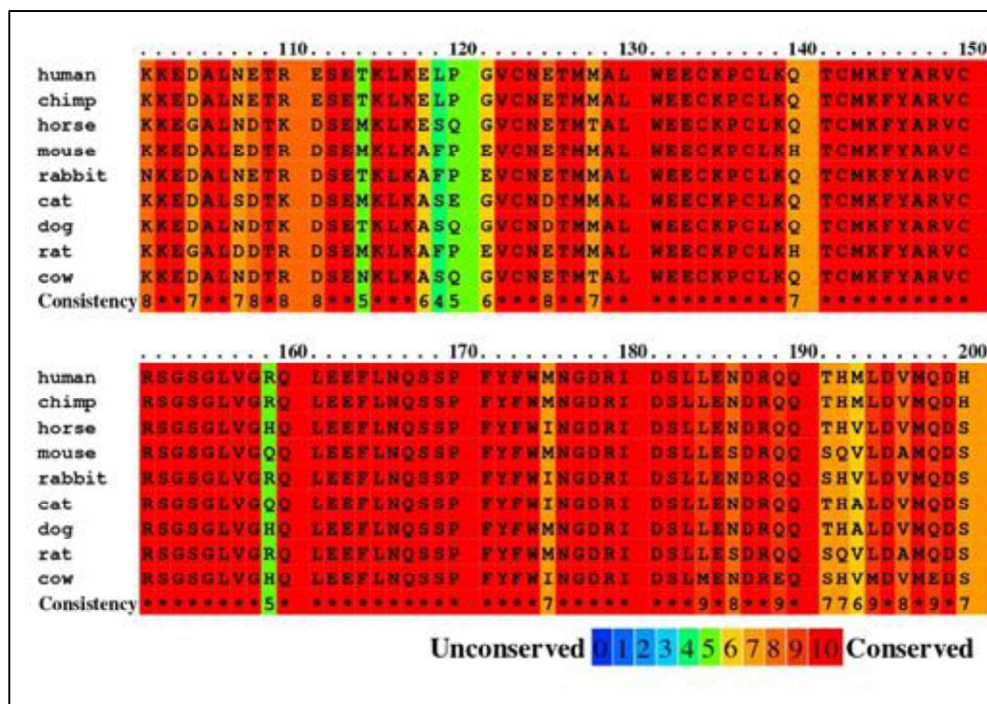


**Figure 43: Sequence alignment of sCLU sequences across different species using PRALINE tool.** The color key at the bottom represents the level of conservation (red: highly conserved, blue: least conserved).

Figure 44 shows cartoon representation of sCLU in complex with different nucleolar proteins NPM1 (A), Fibrillarin (B), UBF (C), and Nucleolin (D). Intriguingly, all the complexes showed the involvement of Phe<sup>152</sup> of sCLU in hydrophobic interaction with interacting partners. The details of different types of interactions observed in these are described below:

**A. sCLU-NPM1 complex:**

In the sCLU-NPM1 complex, the Phe<sup>152</sup> of sCLU is held in a hydrophobic core formed by Met<sup>251</sup> and Leu<sup>261</sup> of NPM1. Additionally, the Tyr<sup>271</sup> of NPM1 also engages in aromatic

interaction with the Phe<sup>152</sup> of sCLU. Interestingly, the Met<sup>251</sup> and Leu<sup>261</sup> of NPM1 are reported to form the hydrophobic core crucial for its interaction with other interacting partners.

**B. sCLU-Fibrillarin complex:**

In the sCLU-Fibrillarin complex, the Phe<sup>152</sup> of sCLU interacts with His<sup>252</sup> of Fibrillarin by cation-pi interaction between the imidazole ring of His<sup>252</sup> and benzyl ring of Phe<sup>152</sup>. Apart from this, other hydrophobic residues like Ala<sup>247</sup> and Leu<sup>248</sup> of Fibrillarin also surround Phe<sup>152</sup> of sCLU, generating a hydrophobic core for interaction.

**C. sCLU-UBF complex:**

In the sCLU-UBF (HMG5) complex, the Phe<sup>152</sup> of sCLU is caged between two Trp<sup>492</sup> and Trp<sup>530</sup> of UBF by strong hydrophobic interactions. In addition, other residues of UBF line and form a hydrophobic pocket which could help in further stabilization of the interaction. The Leu<sup>144</sup> of sCLU is also involved in hydrophobic interaction with Val<sup>496</sup> and Met<sup>515</sup> of UBF

**D. sCLU-Nucleolin complex:**

In the sCLU-RBD domain of Nucleolin interaction, the Phe<sup>150</sup> of sCLU is held in a hydrophobic pocket generated by Trp<sup>452</sup> and Phe<sup>349</sup> of Nucleolin and lies close to Thr<sup>346</sup>. The Phe<sup>152</sup> of sCLU is engaged in hydrophobic interactions with the Leu<sup>400</sup> of Nucleolin.

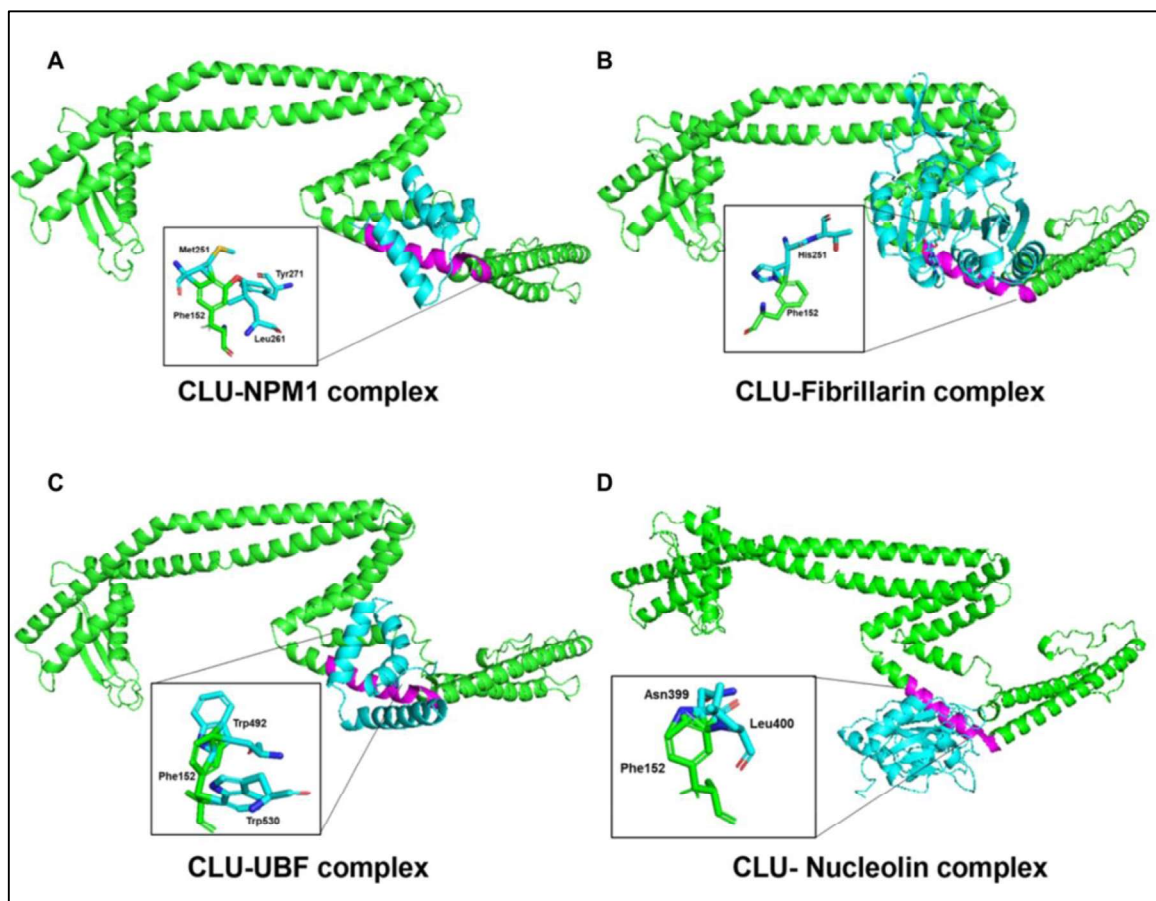


*Figure 44: Docking analysis of CLU with different nucleolar client proteins using Z-DOCK. (A to D) Z-DOCK analysis showing interaction of sCLU in complex with different nucleolar proteins like NPM1, Fibrillarin, UBF, and Nucleolin. Inset designates hydrophobic interaction of Phe<sup>152</sup> of sCLU with different client proteins. The conserved amino acids 140-155 involved in interactions are highlighted in magenta.*

The other potential interactions between sCLU and nucleolar proteins are listed in the table 17 below.

**Table 17: Potential additional interactions between sCLU and nucleolar proteins**

**sCLU -UBF**

sCLU	UBF	Interaction
Asn <sup>155</sup>	Ser <sup>495</sup>	H-bond
Asn <sup>290</sup>	Arg <sup>503</sup>	H-bond
Asn <sup>145</sup>	Asn <sup>521</sup>	H-bond
Ser <sup>148</sup>	Glu <sup>526</sup>	H-bond
Leu <sup>144</sup>	Val <sup>496</sup>	hydrophobic
Leu <sup>144</sup>	Met <sup>529</sup>	hydrophobic

**sCLU -NPM1**

sCLU	NPM1	Interaction
Ser <sup>147</sup>	Cys <sup>275</sup>	H-bond
Asn <sup>145</sup>	Lys <sup>250</sup>	Salt bridge
Thr <sup>272</sup>	Lys <sup>267</sup>	H-bond

**sCLU -Nucleolin**

sCLU	Nucleolin	Interaction
Met <sup>154</sup>	Phe <sup>316</sup>	Methionine-aromatic interaction
Asn <sup>155</sup>	Arg <sup>457</sup>	H-bond

**sCLU -Fibrillarin**

sCLU	Fibrillarin	Interaction
Leu <sup>144</sup>	Phe <sup>253</sup>	hydrophobic
Asn <sup>155</sup>	Glu <sup>289</sup>	H-bond
Thr <sup>272</sup>	Asn <sup>290</sup>	H-bond
Asp <sup>280</sup>	Asn <sup>256</sup>	H-bond

# *Chapter 6*

## *Discussion*

Oral squamous cell carcinoma is one of the highly lethal and prevalent cancers with increased incidences and mortality reported since the last decade. Although the treatment modalities have tremendously improved, the 5-year overall survival rate of oral cancer patients has not significantly changed in the past 20 years [193]. Therefore, understanding the molecular changes and interplay of oncogenes and tumor suppressor genes driving the oral carcinogenesis is essential which will allow a more precise diagnosis and predict the disease prognosis. In one of the earlier studies in the lab to understand the alteration in apoptosis related molecules using ribonuclease protection assay (RPA), we identified TRPM2 or Clusterin (CLU) as one of the downregulated molecules in oral tumor samples and cell lines.

Clusterin is an anti-apoptotic molecule that is overexpressed in most cancers including pancreatic, breast, hepatocellular, and bladder cancers. Its role as an oncogene and underlying signaling pathways driving the carcinogenesis is well studied in these cancers [6]. Contrarily we observed downregulation of CLU transcripts in oral tumor samples and cell lines using RPA which prompted us to further investigate its significance in oral cancers. Since there were no studies that demonstrated the isoform-specific expression of CLU in oral cancers, we first checked the levels of different spliced variants of CLU using isoform specific qRT-PCR. We observed secretory clusterin (sCLU) as the predominant isoform in oral tumor samples. The other variants of CLU including nuclear clusterin ( $\Delta$ Exon2), NR\_038335.1, and NR\_045494.1 were not detectable in oral tumor samples. Interestingly, we observed significant downregulation of sCLU in oral tumors compared to adjacent normal tissues. Since adjacent normal oral tissues may show molecular alterations due to exposure to chewing tobacco carcinogen, a phenomenon termed as ‘field cancerization’ [184,185], we also included normal oral tumor tissue samples obtained from healthy individuals during minor dental surgeries. Compared to healthy normal tissues, downregulation of sCLU transcripts was observed in oral cancer tissues. This observation is in accordance with

Mydlarz et al., 2014 studies in head and neck carcinoma, where they have shown downregulation of sCLU transcripts (referred to as variant-1) in head and neck carcinoma tissue samples which is mediated by upregulation of miR-21 [13]. Although the sample size in this study was very small (n=16), this was the first study to report the isoform specific expression of CLU and its miRNA mediated downregulation in head and neck carcinoma. Further, western blot analysis in oral tumor samples detected the presence of 60kDa pre-secretory form of CLU (psCLU) which is downregulated in the majority of the tumor samples compared to their adjacent normal tissues. Few of the oral tumors which exhibited downregulation of psCLU showed the upregulation of 40 kDa mature form sCLU. Although sCLU is processed from psCLU in ER and golgi via post-translational modifications and proteolytic cleavage, the reason for the disparity in the detection of these two forms in oral tumor samples is unclear. However, we speculate the existence of a stabilized form of sCLU which may be crucial for oral tumorigenesis. Serum proteomic analysis of oral cancer patients using two dimensional electrophoresis and mass spectrometry identified CLU as one of the significantly downregulated proteins supporting our observations in oral tumor samples. Additionally, we performed immunohistochemical studies to study the expression and localization of CLU in oral tumor samples. We observed the presence of CLU in both epithelial and stromal compartments of oral tissues. The stromal compartment is mainly comprised of fibroblast, macrophages, blood vessels, and muscle fibres. CLU staining intensity and percentage positivity were scored independently for both of these compartments. It is now well established that the tumor microenvironment plays an important role in both tumor initiation and progression [194,195].

There are few reports in the context of stromal expression of CLU where higher stromal expression of CLU has been shown to be associated with poor overall and recurrence-free survival of the patients with prostate, esophageal, and triple negative breast

cancers [196–198]. Hence, in this study, we examined the expression of CLU in both of these compartments to understand its functional significance and prognostic role if any. We observed a decrease in intensity and percent positivity of CLU in both tumor epithelium and stromal compartments of oral tumor samples compared to their adjacent normal tissues, which supports our findings from real time PCR and western blotting. Nuclear staining was not observed in any of the tissue samples. However, we did not find any association of CLU expression with clinicopathological parameters like sex, tumor stage, nodal involvement, and differentiation status. Further, univariate analysis showed that low expression of CLU in tumor epithelium is associated with poor overall and recurrence free survival. Contrarily, high expression of CLU in the stromal compartment was shown to be associated poor overall and recurrence-free survival. The differences in the survival outcome of the patients based on CLU expression in epithelium and stromal compartments prompted us to further divide the sample cohort into four subgroups based on their median expression (i.e. percent positive cells) in both of these compartments as follow: 1. Low epithelial, low stroma. 2. High epithelial, low stroma. 3. Low epithelial, high stroma. 4. High epithelial, high stroma. Surprisingly, the low epithelial and high stromal expression subgroup showed highly significant poor overall and recurrence free survival followed by low epithelial and low stroma subgroup. The subgroup with high expression of CLU in both stromal and epithelial compartments showed relatively better survival. These observations indicate that the CLU expression in the oral epithelium of tumor samples impacts the fate of the oral cancer cells and the outcome of the disease progression. In line with our findings, a study in prostate cancer cells exhibiting low expression of CLU in the epithelium and high in the stroma were similarly associated with poor disease-free survival [196]. Further, to understand whether differences in CLU expression in these two compartments are due to differences in isoform expression, laser microdissected samples were used, which showed differential expression of

CLU gene in tumor epithelium and stroma which is being highly expressed in the stromal compartment [199]. Another study in triple negative breast cancer showed that higher stromal expression was associated with poor responsiveness to neo-adjuvant chemotherapy, highlighting the significance of stromal CLU expression for predicting the treatment outcome [198]. Under normal physiological conditions, tumor-associated stroma acts as a barrier to preclude the malignant transformation, but during the tumor initiation and progression, the associated stroma may respond to the molecular signals from tumor cells and modulate the extracellular matrix to promote tumor progression and metastasis. Based on our current findings from this study, we hypothesize that under normal physiological conditions the high levels of CLU in both the compartments mediate the cross-talk between stroma and epithelial compartment that maintains the tissue equilibrium and integrity. On the other hand, post malignant transformation, due to loss of CLU in epithelial compartment, there is a loss of epithelial-stromal signaling as a result of which the expression of tumor inducing factors secreted by associated stroma increases. Contrarily, a recent study in oral cancers has reported the upregulation of CLU in a grade wise manner. Such type of discrepancy has also been reported earlier in the case of colorectal and prostate carcinomas, where use of different antibodies for the detection of CLU, the variation in the IHC protocols such as antigen retrieval and detection, and lack of clarity on the isoform being detected resulted in such ambiguous results.

Since the role of CLU as an oncogene is well established, different mechanisms and signaling pathways responsible for CLU upregulation are well studied in the literature. However, the mechanisms for CLU downregulation and its impact on downstream signaling are not well studied till date. Hence, to explore the possible mechanisms of CLU downregulation in oral cancer, we studied different mechanisms like methylation of CLU promoter, loss of heterozygosity at chromosome 8p locus, and miRNA mediated translational

repression. Methylation and deacetylation of CLU gene promoter have been shown to be responsible for CLU downregulation seen in human neuroblastoma and prostate cancer cell lines [102,103]. In this study, methylation specific PCR analysis did not show any difference in the methylation pattern of tumors and healthy control tissue samples, rather both methylated and unmethylated forms were detected suggesting that there could be a mixed cell population with some being methylated while others are not or another possibility is the presence of both methylated and unmethylated alleles attributed to heterogeneity in tumor samples. However, the sample size used for this study is very less, hence the role of methylation in CLU silencing remains obscure. Studies carried out in colorectal carcinomas have shown that LOH at chromosome 8p locus contributes to downregulation of CLU [86]. Since LOH at chromosome 8p locus in advanced stages of oral cancers has been known [200], we examined LOH in the region spanned by CLU at chromosome 8p using mass spectrometry based MassEXTEND assay. However, all the SNPs (both germline and somatic) screened showed the presence of homozygous allele in adjacent normal tissues, as a result of which the output was 'non-informative', which was later confirmed using sequencing. The major drawback of this assay was less sample size, hence this needs to be performed in a larger cohort to understand its role if any. Further, to understand the role of miRNA in CLU silencing, the miRNAs predicted to target the CLU mRNA were identified using miRNA prediction tools and expression profiling was carried out. In the context of CLU downregulation, the role of miR-21 and miR-17-92 cluster was established in head and neck cancers and neuroblastoma respectively [13,96]. In the case of neuroblastoma, N-myc overexpression leads to activation of miR-17-92 clusters which in turn leads to downregulation of CLU. However, miR-17-92 has been shown not to bind directly to the CLU 3'-UTR, suggesting that it may repress the potential activators of CLU gene expression. In our study, we observed upregulation of miR-21 and miR-15a, suggesting their possible

role in CLU regulation. This needs to be performed in a larger sample size and warrants further studies like luciferase assay and miRNA overexpression studies to identify the binding site of miRNA in CLU 3'-UTR region and confirm the downregulation of CLU. In summary, we observed low levels of sCLU transcripts and protein in oral tumors compared to their adjacent normal; however, the exact mechanism involved in its downregulation is unclear.

Oral cancer cell lines also showed the presence of sCLU as the predominant isoform, which was downregulated in oral cancer cell lines compared to HaCaT, an immortalized skin keratinocyte used as a control in this study and healthy control tissue samples. nCLU transcript levels were very low. A study by Prochnow et al., 2013 also showed the presence of sCLU as the predominant isoform in cancer and non-cancer cell lines. Interestingly, they observed induction of nCLU post proteotoxic stress induced by heat shock, serum deprivation, and proteasomal degradation inhibitor [9]. At the protein level, all oral cancer cell lines showed the presence of 40 kDa mature form of sCLU, however, we did not find downregulation of sCLU protein compared to control cell line HaCaT, despite the downregulation of sCLU transcripts. This suggests that CLU may be stabilized in oral cancer cells. We observed degradation of CLU via both proteasomal and lysosomal degradation pathways as mentioned in earlier reports [186,201]. Since sCLU is a heavily glycosylated molecule, we determined the effect of glycosylation inhibitors on CLU expression. Surprisingly, after Tunicamycin treatment which is a N-linked glycosylation inhibitor we observed a decrease in levels of sCLU, indicating the possible role of glycosylation in imparting stability to sCLU. A similar study carried out by Jin et al., 2017 showed that glycosylation affected the stability of desmosomal proteins Desmogleins (Dsg) 1 and 3. They observed a decrease in levels of Dsg 1 and 3 resulting in their disassembly and loss of cell-cell adhesion [189]. It is speculated that deglycosylation of proteins by tunicamycin may

result in misfolded proteins thus decreasing protein stability. Hence, N-glycans may have a crucial role in maintaining the CLU protein stability.

Since we observed the presence of a secretory form of CLU in all oral cancer cell lines, in order to assess the localization pattern, immunofluorescence studies were carried out. To our surprise, CLU was prominently localized in the nucleolus along with the cytoplasm and nucleus. Since we did not find the presence of nCLU isoform in oral cancer cells, its presence in the nucleolus was a novel observation. Since there were no reports on the nucleolar localization of CLU in any cancer or non-cancer cells; it was essential to ratify this finding with multiple approaches with suitable controls. The co-localization studies with different nucleolar marker proteins representing different sub-regions of nucleoli confirmed its nucleolar localization. As fixation methods and the antibody used for immunofluorescence based detection can result in an artifact or variation in the staining pattern [202–204], we confirmed its nucleolar localization with PFA and methanol both. Subsequently, the possibility of non-specific staining by CLU antibody was ruled out by CLU knockdown studies, which showed a decrease in CLU by both western blotting and immunofluorescence. Nucleolar fractionation studies indisputably confirmed the nucleolar presence of sCLU in oral cancer cells. We also attempted to study the localization of GFP-tagged CLU in these cells. Interestingly, overexpression studies using pEGFP-N1-CLU showed localization of CLU in cytoplasm, nucleus, and nucleolus, although the nucleolar localization was not the same as that observed for endogenous CLU. On the other hand, overexpression of pEGFP-C1-CLU showed localization of CLU mainly in the secretory pathway components ER and golgi. We confirmed this presence in ER and golgi using CLU antibody, which showed CLU staining in the nucleolus along with ER and golgi. These findings from overexpression studies using N- or C- terminally GFP tagged CLU suggest that GFP-tagged CLU may be unable to enter the nucleolus due to the following possibilities: 1) The bulky nature of GFP

tagged CLU does not allow its entry into the nucleolus. 2) The nuclear localization sequence (NLS) is sterically hindered in GFP-tagged CLU as a result of which it is inaccessible to importin- $\beta$ . 3) Poor exchange of GFP tagged CLU with endogenous CLU.

The majority of the nucleolar proteins show the presence of canonical nucleolar localization signal (NoLS), which mediates the nucleolar transport [205]. Analysis of CLU sequence for the presence of NoLS using NoD tool did not reveal any NoLS, indicating its nucleolar localization may be dependent on NLS present in both  $\alpha$  and  $\beta$  chains [85]. Alternatively, sCLU may get imported to the nucleolus by binding to other nucleolar proteins like NPM1 and Nucleolin [206,207]. Taken together, the mechanism of nucleolar accumulation of CLU warrants further investigation.

Since CLU is localized at the FC/DFC interface of the nucleolus, the region where rDNA transcription and processing of rRNA takes place, we examined the effect of nucleases on nucleolar localization of CLU. DNase I had no effect on nucleolar localization, but RNase A treatment showed translocation of nucleolar CLU to the nucleoplasm, suggesting that nucleolar localization of CLU may be ribosomal RNA dependent. Further bioinformatics analysis of sCLU amino acid sequence using online RNA binding region prediction tools showed the presence of putative RNA binding regions at the N and C terminus of sCLU. However, it is not clear whether sCLU binds directly to rRNA or in association with different ribonucleolar proteins.

The nucleolus functions as a 'cellular stress sensor', where any alteration in the morphology and content of nucleolar proteins is an indication of cell growth and proliferation changes, cell cycle deregulation, or senescence [135]. It has been well established that nucleolar stress induced by transcriptional inhibition induces segregation of nucleolar components, where FC and DFC region proteins form bipartite cap-like structures at the nucleolar periphery termed as 'nucleolar caps' or 'necklace like pattern', whereas the

GC region components remain at the nucleolar center in contact with DFC region [208,209]. We also observed similar cap-like structures formed by CLU with other FC/DFC region proteins like Fibrillarin and NPM1 post inhibition of ribosome biosynthesis induced by actinomycin D and doxorubicin resulting in nucleolar stress. It has been suggested that nucleolar proteins or rDNA translocated at nucleolar caps get access to different DNA repair related proteins to further activate different signaling pathways like DNA repair, apoptosis, or senescence [135]. Interestingly, we also observed co-localization of cajal bodies with CLU at the nucleolar caps. Cajal bodies are the site for small nuclear ribonucleoproteins (snRNPs) assembly and the exact significance of its association with cap structures is not known. It is speculated that inhibition of ribogenesis results in post-translational modifications of Coilin (marker for cajal body) like SUMOylation and phosphorylation resulting in disassembly of cajal bodies and its association with nucleolar caps [210]. Such type of nucleolar cap formation was observed only in the case of ‘nucleolar stress’ but not under metabolic stress induced by radiation or hypoxia.

Since nucleolus is the main site for ribosome biosynthesis, we evaluated the effect of CLU knockdown on ribosome biogenesis. Primarily we observed an increase in 45S, 28S, and 18S rRNA transcripts post CLU knockdown, suggestive of its role in the negative regulation of ribogenesis. Tumor suppressor proteins like p14ARF and pNO40 have been shown to negatively regulate ribogenesis by binding to UBF, a nucleolar transcription factor, thus decreasing its occupancy at the rDNA promoter [211,212]. Another tumor suppressor protein MTG16a has been shown to inhibit ribogenesis in breast cancer cells by interacting with nucleolar remodeling complex (NoRC) which recruits histone deacetylases at the rDNA promoter chromatin thereby suppressing rDNA transcription [213]. Future mass spectrometry-based studies to understand the novel interacting partners of CLU in the nucleolus are warranted which will provide more insights into the role of CLU in the

regulation of ribogenesis. In support of this observation, we also observed an increase in the proliferation of CLU knockdown clones, possibly by modulating the ERK and NF- $\kappa$ B pathways.

CLU knockdown studies in oral cancer cells also revealed alterations in nuclear morphologies as seen by aberrant nuclear shapes like irregular, lobulated, and dumbbell. Aberrant nuclear shapes are usually due to defects in the assembly of the post-mitotic nuclear envelope or structural changes of cytoskeletal protein [214,215]. However, no change in the expression of nuclear envelope protein Lamin A/C was observed post CLU knockdown, thus excluding this possibility. Interestingly, we observed a decrease in nucleolar proteins NPM1 and Fibrillarin, which were earlier reported to regulate nuclear shape [191,214]. Although the exact mechanism by which Fibrillarin regulates nuclear shape is not known, NPM1 is known to regulate the cytoskeletal structure through tubulin and actin. Our present study also demonstrated the presence of shrunk tubulin filaments post CLU knockdown, possibly contributing to the abnormal nuclear shapes, suggesting that this could be an independent effect of CLU knockdown or decreased levels of NPM1.

Decreased levels of nucleolar proteins post CLU knockdown suggest that CLU may have a chaperone like function in the stabilization of these proteins. To explore this possibility an *in silico* studies were carried out to understand the interaction between CLU and these nucleolar proteins. Due to the heavy glycosylated nature of sCLU, there is no crystallographic data available for CLU. The structure of sCLU predicted using trRosetta tool indicated that sCLU is mainly comprised of amphipathic  $\alpha$  helices and a small region of beta sheets. The arrangement of these  $\alpha$ - helices may assist in binding and masking unstructured regions of interacting client proteins thus stabilizing it. This is supported by previous reports about secondary structure of CLU which has shown that CLU is comprised of 60%  $\alpha$  helices which possibly shield the exposed hydrophobic regions of the interacting partners and

stabilizes them [88]. Docking studies with different nucleolar proteins showed that the conserved  $\alpha$ -helical region between 140-155 amino acid residues of CLU is principally involved in the interaction, suggesting a similar mode of interaction. Careful analysis showed that the Phe152 of CLU was held in a hydrophobic core created by residues of the binding partner in all the docked complexes, underlining the functional significance of this residue. Intriguingly, in case of its interaction with UBF and NPM1, amino acid residues involved in the interaction with Phe152 of CLU form the hydrophobic core of the protein, signifying the possible role of CLU in maintaining their stability [216,217]. These interactions need to be validated further using co-immunoprecipitation experiments. Thus our study highlights the chaperonic role of CLU in the stabilization of these nucleolar proteins in oral cancer cells.

*Chapter 7*  
*Summary and*  
*Conclusions*

The present study aimed to identify the expression of different transcript variants of CLU and its functional significance in human oral cancer cells. This is the first comprehensive study to understand the expression, localization, and intracellular function of CLU in human oral cancer tissues and cell lines.

**The important findings from this study are as follow:**

- The isoform specific qRT-PCR in oral cancer tissues and cell lines showed the presence of sCLU as the predominant isoform. The transcript levels of other transcript variants including nCLU, NR\_038335.1, and NR\_045494.1 were very low or undetectable.
- The sCLU transcript levels were significantly downregulated in oral tumors compared to their adjacent normal tissues and healthy control tissues obtained during minor dental surgeries. Similarly, we observed downregulation of pre-secretory form of CLU (psCLU) in the majority of the oral tumors compared to its adjacent normal tissue. Immunohistochemical analysis of CLU expression in oral tissue samples showed cytoplasmic staining in both epithelial and cancer associated stromal compartments. Interestingly, low epithelial and high stromal expression of CLU was found to be associated with poor overall and recurrence-free survival of the patients, highlighting its prognostic significance.
- To understand the possible mechanisms for CLU downregulation in oral tumors, we studied methylation of CLU promoter, LOH at chromosome 8p, and miRNA mediated regulation in 10 randomly selected paired oral tissue samples. However, data obtained from methylation- specific PCR and LOH was inconclusive possibly due to the smaller sample size; hence needs to be performed in a larger sample cohort to understand its role in CLU regulation if any. The expression analysis of miRNAs which are predicted to target the CLU gene, showed overexpression of miR-21, miR-15a, and miR-17-3p, which may have a role in CLU downregulation in oral tumors. This needs to be performed in a larger sample cohort

and needs further validation using luciferase-based assay to confirm the binding of miRNA to CLU 3'-UTR.

- All oral cancer cell lines showed downregulation of sCLU transcripts compared to HaCaT, an immortalized skin keratinocyte cell line. However, at the protein level, all oral cancer cell lines showed the presence of a significant amount of protein possibly due to its increased stability. Cycloheximide chase assay in oral cancer cell lines revealed that sCLU is stable for up to 24 hr. Further, treatment of these cells with N-linked glycosylation inhibitor tunicamycin showed a decrease in sCLU levels, suggesting the possible role of glycosylation in imparting stability to sCLU. sCLU degradation was shown to be mediated by the proteasome and lysosomal pathways.
- We demonstrated for the first time the nucleolar localization of CLU in oral cancer cell lines. The nucleolar localization of CLU was confirmed by its co-localization with different nucleolar markers and different fixation-permeabilization techniques. sCLU was mainly localized at the FC and DFC compartments of the nucleolus, the site of rDNA transcription and processing. Nucleolar fractionation studies indisputably confirmed the presence of sCLU in the nucleolar fraction. Also, CLU knockdown studies confirmed the specificity of the CLU antibody used for western blotting and immunofluorescence based studies.
- The study involving overexpression of N- and C-terminally GFP tagged CLU protein in oral cancer cells either showed pan-cellular localization or in the ER and golgi, the secretory pathway components. We did not observe the nucleolar localization of GFP tagged CLU either due to sterically hindered NLS or poor exchange with intracellular endogenous CLU present in the nucleolus.
- Analysis of the sCLU amino acid sequence showed the presence of NLS but no NoLS was detected, suggesting that transport of CLU to nucleolus may be NLS dependent. Further

studies involving site-directed mutagenesis of NLS of sCLU and its effect on the nucleolar localization are currently ongoing in the lab.

- sCLU, like other nucleolar proteins, showed the formation of ‘nucleolar caps’ or ‘nucleolar segregation pattern’ post-treatment with actinomycin D or doxorubicin, a characteristic phenomenon observed post ribosome biosynthesis inhibition. Also, sCLU was associated with cajal bodies at the nucleolar caps post ribogenesis inhibition, suggesting its possible role in nucleolar stress response. However, such types of nucleolar caps were not seen post metabolic stress conditions like radiation and hypoxia.
- RNase A treatment showed translocation of nucleolar CLU to the nucleoplasm, indicating that nucleolar localization of CLU may be rRNA or ribonucleoprotein dependent. This was supported by the presence of putative RNA binding regions at the N and C terminus of sCLU predicted by RNABindR and PPRInt.
- CLU knockdown studies in oral cancer cells showed a significant increase in 28S and 18S rRNAs. The increase in 45S rRNA was not statistically significant. This was also confirmed by the 5-FUrd incorporation assay which showed increased uptake of 5-FUrd in CLU knockdown cells, suggesting the role of nucleolar CLU in the negative regulation of ribogenesis. On a similar line, CLU knockdown clones showed increased proliferation. This suggests the possible tumor suppressor like role of sCLU in oral cancer cells.
- Intriguingly, we also observed altered nuclear shapes post knockdown of CLU. CLU silencing resulted in aberrant nuclear morphologies like ruffled, irregular, and lobulated. The knockdown of CLU resulted in a decrease in the expression of nucleolar proteins NPM1 and Fibrillarin. These two proteins were earlier reported to regulate the nuclear shape possibly by maintaining the cytoskeletal structures like tubulin and actin filaments. In this study, we observed shrunk tubulin filaments in CLU silenced cells resulting in abnormal nuclear shape.

This suggests the role of CLU in nuclear shape maintenance mediated by regulating the levels of nucleolar proteins like NPM1 and Fibrillarin.

- Since NPM1 and Fibrillarin levels were downregulated post sCLU knockdown, we wanted to assess whether sCLU can interact with these nucleolar proteins and mediate chaperonic functions. Hence, to explore this possibility we predicted the structure of sCLU and studied its interaction with different nucleolar proteins like NPM1, Fibrillarin, UBF, and Nucleolin using an *in silico* approach. Interestingly, docking studies revealed the involvement of the amino acid region 140-155 of sCLU in interaction with all the complexes studied. Notably, all the docking complexes showed that the Phe152 residue of sCLU is held in a hydrophobic core created by the residues of the interacting partners.

# *Chapter 8*

## *References*

- [1] A.D. Shrestha, P. Vedsted, P. Kallestrup, D. Neupane, Prevalence and incidence of oral cancer in low- and middle-income countries: A scoping review, *European Journal of Cancer Care*. 29 (2020) 1–7. <https://doi.org/10.1111/ecc.13207>.
- [2] V.V. Boras, A. Fucic, M. Virag, D. Gabric, I. Blivajs, C. Tomasovic-Loncaric, Z. Rakusic, V. Bisof, N. Le Novere, D.V. Vrdoljak, Significance of stroma in biology of oral squamous cell carcinoma, *Tumori*. 104 (2018) 9–14. <https://doi.org/10.5301/tj.5000673>.
- [3] C.F. Lauritano D, Lucchese A, Contaldo M, Serpico R, Lo Muzio L, Biolcati F, Oral squamous cell carcinoma: diagnostic markers and prognostic indicators., *J Biol Regul Homeost Agents*. 30(2 Suppl (2016) 169–76.
- [4] T. Radhika, N. Jeddy, S. Nithya, R.M. Muthumeenakshi, Salivary biomarkers in oral squamous cell carcinoma – An insight, *Journal of Oral Biology and Craniofacial Research*. 6 (2016) S51–S54. <https://doi.org/10.1016/j.jobcr.2016.07.003>.
- [5] S. Gupta, V.S. Kushwaha, S. Verma, H. Khan, M.L.B. Bhatt, N. Husain, M.P.S. Negi, V.V. Bhosale, A. Ghatak, Understanding molecular markers in recurrent oral squamous cell carcinoma treated with chemoradiation, *Heliyon*. 2 (2016). <https://doi.org/10.1016/j.heliyon.2016.e00206>.
- [6] A. Krishna, S. Singh, V. Kumar, U. Pal, Molecular concept in human oral cancer, *National Journal of Maxillofacial Surgery*. 6 (2015) 9. <https://doi.org/10.4103/0975-5950.168235>.
- [7] S.E. Jones, C. Jomary, Clusterin, *International Journal of Biochemistry and Cell Biology*. 34 (2002) 427–431. [https://doi.org/10.1016/S1357-2725\(01\)00155-8](https://doi.org/10.1016/S1357-2725(01)00155-8).
- [8] R. Kadam, T. Teni, Clusterin in cancer: Dual role as a tumor suppressor gene and an oncogene, *Biomedical Research Journal*. (2016). <https://doi.org/10.4103/2349-3666.240609>.

- [9] H. Prochnow, R. Gollan, P. Rohne, M. Hassemer, C. Koch-Brandt, M. Baiersdörfer, Non-Secreted Clusterin Isoforms Are Translated in Rare Amounts from Distinct Human mRNA Variants and Do Not Affect Bax-Mediated Apoptosis or the NF- $\kappa$ B Signaling Pathway, *PLoS ONE*. 8 (2013) 1–15. <https://doi.org/10.1371/journal.pone.0075303>.
- [10] O. Chayka, D. Corvetta, M. Dews, A.E. Caccamo, I. Piotrowska, G. Santilli, S. Gibson, N.J. Sebire, N. Himoudi, M.D. Hogarty, J. Anderson, S. Bettuzzi, A. Thomas-Tikhonenko, A. Sala, Clusterin, a haploinsufficient tumor suppressor gene in neuroblastomas, *Journal of the National Cancer Institute*. 101 (2009) 663–677. <https://doi.org/10.1093/jnci/djp063>.
- [11] B. Liu, M.T.Z. Han, J. Zhang, P. Lu, J. Li, N. Song, Z. Wang, C. Yin, W. Zhang, Downregulation of clusterin expression in human testicular seminoma, *Cellular Physiology and Biochemistry*. 32 (2013) 1117–1123. <https://doi.org/10.1159/000354511>.
- [12] L.Y. Zhang, W.T. Ying, Y.S. Mao, H.Z. He, Y. Liu, H.X. Wang, F. Liu, K. Wang, D.C. Zhang, Y. Wang, M. Wu, X.H. Qian, X.H. Zhao, Loss of clusterin both in serum and tissue correlates with the tumorigenesis of esophageal squamous cell carcinoma via proteomics approaches, *World Journal of Gastroenterology*. 9 (2003) 650–654. <https://doi.org/10.3748/wjg.v9.i4.650>.
- [13] W. Mydlarz, M. Uemura, S. Ahn, P. Hennessey, S. Chang, S. Demokan, W. Sun, C. Shao, J. Bishop, J. Krosting, E. Mambo, W. Westra, P. Ha, D. Sidransky, J. Califano, Clusterin is a gene-specific target of microrna-21 in head and neck squamous cell carcinoma, *Clinical Cancer Research*. 20 (2014) 868–877. <https://doi.org/10.1158/1078-0432.CCR-13-2675>.
- [14] Y. Chen, S.N. Azman, J.P. Kerishnan, R.B. Zain, Y.N. Chen, Y.L. Wong, S.C.B.

- Gopinath, Identification of host-immune response protein candidates in the sera of human oral squamous cell carcinoma patients, *PLoS ONE*. 9 (2014). <https://doi.org/10.1371/journal.pone.0109012>.
- [15] P.P. Naik, S. Mukhopadhyay, P.P. Praharaj, C.S. Bhol, D.P. Panigrahi, K.K. Mahapatra, S. Patra, S. Saha, A.K. Panda, K. Panda, S. Paul, P. Aich, S.K. Patra, S.K. Bhutia, Secretory clusterin promotes oral cancer cell survival via inhibiting apoptosis by activation of autophagy in Akt/mTOR/ULK1 dependent pathway, *Life Sciences*. (2020) 118722. <https://doi.org/10.1016/j.lfs.2020.118722>.
- [16] G. Sarode, N. Maniyar, S.C. Sarode, M. Jafer, S. Patil, K.H. Awan, Epidemiologic aspects of oral cancer, *Disease-a-Month*. 66 (2020) 100988. <https://doi.org/10.1016/j.disamonth.2020.100988>.
- [17] P.K. Sahu, S. Kumar, Epidemiological Aspects of Oral Cancer in North Indian Population, *Indian Journal of Otolaryngology and Head and Neck Surgery*. 71 (2019) 944–948. <https://doi.org/10.1007/s12070-019-01629-7>.
- [18] K.R. Coelho, Challenges of the oral cancer burden in India, *Journal of Cancer Epidemiology*. 2012 (2012). <https://doi.org/10.1155/2012/701932>.
- [19] S.B. Thavarool, G. Muttath, S. Nayanar, K. Duraisamy, P. Bhat, K. Shringarpure, P. Nayak, J.P. Tripathy, A. Thaddeus, S. Philip, B. Satheesan, Improved survival among oral cancer patients: Findings from a retrospective study at a tertiary care cancer centre in rural Kerala, India, *World Journal of Surgical Oncology*. 17 (2019) 1–7. <https://doi.org/10.1186/s12957-018-1550-z>.
- [20] H. Ram, J. Sarkar, H. Kumar, R. Konwar, M.L.B. Bhatt, S. Mohammad, Oral Cancer: Risk Factors and Molecular Pathogenesis, *Journal of Maxillofacial and Oral Surgery*. 10 (2011) 132–137. <https://doi.org/10.1007/s12663-011-0195-z>.
- [21] S. Warnakulasuriya, Clinical features and presentation of oral potentially malignant

- disorders, *Oral Surgery, Oral Medicine, Oral Pathology and Oral Radiology*. 125 (2018) 582–590. <https://doi.org/10.1016/j.oooo.2018.03.011>.
- [22] I. van der Waal, Potentially malignant disorders of the oral and oropharyngeal mucosa; terminology, classification and present concepts of management, *Oral Oncology*. 45 (2009) 317–323. <https://doi.org/10.1016/j.oraloncology.2008.05.016>.
- [23] B. George, S.T. Sebastian, R.R. Soman, V. M., Mulamoottil, M.K. Johny, Prevalence of Precancerous Lesions in an Adult Population, *Indian Journal of Dental Research*. 30 (2019) 500–505. [https://doi.org/0.4103/ijdr.IJDR\\_138\\_18](https://doi.org/0.4103/ijdr.IJDR_138_18).
- [24] M.P. Rethman, W. Carpenter, E.E.W. Cohen, J. Epstein, C.A. Evans, C.M. Flalfz, F.J. Graham, P.P. Hujoel, J.R. Kalmar, W.M. Koch, P.M. Lambert, M.W. Lingen, B.W. Oettmeier, L.L. Patton, D. Perkins, B.C. Reid, J.J. Scclubba, S.L. Tomar, A.D. Wyatt, K. Aravamudhan, J. Frantsve-Hawley, J.L. Cleveland, D.M. Meyer, Evidence-based clinical recommendations regarding screening for oral squamous cell carcinomas, *Journal of the American Dental Association*. 141 (2010) 509–520. <https://doi.org/10.14219/jada.archive.2010.0223>.
- [25] A.F. Bewley, D.G. Farwell, Oral leukoplakia and oral cavity squamous cell carcinoma, *Clinics in Dermatology*. 35 (2017) 461–467. <https://doi.org/10.1016/j.clindermatol.2017.06.008>.
- [26] V.C. Carrard, I. Van Der Waal, A clinical diagnosis of oral leukoplakia; A guide for dentists, *Medicina Oral Patologia Oral y Cirugia Bucal*. 23 (2018) e59–e64. <https://doi.org/10.4317/medoral.22292>.
- [27] S. Abati, C. Bramati, S. Bondi, A. Lissoni, M. Trimarchi, Oral cancer and precancer: A narrative review on the relevance of early diagnosis, *International Journal of Environmental Research and Public Health*. 17 (2020) 1–14. <https://doi.org/10.3390/ijerph17249160>.

- [28] P.A. Reichart, H.P. Philipsen, Oral erythroplakia - A review, *Oral Oncology*. 41 (2005) 551–561. <https://doi.org/10.1016/j.oraloncology.2004.12.003>.
- [29] N.R. Rao, A. Villa, C.B. More, R.D. Jayasinghe, A.R. Kerr, N.W. Johnson, Oral submucous fibrosis: A contemporary narrative review with a proposed inter-professional approach for an early diagnosis and clinical management, *Journal of Otolaryngology - Head and Neck Surgery*. 49 (2020) 1–11. <https://doi.org/10.1186/s40463-020-0399-7>.
- [30] M.B.C. Maymone, R.O. Greer, J. Kesecker, P.C. Sahitya, L.K. Burdine, A.D. Cheng, A.C. Maymone, N.A. Vashi, Premalignant and malignant oral mucosal lesions: Clinical and pathological findings, *Journal of the American Academy of Dermatology*. 81 (2019) 59–71. <https://doi.org/10.1016/j.jaad.2018.09.060>.
- [31] G. Arakeri, P.A. Brennan, Oral submucous fibrosis: An overview of the aetiology, pathogenesis, classification, and principles of management, *British Journal of Oral and Maxillofacial Surgery*. 51 (2013) 587–593. <https://doi.org/10.1016/j.bjoms.2012.08.014>.
- [32] M. Sharma, S.S. Shetty, R. Radhakrishnan, Oral Submucous Fibrosis as an Overhealing Wound: Implications in Malignant Transformation, *Recent Patents on Anti-Cancer Drug Discovery*. 13 (2018) 272–291. <https://doi.org/10.2174/1574892813666180227103147>.
- [33] M. Kumar, R. Nanavati, T. Modi, C. Dobariya, Oral cancer: Etiology and risk factors: A review, *Journal of Cancer Research and Therapeutics*. 12 (2016) 458–463. <https://doi.org/10.4103/0973-1482.186696>.
- [34] D.N.S.& R.M. Sanjay Gupta, Ruchika Gupta, Relationship between type of smokeless tobacco & risk of cancer: A systematic review, *Indian Journal of Medical Research*. 148 (2018) 56–76. [https://doi.org/10.4103/ijmr.IJMR\\_2023\\_17](https://doi.org/10.4103/ijmr.IJMR_2023_17).

- [35] K.A.A.S. Warnakulasuriya, N.W. Johnson, K.M. Linklater, J. Bell, Cancer of mouth, pharynx and nasopharynx in Asian and Chinese immigrants resident in Thames regions, *Oral Oncology*. 35 (1999) 471–475. [https://doi.org/10.1016/S1368-8375\(99\)00019-6](https://doi.org/10.1016/S1368-8375(99)00019-6).
- [36] J. Hukkanen, P. Jacob, M. Peng, D. Dempsey, N.L. Benowitz, Effect of nicotine on cytochrome P450 1A2 activity, *British Journal of Clinical Pharmacology*. 72 (2011) 836–838. <https://doi.org/10.1111/j.1365-2125.2011.04023.x>.
- [37] G. Shah, P. Chaturvedi, S. Vaishampayan, Arecanut as an emerging etiology of oral cancers in India, *Indian Journal of Medical and Paediatric Oncology*. 33 (2012) 71–79. <https://doi.org/10.4103/0971-5851.99726>.
- [38] S.M. Pickwell, S. Schimelpfening, L.A. Palinkas, “Betelmania” - Betel quid chewing by Cambodian women in the United States and its potential health effects, *Western Journal of Medicine*. 160 (1994) 326–330.
- [39] U.J. Nair, G. Obe, M. Friesen, M.T. Goldberg, H. Bartsch, Role of lime in the generation of reactive oxygen species from betel-quid ingredients, *Environmental Health Perspectives*. 98 (1992) 203–205. <https://doi.org/10.1289/ehp.9298203>.
- [40] Y.J. Liu, W. Peng, M.B. Hu, M. Xu, C.J. Wu, The pharmacology, toxicology and potential applications of arecoline: a review, *Pharmaceutical Biology*. 54 (2016) 2753–2760. <https://doi.org/10.3109/13880209.2016.1160251>.
- [41] Q. Peng, Y. Wang, H. Quan, Y. Li, Z. Tang, Oral verrucous carcinoma: From multifactorial etiology to diverse treatment regimens (Review), *International Journal of Oncology*. 49 (2016) 59–73. <https://doi.org/10.3892/ijo.2016.3501>.
- [42] T. V. Evstifeeva, D.G. Zaridze, Nass use, cigarette smoking, alcohol consumption and risk of oral and oesophageal precancer, *European Journal of Cancer. Part B: Oral Oncology*. 28 (1992) 29–35. [https://doi.org/10.1016/0964-1955\(92\)90008-O](https://doi.org/10.1016/0964-1955(92)90008-O).

- [43] G.R. Ogden, A.J. Wight, Aetiology of oral cancer: Alcohol, *British Journal of Oral and Maxillofacial Surgery*. 36 (1998) 247–251. [https://doi.org/10.1016/S0266-4356\(98\)90707-0](https://doi.org/10.1016/S0266-4356(98)90707-0).
- [44] W.H. Westra, The changing face of head and neck cancer in the 21st century: The impact of hpv on the epidemiology and pathology of oral cancer, *Head and Neck Pathology*. 3 (2009) 78–81. <https://doi.org/10.1007/s12105-009-0100-y>.
- [45] F. Dayyani, C.J. Etzel, M. Liu, C.H. Ho, S.M. Lippman, A.S. Tsao, Meta-analysis of the impact of human papillomavirus (HPV) on cancer risk and overall survival in head and neck squamous cell carcinomas (HNSCC), *Head and Neck Oncology*. 2 (2010) 1–11. <https://doi.org/10.1186/1758-3284-2-15>.
- [46] E.J. Shillitoe, The role of viruses in squamous cell carcinoma of the oropharyngeal mucosa, *Oral Oncology*. 45 (2009) 351–355. <https://doi.org/10.1016/j.oraloncology.2008.08.001>.
- [47] R.A.G. Khammissa, J. Fourie, R. Chandran, J. Lemmer, L. Feller, Epstein-Barr virus and its association with oral hairy leukoplakia: A short review, *International Journal of Dentistry*. 2016 (2016). <https://doi.org/10.1155/2016/4941783>.
- [48] S.M. Kim, Human papilloma virus in oral cancer, *Journal of the Korean Association of Oral and Maxillofacial Surgeons*. 42 (2016) 327. <https://doi.org/10.5125/jkaoms.2016.42.6.327>.
- [49] S. Yete, W. D'Souza, D. Saranath, High-Risk Human Papillomavirus in Oral Cancer: Clinical Implications, *Oncology (Switzerland)*. 94 (2018) 133–141. <https://doi.org/10.1159/000485322>.
- [50] M.P. Prasad, T.P. Krishna, S. Pasricha, M.A. Quereshi, K. Krishnaswamy, Diet and oral cancer - a case control study., *Asia Pacific Journal of Clinical Nutrition*. 4 (1995) 259–25964.

- [51] G. Pöschl, H.K. Seitz, Alcohol and cancer, *Alcohol and Alcoholism*. 39 (2004) 155–165. <https://doi.org/10.1093/alcalc/agh057>.
- [52] J. Prelec, Treatment modalities of oral cancer, *Can J Dent Hyg* 2014;48(1):13-19. 48 (2013) 13–19.
- [53] J.P. Shah, Z. Gil, Current concepts in management of oral cancer - Surgery, *Oral Oncology*. 45 (2009) 394–401. <https://doi.org/10.1016/j.oraloncology.2008.05.017>.
- [54] H. Deng, P.J. Sambrook, R.M. Logan, The treatment of oral cancer: An overview for dental professionals, *Australian Dental Journal*. 56 (2011) 244–252. <https://doi.org/10.1111/j.1834-7819.2011.01349.x>.
- [55] J.A. Woolgar, S. Rogers, C.R. West, R.D. Errington, J.S. Brown, E.D. Vaughan, Survival and patterns of recurrence in 200 oral cancer patients treated by radical surgery and neck dissection, *Oral Oncology*. 35 (1999) 257–265. [https://doi.org/10.1016/S1368-8375\(98\)00113-4](https://doi.org/10.1016/S1368-8375(98)00113-4).
- [56] C.F. Poh, D.W. Anderson, J. Scott Durham, J. Chen, K.W. Berean, C.E. MacAulay, M.P. Rosin, Fluorescence visualization-guided surgery for early-stage oral cancer, *JAMA Otolaryngology - Head and Neck Surgery*. 142 (2016) 209–216. <https://doi.org/10.1001/jamaoto.2015.3211>.
- [57] Robert I. Haddad, Recent Advances in Head and Neck Cancer, *N Engl J Med*. 359 (2008) 143–54.
- [58] A. Argiris, N.C. Program, M. V Karamouzis, N.C. Program, D. Raben, R.L. Ferris, N.C. Program, C. Immunology, I. Program, Head and neck cancer Athanassios, *Lancet*. 371 (2008) 1695–1709. [https://doi.org/10.1016/S0140-6736\(08\)60728-X.Head](https://doi.org/10.1016/S0140-6736(08)60728-X.Head).
- [59] J. Alvarez-Moret, F. Pohl, O. Koelbl, B. Dobler, Evaluation of volumetric modulated arc therapy (VMAT) with Oncentra MasterPlan® for the treatment of head and neck

- cancer, *Radiation Oncology*. 5 (2010) 1–10. <https://doi.org/10.1186/1748-717X-5-110>.
- [60] J.J. J Cooper, T Pajak, Forastiere A, Postoperative Concurrent Radiotherapy and Chemotherapy for High-Risk Squamous-Cell Carcinoma of the Head and Neck, *N Engl J Med*. 350 (2004) 1937–44.
- [61] R.S. Rao, S. Patil, S. Ghosh, K. Kumari, Current aspects and future strategies in oral cancer research: A review, *Journal of Medicine, Radiology, Pathology and Surgery*. 1 (2015) 8–13. <https://doi.org/10.15713/ins.jmrps.15>.
- [62] N.N. Danial, S.J. Korsmeyer, Cell Death: Critical Control Points, *Cell*. 116 (2004) 205–219. [https://doi.org/10.1016/S0092-8674\(04\)00046-7](https://doi.org/10.1016/S0092-8674(04)00046-7).
- [63] D. Hanahan, R.A. Weinberg, Hallmarks of cancer: The next generation, *Cell*. 144 (2011) 646–674. <https://doi.org/10.1016/j.cell.2011.02.013>.
- [64] S. Elmore, Apoptosis: A Review of Programmed Cell Death, *Toxicologic Pathology*. 35 (2007) 495–516. <https://doi.org/10.1080/01926230701320337>.
- [65] M. MacFarlane, A.C. Williams, Apoptosis and disease: A life or death decision. Conference and workshop on apoptosis and disease, *EMBO Reports*. 5 (2004) 674–678. <https://doi.org/10.1038/sj.embor.7400191>.
- [66] C.M. Pfeffer, A.T.K. Singh, Apoptosis: A target for anticancer therapy, *International Journal of Molecular Sciences*. 19 (2018). <https://doi.org/10.3390/ijms19020448>.
- [67] S. Fulda, K.M. Debatin, Extrinsic versus intrinsic apoptosis pathways in anticancer chemotherapy, *Oncogene*. 25 (2006) 4798–4811. <https://doi.org/10.1038/sj.onc.1209608>.
- [68] G. Ichim, S.W.G. Tait, A fate worse than death: Apoptosis as an oncogenic process, *Nature Reviews Cancer*. 16 (2016) 539–548. <https://doi.org/10.1038/nrc.2016.58>.
- [69] J.M. Adams, S. Cory, The Bcl-2 apoptotic switch in cancer development and therapy, *Oncogene*. 26 (2007) 1324–1337. <https://doi.org/10.1038/sj.onc.1210220>.

- [70] E. L. Omonosova, G. C. Hinnadurai, BH3-only proteins in apoptosis and beyond: An overview, *Oncogene*. 27 (2008) S2–S19. <https://doi.org/10.1038/onc.2009.39>.
- [71] I. Tamm, Y. Wang, E. Sausville, D.A. Scudiero, N. Vigna, T. Oltersdorf, J.C. Reed, IAP-family protein Survivin inhibits caspase activity and apoptosis induced by Fas (CD95), bax, caspases, and anticancer drugs, *Cancer Research*. 58 (1998) 5315–5320.
- [72] G.S. Salvesen, C.S. Duckett, IAP proteins: Blocking the road to death's door, *Nature Reviews Molecular Cell Biology*. 3 (2002) 401–410. <https://doi.org/10.1038/nrm830>.
- [73] P. Hensley, M. Mishra, N. Kyprianou, Targeting caspases in cancer therapeutics, *Biological Chemistry*. 394 (2013) 831–843. <https://doi.org/10.1515/hsz-2013-0128>.
- [74] A. Ashkenazi, Targeting the extrinsic apoptosis pathway in cancer, *Cytokine and Growth Factor Reviews*. 19 (2008) 325–331. <https://doi.org/10.1016/j.cytogfr.2008.04.001>.
- [75] V. Pavet, M.M. Portal, J.C. Moulin, R. Herbrecht, H. Gronemeyer, Towards novel paradigms for cancer therapy, *Oncogene*. 30 (2011) 1–20. <https://doi.org/10.1038/onc.2010.460>.
- [76] I.B. Fritz, B. Murphy, Insights into a Multifunctional Protein, 8 (1993) 41–45.
- [77] M.E. Rosenberg, J. Silkensen, Clusterin: Physiologic and pathophysiologic considerations, *International Journal of Biochemistry and Cell Biology*. 27 (1995) 633–645. [https://doi.org/10.1016/1357-2725\(95\)00027-M](https://doi.org/10.1016/1357-2725(95)00027-M).
- [78] S. Poon, S.B. Easterbrook-Smith, M.S. Rybchyn, J.A. Carver, M.R. Wilson, Clusterin is an ATP - Independent chaperone with very broad substrate specificity that stabilizes stressed proteins in a folding-competent state, *Biochemistry*. 39 (2000) 15953–15960. <https://doi.org/10.1021/bi002189x>.
- [79] B. Shannan, M. Seifert, K. Leskov, J. Willis, D. Boothman, W. Tilgen, J. Reichrath,

- Challenge and promise: Roles for clusterin in pathogenesis, progression and therapy of cancer, *Cell Death and Differentiation*. 13 (2006) 12–19. <https://doi.org/10.1038/sj.cdd.4401779>.
- [80] I.P. Trougakos, The molecular chaperone apolipoprotein J/Clusterin as a sensor of oxidative stress: Implications in therapeutic approaches - A mini-review, *Gerontology*. 59 (2013) 514–523. <https://doi.org/10.1159/000351207>.
- [81] M. Purrello, S. Bettuzzi, C. Di Pietro, E. Mirabile, M. Di Blasi, R. Rimini, K.H. Grzeschik, C. Ingletti, A. Corti, G. Sichel, The gene for SP-40,40, human homolog of rat sulfated glycoprotein 2, rat clusterin, and rat testosterone-repressed prostate message 2, maps to chromosome 8, *Genomics*. 10 (1991) 151–156. [https://doi.org/10.1016/0888-7543\(91\)90495-Z](https://doi.org/10.1016/0888-7543(91)90495-Z).
- [82] F. Rizzi, S. Bettuzzi, The clusterin paradigm in prostate and breast carcinogenesis, *Endocrine-Related Cancer*. 17 (2010) 1–17. <https://doi.org/10.1677/ERC-09-0140>.
- [83] P. Rohne, H. Prochnow, C. Koch-Brandt, The CLU-files: Disentanglement of a mystery, *Biomolecular Concepts*. 7 (2016) 1–15. <https://doi.org/10.1515/bmc-2015-0026>.
- [84] J. O’Sullivan, L. Whyte, J. Drake, M. Tenniswood, Alterations in the post-translational modification and intracellular trafficking of clusterin in MCF-7 cells during apoptosis, *Cell Death and Differentiation*. 10 (2003) 914–927. <https://doi.org/10.1038/sj.cdd.4401254>.
- [85] K.S. Leskov, D.Y. Klovov, J. Li, T.J. Kinsella, D.A. Boothman, Synthesis and functional analyses of nuclear clusterin, a cell death protein, *Journal of Biological Chemistry*. 278 (2003) 11590–11600. <https://doi.org/10.1074/jbc.M209233200>.
- [86] C.L. Andersen, T. Schepeler, K. Thorsen, K. Birkenkamp-Demtröder, F. Mansilla, L.A. Aaltonen, S. Laurberg, T.F. Ørntoft, Clusterin expression in normal mucosa and

- colorectal cancer, *Molecular and Cellular Proteomics*. 6 (2007) 1039–1048.  
<https://doi.org/10.1074/mcp.M600261-MCP200>.
- [87] I.F. Ling, J. Bhongsatiern, J.F. Simpson, D.W. Fardo, S. Estus, Genetics of clusterin isoform expression and Alzheimer's disease risk, *PLoS ONE*. 7 (2012).  
<https://doi.org/10.1371/journal.pone.0033923>.
- [88] A.R. Wyatt, J.J. Yerbury, M.R. Wilson, Structural characterization of clusterin-chaperone client protein complexes, *Journal of Biological Chemistry*. 284 (2009) 21920–21927. <https://doi.org/10.1074/jbc.M109.033688>.
- [89] A.R. Wyatt, J.J. Yerbury, M.R. Wilson, Structural characterization of clusterin-chaperone client protein complexes, *Journal of Biological Chemistry*. 284 (2009) 21920–21927. <https://doi.org/10.1074/jbc.M109.033688>.
- [90] A. Londou, A. Mikrou, I.K. Zarkadis, Cloning and characterization of two clusterin isoforms in rainbow trout, *Molecular Immunology*. 45 (2008) 470–478.  
<https://doi.org/10.1016/j.molimm.2007.05.027>.
- [91] R.W. Bailey, A.K. Dunker, C.J. Brown, E.C. Garner, M.D. Griswold, Clusterin, a binding protein with a molten globule-like region, *Biochemistry*. 40 (2001) 11828–11840. <https://doi.org/10.1021/bi010135x>.
- [92] A.K. Dunker, J.D. Lawson, C.J. Brown, R.M. Williams, P. Romero, J.S. Oh, C.J. Oldfield, A.M. Campen, C.M. Ratliff, K.W. Hipps, J. Ausio, M.S. Nissen, R. Reeves, C.H. Kang, C.R. Kissinger, R.W. Bailey, M.D. Griswold, W. Chiu, E.C. Garner, Z. Obradovic, Intrinsically disordered protein, *Journal of Molecular Graphics and Modelling*. 19 (2001) 26–59. [https://doi.org/10.1016/S1093-3263\(00\)00138-8](https://doi.org/10.1016/S1093-3263(00)00138-8).
- [93] J.A. Carver, A. Rekas, D.C. Thorn, M.R. Wilson, Small Heat-shock Proteins and Clusterin: Intra- and Extracellular Molecular Chaperones with a Common Mechanism of Action and Function?, *IUBMB Life*. 55 (2003) 661–668.

<https://doi.org/10.1080/15216540310001640498>.

- [94] D.H. Lee, J.H. Ha, Y. Kim, K.H. Bae, J.Y. Park, W.S. Choi, H.S. Yoon, S.G. Park, B.C. Park, G.S. Yi, S.W. Chi, Interaction of a putative BH3 domain of clusterin with anti-apoptotic Bcl-2 family proteins as revealed by NMR spectroscopy, *Biochemical and Biophysical Research Communications*. 408 (2011) 541–547. <https://doi.org/10.1016/j.bbrc.2011.04.054>.
- [95] T. Koltai, Clusterin: A key player in cancer chemoresistance and its inhibition, *OncoTargets and Therapy*. 7 (2014) 447–456. <https://doi.org/10.2147/OTT.S58622>.
- [96] O. Chayka, D. Corvetta, M. Dews, A.E. Caccamo, I. Piotrowska, G. Santilli, S. Gibson, N.J. Sebire, N. Himoudi, M.D. Hogarty, J. Anderson, S. Bettuzzi, A. Thomas-Tikhonenko, A. Sala, Clusterin, a haploinsufficient tumor suppressor gene in neuroblastomas, *Journal of the National Cancer Institute*. 101 (2009) 663–677. <https://doi.org/10.1093/jnci/djp063>.
- [97] B. Liu, M.T.Z. Han, J. Zhang, P. Lu, J. Li, N. Song, Z. Wang, C. Yin, W. Zhang, Downregulation of clusterin expression in human testicular seminoma, *Cellular Physiology and Biochemistry*. 32 (2013) 1117–1123. <https://doi.org/10.1159/000354511>.
- [98] B. Zhang, K. Zhang, Z. Liu, F. Hao, M. Wang, X. Li, Z. Yin, H. Liang, Secreted Clusterin gene silencing enhances chemosensitivity of A549 cells to cisplatin through AKT and ERK1/2 pathways in vitro, *Cellular Physiology and Biochemistry*. 33 (2014) 1162–1175. <https://doi.org/10.1159/000358685>.
- [99] J.C. Chuang, P.A. Jones, Epigenetics and microRNAs, *Pediatric Research*. 61 (2007) 24–29. <https://doi.org/10.1203/pdr.0b013e3180457684>.
- [100] P. Lund, K. Weißhaupt, T. Mikeska, D. Jammass, X. Chen, R.J. Kuban, U. Ungethüm, U. Krapfenbauer, H.P. Herzog, R. Schäfer, J. Walter, C. Sers, Oncogenic HRAS

- suppresses clusterin expression through promoter hypermethylation, *Oncogene*. 25 (2006) 4890–4903. <https://doi.org/10.1038/sj.onc.1209502>.
- [101] D.M.E.I. Hellebrekers, V. Melotte, E. Viré, E. Langenkamp, G. Molema, F. Fuks, J.G. Herman, W. Van Criekinge, A.W. Griffioen, M. Van Engeland, Identification of epigenetically silenced genes in tumor endothelial cells, *Cancer Research*. 67 (2007) 4138–4148. <https://doi.org/10.1158/0008-5472.CAN-06-3032>.
- [102] T. Nuutinen, T. Suuronen, S. Kyrlylenko, J. Huuskonen, A. Salminen, Induction of clusterin/apoJ expression by histone deacetylase inhibitors in neural cells, *Neurochemistry International*. 47 (2005) 528–538. <https://doi.org/10.1016/j.neuint.2005.07.007>.
- [103] H.E. Rauhala, K.P. Porkka, O.R. Saramäki, T.L.J. Tammela, T. Visakorpi, Clusterin is epigenetically regulated in prostate cancer, *International Journal of Cancer*. 123 (2008) 1601–1609. <https://doi.org/10.1002/ijc.23658>.
- [104] F.T. Liao, Y.J. Lee, J.L. Ko, C.C. Tsai, C.J. Tseng, G.T. Sheu, Hepatitis delta virus epigenetically enhances clusterin expression via histone acetylation in human hepatocellular carcinoma cells, *Journal of General Virology*. 90 (2009) 1124–1134. <https://doi.org/10.1099/vir.0.007211-0>.
- [105] J. Park, S.Y. Park, E. Shin, S.H. Lee, Y.S. Kim, D.H. Lee, G.S. Roh, H.J. Kim, S.S. Kang, G.J. Cho, B.Y. Jeong, H. Kim, W.S. Choi, Hypoxia inducible factor-1 $\alpha$  directly regulates nuclear clusterin transcription by interacting with hypoxia response elements in the clusterin promoter, *Molecules and Cells*. 37 (2014) 178–186. <https://doi.org/10.14348/molcells.2014.2349>.
- [106] A. Serrano, M. Redondo, T. Tellez, I. Castro-Vega, M.J. Roldan, R. Mendez, A. Rueda, E. Jimenez, Regulation of clusterin expression in human cancer via DNA methylation, *Tumor Biology*. 30 (2009) 286–291. <https://doi.org/10.1159/000259912>.

- [107] S. Amente, G. Milazzo, M.C. Sorrentino, G. Di Palo, L. Lania, G. Perini, B. Majello, Lysine-specific demethylase ( LSD1 / KDM1A ) and MYCN cooperatively repress tumor suppressor genes in neuroblastoma, 6 (2015).
- [108] F. Erhard, J. Haas, D. Lieber, G. Malterer, L. Jaskiewicz, M. Zavolan, L. Dołken, R. Zimmer, Widespread context dependency of microRNA-mediated regulation, *Genome Research*. 24 (2014) 906–919. <https://doi.org/10.1101/gr.166702.113>.
- [109] A. Sala, S. Bettuzzi, S. Pucci, O. Chayka, M. Dews, A. Thomas-Tikhonenko, Regulation of CLU gene expression by oncogenes and epigenetic factors: Implications for tumorigenesis, *Advances in Cancer Research*. 105 (2009) 115–132. [https://doi.org/10.1016/S0065-230X\(09\)05007-6](https://doi.org/10.1016/S0065-230X(09)05007-6).
- [110] I.P. Trougakos, M. Lourda, M.H. Antonelou, D. Kletsas, V.G. Gorgoulis, I.S. Papassideri, Y. Zou, L.H. Margaritis, D.A. Boothman, E.S. Gonos, Intracellular clusterin inhibits mitochondrial apoptosis by suppressing p53-activating stress signals and stabilizing the cytosolic Ku70-bax protein complex, *Clinical Cancer Research*. 15 (2009) 48–59. <https://doi.org/10.1158/1078-0432.CCR-08-1805>.
- [111] F. Zhang, M. Kumano, E. Beraldi, L. Fazli, C. Du, S. Moore, P. Sorensen, A. Zoubeidi, M.E. Gleave, Clusterin facilitates stress-induced lipidation of LC3 and autophagosome biogenesis to enhance cancer cell survival, *Nature Communications*. 5 (2014) 1–13. <https://doi.org/10.1038/ncomms6775>.
- [112] M. Xu, X. Chen, Y. Han, C. Ma, L. Ma, S. Li, Clusterin silencing sensitizes pancreatic cancer MIA-PaCa-2 cells to gemcitabine via regulation of NF- $\kappa$ B/BCL-2 signaling, *International Journal of Clinical and Experimental Medicine*. 8 (2015) 12476–12486.
- [113] Y. Tang, F. Liu, C. Zheng, S. Sun, Y. Jiang, Knockdown of clusterin sensitizes pancreatic cancer cells to gemcitabine chemotherapy by ERK1/2 inactivation, *Journal of Experimental and Clinical Cancer Research*. 31 (2012) 1–10.

<https://doi.org/10.1186/1756-9966-31-73>.

- [114] T.Y. Chou, W.C. Chen, A.C. Lee, S.M. Hung, N.Y. Shih, M.Y. Chen, Clusterin silencing in human lung adenocarcinoma cells induces a mesenchymal-to-epithelial transition through modulating the ERK/Slug pathway, *Cellular Signalling*. 21 (2009) 704–711. <https://doi.org/10.1016/j.cellsig.2009.01.008>.
- [115] Y.J. Shim, Y.J. Shin, S.Y. Jeong, S.W. Kang, B.M. Kim, I.S. Park, B.H. Min, Epidermal growth factor receptor is involved in clusterin-induced astrocyte proliferation, *NeuroReport*. 20 (2009) 435–439. <https://doi.org/10.1097/WNR.0b013e3283262df8>.
- [116] P. WONG, D. TAILLEFER, J. LAKINS, J. PINEAULT, G. CHADER, M. TENNISWOOD, Molecular characterization of human TRPM- 2/clusterin, a gene associated with sperm maturation, apoptosis and neurodegeneration, *European Journal of Biochemistry*. 221 (1994) 917–925. <https://doi.org/10.1111/j.1432-1033.1994.tb18807.x>.
- [117] G. Jin, P.H. Howe, Transforming growth factor  $\beta$  regulates clusterin gene expression via modulation of transcription factor c-Fos, *European Journal of Biochemistry*. 263 (1999) 534–542. <https://doi.org/10.1046/j.1432-1327.1999.00533.x>.
- [118] K.B. Reddy, G. Jin, M.C. Karode, J.A.K. Harmony, P.H. Howe, Reddy KB, *Biochemistry* 1996 6157-6163 Transforming Growth Factor  $\beta$  (TGF $\beta$ )-Induced Nuclear Localization of.pdf, 2960 (1996) 6157–6163.
- [119] K.B. Lee, J.H. Jeon, I. Choi, O.Y. Kwon, K. Yu, K.H. You, Clusterin, a novel modulator of TGF- $\beta$  signaling, is involved in Smad2/3 stability, *Biochemical and Biophysical Research Communications*. 366 (2008) 905–909. <https://doi.org/10.1016/j.bbrc.2007.12.033>.
- [120] M. Shiota, A. Zardan, A. Takeuchi, M. Kumano, E. Beraldi, S. Naito, A. Zoubeidi,

- M.E. Gleave, Clusterin mediates TGF- $\beta$ -induced epithelial-mesenchymal transition and metastasis via Twist1 in prostate cancer cells, *Cancer Research*. 72 (2012) 5261–5272. <https://doi.org/10.1158/0008-5472.CAN-12-0254>.
- [121] H. Ammar, J.L. Closset, Clusterin activates survival through the phosphatidylinositol 3-kinase/akt pathway, *Journal of Biological Chemistry*. 283 (2008) 12851–12861. <https://doi.org/10.1074/jbc.M800403200>.
- [122] E.M. Goetz, B. Shankar, Y. Zou, J.C. Morales, X. Luo, S. Araki, R. Bachoo, L.D. Mayo, D.A. Boothman, ATM-dependent IGF-1 induction regulates secretory clusterin expression after DNA damage and in genetic instability, *Oncogene*. 30 (2011) 3745–3754. <https://doi.org/10.1038/onc.2011.92>.
- [123] H. Jo, Y. Jia, K.K. Subramanian, H. Hattori, H.R. Luo, Cancer Cell-Derived Clusterin Modulates the Phosphatidylinositol 3'-Kinase-Akt Pathway through Attenuation of Insulin-Like Growth Factor 1 during Serum Deprivation, *Molecular and Cellular Biology*. 28 (2008) 4285–4299. <https://doi.org/10.1128/mcb.01240-07>.
- [124] J.Y. Lee, H.J. Kim, S.B. Rho, S.H. Lee, eIF3f reduces tumor growth by directly interrupting clusterin with anti-apoptotic property in cancer cells, *Oncotarget*. 7 (2016) 18541–18557. <https://doi.org/10.18632/oncotarget.8105>.
- [125] A. Takeuchi, M. Shiota, E. Beraldi, D. Thaper, K. Takahara, N. Ibuki, M. Pollak, M.E. Cox, S. Naito, M.E. Gleave, A. Zoubeidi, Insulin-like growth factor-I induces CLU expression through Twist1 to promote prostate cancer growth, *Molecular and Cellular Endocrinology*. 384 (2014) 117–125. <https://doi.org/10.1016/j.mce.2014.01.012>.
- [126] G. Santilli, B.J. Aronow, A. Sala, Essential requirement of apolipoprotein J (clusterin) signaling for I $\kappa$ B expression and regulation of NF- $\kappa$ B activity, *Journal of Biological Chemistry*. 278 (2003) 38214–38219. <https://doi.org/10.1074/jbc.C300252200>.
- [127] V. Devauchelle, A. Essabbani, G. De Pinieux, S. Germain, L. Tourneur, S. Mistou, F.

- Margottin-Goguet, P. Anract, H. Migaud, D. Le Nen, T. Lequerré, A. Saraux, M. Dougados, M. Breban, C. Fournier, G. Chiochia, Characterization and Functional Consequences of Underexpression of Clusterin in Rheumatoid Arthritis, *The Journal of Immunology*. 177 (2006) 6471–6479. <https://doi.org/10.4049/jimmunol.177.9.6471>.
- [128] L. Debure, J.L. Vayssière, V. Rincheval, F. Loison, Y. Le Dréan, D. Michel, Intracellular clusterin causes juxtannuclear aggregate formation and mitochondrial alteration, *Journal of Cell Science*. 116 (2003) 3109–3121. <https://doi.org/10.1242/jcs.00619>.
- [129] K. Bettens, S. Vermeulen, C. Van Cauwenberghe, B. Heeman, B. Asselbergh, C. Robberecht, S. Engelborghs, M. Vandenbulcke, R. Vandenberghe, P.P. De Deyn, M. Cruts, C. Van Broeckhoven, K. Sleegers, Reduced secreted clusterin as a mechanism for Alzheimer-associated CLU mutations, *Molecular Neurodegeneration*. 10 (2015) 1–12. <https://doi.org/10.1186/s13024-015-0024-9>.
- [130] S.K. Herring, H.J. Moon, P. Rawal, A. Chhibber, L. Zhao, Brain clusterin protein isoforms and mitochondrial localization, *ELife*. 8 (2019) 1–31. <https://doi.org/10.7554/eLife.48255>.
- [131] S.R. Matukumalli, R. Tangirala, C.M. Rao, Clusterin: Full-length protein and one of its chains show opposing effects on cellular lipid accumulation, *Scientific Reports*. 7 (2017) 1–13. <https://doi.org/10.1038/srep41235>.
- [132] M. Dunder, T. Misteli, Nucleolomics: An inventory of the nucleolus, *Molecular Cell*. 9 (2002) 5–7. [https://doi.org/10.1016/S1097-2765\(02\)00433-1](https://doi.org/10.1016/S1097-2765(02)00433-1).
- [133] M.O.J. Olson, M. Dunder, The moving parts of the nucleolus, *Histochemistry and Cell Biology*. 123 (2005) 203–216. <https://doi.org/10.1007/s00418-005-0754-9>.
- [134] V. Tiku, A. Antebi, Nucleolar Function in Lifespan Regulation, 2018. 28 (n.d.) 662–672.

- [135] S. Boulon, B.J. Westman, S. Hutten, F.M. Boisvert, A.I. Lamond, The Nucleolus under Stress, *Molecular Cell*. 40 (2010) 216–227. <https://doi.org/10.1016/j.molcel.2010.09.024>.
- [136] J.S. Andersen, Y.W. Lam, A.K.L. Leung, S.E. Ong, C.E. Lyon, A.I. Lamond, M. Mann, Nucleolar proteome dynamics, *Nature*. 433 (2005) 77–83. <https://doi.org/10.1038/nature03207>.
- [137] D. Chen, A.S. Belmont, S. Huang, Upstream binding factor association induces large-scale chromatin decondensation, *Proceedings of the National Academy of Sciences of the United States of America*. 101 (2004) 15106–15111. <https://doi.org/10.1073/pnas.0404767101>.
- [138] A.C. O’Sullivan, G.J. Sullivan, B. McStay, UBF Binding In Vivo Is Not Restricted to Regulatory Sequences within the Vertebrate Ribosomal DNA Repeat, *Molecular and Cellular Biology*. 22 (2002) 657–658. <https://doi.org/10.1128/mcb.22.2.657-668.2002>.
- [139] S. Snaar, K. Wiesmeijer, A.G. Jochemsen, H.J. Tanke, R.W. Dirks, Mutational analysis of fibrillarin and its mobility in living human cells, *Journal of Cell Biology*. 151 (2000) 653–662. <https://doi.org/10.1083/jcb.151.3.653>.
- [140] M.Y. Shubina, Y.R. Musinova, E. V. Sheval, Nucleolar methyltransferase fibrillarin: Evolution of structure and functions, *Biochemistry (Moscow)*. 81 (2016) 941–950. <https://doi.org/10.1134/S0006297916090030>.
- [141] V. Sirri, D. Hernandez-Verdun, P. Roussel, Cyclin-dependent kinases govern formation and maintenance of the nucleolus, *Journal of Cell Biology*. 156 (2002) 969–981. <https://doi.org/10.1083/jcb.200201024>.
- [142] M. Okuwaki, The structure and functions of NPM1/Nucleophsmin/B23, a multifunctional nucleolar acidic protein, *Journal of Biochemistry*. 143 (2008) 441–448. <https://doi.org/10.1093/jb/mvm222>.

- [143] A. Szebeni, J.E. Herrera, M.O.J. Olson, Interaction of Nucleolar Protein B23 with Peptides Related to Nuclear Localization Signals, *Biochemistry*. 34 (1995) 8037–8042. <https://doi.org/10.1021/bi00025a009>.
- [144] A.Y.C. Tan, D.A. Westerman, D.A. Carney, J.F. Seymour, S. Juneja, A. Dobrovic, Detection of NPM1 exon 12 mutations and FLT3 - Internal tandem duplications by high resolution melting analysis in normal karyotype acute myeloid leukemia, *Journal of Hematology and Oncology*. 1 (2008) 1–5. <https://doi.org/10.1186/1756-8722-1-10>.
- [145] R. Tuteja, N. Tuteja, Nucleolin: A multifunctional major nucleolar phosphoprotein, 1998. <https://doi.org/10.1080/10409239891204260>.
- [146] S. Storck, M. Shukla, S. Dimitrov, P. Bouvet, Functions of the histone chaperone nucleolin in diseases, *Subcellular Biochemistry*. 41 (2007) 125–144. [https://doi.org/10.1007/1-4020-5466-1\\_7](https://doi.org/10.1007/1-4020-5466-1_7).
- [147] D. Angelov, V.A. Bondarenko, S. Almagro, H. Menoni, F. Mongélard, F. Hans, F. Mietton, V.M. Studitsky, A. Hamiche, S. Dimitrov, P. Bouvet, Nucleolin is a histone chaperone with FACT-like activity and assists remodeling of nucleosomes, *EMBO Journal*. 25 (2006) 1669–1679. <https://doi.org/10.1038/sj.emboj.7601046>.
- [148] J.G. Gall, The centennial of the Cajal body, *Nature Reviews Molecular Cell Biology*. 4 (2003) 975–980. <https://doi.org/10.1038/nrm1262>.
- [149] K.M. Neugebauer, Special focus on the Cajal Body, *RNA Biology*. 14 (2017) 669–670. <https://doi.org/10.1080/15476286.2017.1316928>.
- [150] M. Platani, I. Goldberg, J.R. Swedlow, A.I. Lamond, In vivo analysis of Cajal body movement, separation, and joining in live human cells, *Journal of Cell Biology*. 151 (2000) 1561–1574. <https://doi.org/10.1083/jcb.151.7.1561>.
- [151] G.E. Morris, The Cajal body, *Biochimica et Biophysica Acta - Molecular Cell Research*. 1783 (2008) 2108–2115. <https://doi.org/10.1016/j.bbamcr.2008.07.016>.

- [152] A.S. Pfister, Emerging role of the nucleolar stress response in autophagy, *Frontiers in Cellular Neuroscience*. 13 (2019) 1–18. <https://doi.org/10.3389/fncel.2019.00156>.
- [153] K. Yang, J. Yang, J. Yi, Nucleolar stress: Hallmarks, sensing mechanism and diseases, *Cell Stress*. 2 (2018) 125–140. <https://doi.org/10.15698/cst2018.06.139>.
- [154] C.M. Yaron Shav-Tal,\*† Janna Blechman,\* Xavier Darzacq, and D.Z. Billy T. Dye,§ James G. Patton,§ Robert H. Singer, Dynamic Sorting of Nuclear Components into Distinct Nucleolar Caps during Transcriptional Inhibition, *Mol Biol Cell*. 15 (2005) 2395–2413. <https://doi.org/10.1091/mbc.E04>.
- [155] D.H. Larsen, M. Stucki, Nucleolar responses to DNA double-strand breaks, *Nucleic Acids Research*. 44 (2016) 538–544. <https://doi.org/10.1093/nar/gkv1312>.
- [156] H. Mangan, M. Gailín, B. McStay, Integrating the genomic architecture of human nucleolar organizer regions with the biophysical properties of nucleoli, *FEBS Journal*. 284 (2017) 3977–3985. <https://doi.org/10.1111/febs.14108>.
- [157] Y. Zhang, H. Lu, Signaling to p53: Ribosomal Proteins Find Their Way, *Cancer Cell*. 16 (2009) 369–377. <https://doi.org/10.1016/j.ccr.2009.09.024>.
- [158] Y. Ofir-Rosenfeld, K. Boggs, D. Michael, M.B. Kastan, M. Oren, Mdm2 Regulates p53 mRNA Translation through Inhibitory Interactions with Ribosomal Protein L26, *Molecular Cell*. 32 (2008) 180–189. <https://doi.org/10.1016/j.molcel.2008.08.031>.
- [159] K. Holmberg Olausson, M. Nistér, M. Lindström, p53 -Dependent and -Independent Nucleolar Stress Responses, *Cells*. 1 (2012) 774–798. <https://doi.org/10.3390/cells1040774>.
- [160] M.S. Dai, H. Arnold, X.X. Sun, R. Sears, H. Lu, Inhibition of c-Myc activity by ribosomal protein L11, *EMBO Journal*. 26 (2007) 3332–3345. <https://doi.org/10.1038/sj.emboj.7601776>.
- [161] S. Jayaraman, S. Chittiboyina, Y. Bai, P.C. Abad, P.A. Vidi, C. V. Stauffacher, S.A.

- Lelièvre, The nuclear mitotic apparatus protein NuMA controls rDNA transcription and mediates the nucleolar stress response in a p53-independent manner, *Nucleic Acids Research*. 45 (2017) 11725–11742. <https://doi.org/10.1093/nar/gkx782>.
- [162] S.J. Lo, L.C. Fan, Y.F. Tsai, K.Y. Lin, H.L. Huang, T.H. Wang, H. Liu, T.C. Chen, S.F. Huang, C.J. Chang, Y.J. Lin, B.Y.M. Yung, S.Y. Hsieh, A novel interaction of nucleophosmin with BCL2-associated X protein regulating death evasion and drug sensitivity in human hepatoma cells, *Hepatology*. 57 (2013) 1893–1905. <https://doi.org/10.1002/hep.26209>.
- [163] J. Pelletier, G. Thomas, S. Volarevi, Ribosome biogenesis in cancer: New players and therapeutic avenues, *Nature Reviews Cancer*. 18 (2017) 51–63. <https://doi.org/10.1038/nrc.2017.104>.
- [164] D.M. Stults, M.W. Killen, H.H. Pierce, A.J. Pierce, Genomic architecture and inheritance of human ribosomal RNA gene clusters, *Genome Research*. 18 (2008) 13–18. <https://doi.org/10.1101/gr.6858507>.
- [165] D.L.J. Lafontaine, Noncoding RNAs in eukaryotic ribosome biogenesis and function, *Nature Structural and Molecular Biology*. 22 (2015) 11–19. <https://doi.org/10.1038/nsmb.2939>.
- [166] P. Boukamp, R.T. Petrussevska, D. Breitkreutz, J. Hornung, A. Markham, N.E. Fusenig, Normal keratinization in a spontaneously immortalized aneuploid human keratinocyte cell line, *Journal of Cell Biology*. 106 (1988) 761–771. <https://doi.org/10.1083/jcb.106.3.761>.
- [167] S.E. Chang, S. Foster, D. Betts, W.E. Marnock, DOK, a cell line established from human dysplastic oral mucosa, shows a partially transformed non-malignant phenotype, *International Journal of Cancer*. 52 (1992) 896–902. <https://doi.org/10.1002/ijc.2910520612>.

- [168] R.J. Tatake, N. Rajaram, R.N. Damle, B. Balsara, A.N. Bhisey, S.G. Gangal, Establishment and characterization of four new squamous cell carcinoma cell lines derived from oral tumors, *Journal of Cancer Research and Clinical Oncology*. 116 (1990) 179–186. <https://doi.org/10.1007/BF01612674>.
- [169] J.S. White, J.L. Weissfeld, C.C.R. Ragin, K.M. Rossie, C.L. Martin, M. Shuster, C.S. Ishwad, J.C. Law, E.N. Myers, J.T. Johnson, S.M. Gollin, The influence of clinical and demographic risk factors on the establishment of head and neck squamous cell carcinoma cell lines, *Oral Oncology*. 43 (2007) 701–712. <https://doi.org/10.1016/j.oraloncology.2006.09.001>.
- [170] J.G. Rheinwald, M.A. Beckett, Tumorigenic Keratinocyte Lines Requiring Anchorage and Fibroblast Support Cultured from Human Squamous Cell Carcinomas, *Cancer Research*. 41 (1981) 1657–1663.
- [171] K.J. Livak, T.D. Schmittgen, Analysis of relative gene expression data using real-time quantitative PCR and the  $2^{-\Delta\Delta CT}$  method, *Methods*. 25 (2001) 402–408. <https://doi.org/10.1006/meth.2001.1262>.
- [172] Ayantika Sen Gupta, Kundan Sengupta, Lamin B2 Modulates Nucleolar Morphology, Dynamics, and Function, *Molecular and Cellular Biology*. 37 (2017) 1–22.
- [173] Z.F. Li, Y.W. Lam, A new rapid method for isolating nucleoli, *Methods in Molecular Biology*. 1228 (2015) 35–42. [https://doi.org/10.1007/978-1-4939-1680-1\\_4](https://doi.org/10.1007/978-1-4939-1680-1_4).
- [174] S. Gabriel, L. Ziaugra, D. Tabbaa, SNP genotyping using the sequenom massARRAY iPLEX Platform, *Current Protocols in Human Genetics*. (2009) 1–18. <https://doi.org/10.1002/0471142905.hg0212s60>.
- [175] C. Chen, D.A. Ridzon, A.J. Broomer, Z. Zhou, D.H. Lee, J.T. Nguyen, M. Barbisin, N.L. Xu, V.R. Mahuvakar, M.R. Andersen, K.Q. Lao, K.J. Livak, K.J. Guegler, Real-time quantification of microRNAs by stem-loop RT-PCR, *Nucleic Acids Research*. 33

- (2005) 1–9. <https://doi.org/10.1093/nar/gni178>.
- [176] L. Malaguarnera, G. Nunnari, M. Di Rosa, Nuclear import sequence identification in hOAS3 protein, *Inflammation Research*. 65 (2016) 895–904. <https://doi.org/10.1007/s00011-016-0972-8>.
- [177] M.S. Scott, F.M. Boisvert, M.D. McDowall, A.I. Lamond, G.J. Barton, Characterization and prediction of protein nucleolar localization sequences, *Nucleic Acids Research*. 38 (2010) 7388–7399. <https://doi.org/10.1093/nar/gkq653>.
- [178] M. Terribilini, J.D. Sander, J.H. Lee, P. Zaback, R.L. Jernigan, V. Honavar, D. Dobbs, RNABindR: A server for analyzing and predicting RNA-binding sites in proteins, *Nucleic Acids Research*. 35 (2007) 578–584. <https://doi.org/10.1093/nar/gkm294>.
- [179] M. Kumar, M.M. Gromiha, G.P.S. Raghava, Prediction of RNA binding sites in a protein using SVM and PSSM profile, *Proteins: Structure, Function and Genetics*. 71 (2008) 189–194. <https://doi.org/10.1002/prot.21677>.
- [180] J. Yang, I. Anishchenko, H. Park, Z. Peng, S. Ovchinnikov, D. Baker, Improved protein structure prediction using predicted interresidue orientations, *Proceedings of the National Academy of Sciences of the United States of America*. 117 (2020) 1496–1503. <https://doi.org/10.1073/pnas.1914677117>.
- [181] E. Krieger, K. Joo, J. Lee, J. Lee, S. Raman, J. Thompson, M. Tyka, D. Baker, K. Karplus, Improving physical realism, stereochemistry, and side-chain accuracy in homology modeling: Four approaches that performed well in CASP8., *Proteins*. 77 Suppl 9 (2009) 114–122. <https://doi.org/10.1002/prot.22570>.
- [182] V.A. Simossis, J. Heringa, PRALINE: A multiple sequence alignment toolbox that integrates homology-extended and secondary structure information, *Nucleic Acids Research*. 33 (2005) 289–294. <https://doi.org/10.1093/nar/gki390>.
- [183] B.G. Pierce, K. Wiehe, H. Hwang, B.-H. Kim, T. Vreven, Z. Weng, ZDOCK server:

- interactive docking prediction of protein-protein complexes and symmetric multimers., *Bioinformatics* (Oxford, England). 30 (2014) 1771–1773. <https://doi.org/10.1093/bioinformatics/btu097>.
- [184] G.D. Dakubo, J.P. Jakupciak, M.A. Birch-Machin, R.L. Parr, Clinical implications and utility of field cancerization, *Cancer Cell International*. 7 (2007) 1–12. <https://doi.org/10.1186/1475-2867-7-2>.
- [185] L. Chatra, R. Prabhu, P. Rao, K. Shahin, P. Shenai, K. Veena, M. Aparna, Field cancerization: A review, *Archives of Medicine and Health Sciences*. 1 (2013) 136. <https://doi.org/10.4103/2321-4848.123026>.
- [186] M. Bonacini, M. Coletta, I. Ramazzina, V. Naponelli, A. Modernelli, P. Davalli, S. Bettuzzi, F. Rizzi, Distinct promoters, subjected to epigenetic regulation, drive the expression of two clusterin mRNAs in prostate cancer cells, *Biochimica et Biophysica Acta - Gene Regulatory Mechanisms*. 1849 (2015) 44–54. <https://doi.org/10.1016/j.bbagr.2014.11.003>.
- [187] R.J. SOLÁ, K. GRIEBENOW, Effects of Glycosylation on the Stability of Protein Pharmaceuticals, *J Pharm Sci*. 98 (2009) 1223–1245.
- [188] D. Shental-Bechor, Y. Levy, Effect of glycosylation on protein folding: A close look at thermodynamic stabilization, *Proceedings of the National Academy of Sciences of the United States of America*. 105 (2008) 8256–8261. <https://doi.org/10.1073/pnas.0801340105>.
- [189] S.P. Jin, J.H. Chung, Inhibition of N-glycosylation by tunicamycin attenuates cell–cell adhesion via impaired desmosome formation in normal human epidermal keratinocytes, *Bioscience Reports*. 38 (2018) 1–11. <https://doi.org/10.1042/BSR20171641>.
- [190] A. Vasconcelos-dos-Santos, I.A. Oliveira, M.C. Lucena, N.R. Mantuano, S.A. Whelan,

- W.B. Dias, A.R. Todeschini, Biosynthetic machinery involved in aberrant glycosylation: Promising targets for developing of drugs against cancer, *Frontiers in Oncology*. 5 (2015) 1–23. <https://doi.org/10.3389/fonc.2015.00138>.
- [191] M.A. Amin, S. Matsunaga, N. Ma, H. Takata, M. Yokoyama, S. Uchiyama, K. Fukui, Fibrillarin, a nucleolar protein, is required for normal nuclear morphology and cellular growth in HeLa cells, *Biochemical and Biophysical Research Communications*. 360 (2007) 320–326. <https://doi.org/10.1016/j.bbrc.2007.06.092>.
- [192] M.A. Amin, S. Matsunaga, S. Uchiyama, K. Fukui, Depletion of nucleophosmin leads to distortion of nucleolar and nuclear structures in HeLa cells, *Biochemical Journal*. 415 (2008) 345–351. <https://doi.org/10.1042/bj20081411>.
- [193] S.T. Chou, H.Y. Peng, K.C. Mo, Y.M. Hsu, G.H. Wu, J.R. Hsiao, S.F. Lin, H.D. Wang, S.G. Shiah, MicroRNA-486-3p functions as a tumor suppressor in oral cancer by targeting DDR1, *Journal of Experimental and Clinical Cancer Research*. 38 (2019) 1–14. <https://doi.org/10.1186/s13046-019-1283-z>.
- [194] K.C. Valkenburg, A.E. De Groot, K.J. Pienta, Targeting the tumour stroma to improve cancer therapy, *Nature Reviews Clinical Oncology*. 15 (2018) 366–381. <https://doi.org/10.1038/s41571-018-0007-1>.
- [195] D. Tarin, Role of the host stroma in cancer and its therapeutic significance, *Cancer and Metastasis Reviews*. 32 (2013) 553–566. <https://doi.org/10.1007/s10555-013-9438-4>.
- [196] M. Pins, J. Fiadjoe, F. Korley, M. Wong, A. Rademaker, B. Jovanovic, T. Yoo1, J. Kozlowski, A. Raji, X. Yang, C. Lee1, Clusterin as a possible predictor for biochemical recurrence of prostate cancer following radical prostatectomy with intermediate Gleason scores: a preliminary report, *Prostate Cancer Prostatic Dis*. 7 (2004) 243–248.
- [197] L.R. He, M.Z. Liu, B.K. Li, H.L. Rao, Y.J. Liao, L.J. Zhang, X.Y. Guan, Y.X. Zeng,

- D. Xie, Clusterin as a predictor for chemoradiotherapy sensitivity and patient survival in esophageal squamous cell carcinoma, *Cancer Science*. 100 (2009) 2354–2360. <https://doi.org/10.1111/j.1349-7006.2009.01349.x>.
- [198] Y. Wang, A.S. Brodsky, J. Xiong, M.L. Lopresti, D. Yang, M.B. Resnick, Stromal Clusterin Expression Predicts Therapeutic Response to Neoadjuvant Chemotherapy in Triple Negative Breast Cancer, *Clinical Breast Cancer*. 18 (2018) e373–e379. <https://doi.org/10.1016/j.clbc.2017.08.007>.
- [199] S. Bettuzzi, P. Davalli, S. Davoli, O. Chayka, F. Rizzi, L. Belloni, D. Pellacani, G. Fregni, S. Astancolle, M. Fassan, A. Corti, R. Baffa, A. Sala, Genetic inactivation of ApoJ/clusterin: Effects on prostate tumourigenesis and metastatic spread, *Oncogene*. 28 (2009) 4344–4352. <https://doi.org/10.1038/onc.2009.286>.
- [200] K. Ono, A. Miyakawa, M. Fukuda, M. Shiiba, K. Uzawa, T. Watanabe, T. Miya, H. Yokoe, Y. Imai, H. Tanzawa, Allelic loss on the short arm of chromosome 8 in oral squamous cell carcinoma., *Oncology Reports*. 6 (1999) 785–789. <https://doi.org/10.3892/or.6.4.785>.
- [201] M. Deb, D. Sengupta, S.K. Rath, S. Kar, S. Parbin, A. Shilpi, N. Pradhan, S.K. Bhutia, S. Roy, S.K. Patra, Clusterin gene is predominantly regulated by histone modifications in human colon cancer and ectopic expression of the nuclear isoform induces cell death, *Biochimica et Biophysica Acta - Molecular Basis of Disease*. 1852 (2015) 1630–1645. <https://doi.org/10.1016/j.bbadis.2015.04.021>.
- [202] M. Guerra-Rebollo, F. Mateo, K. Franke, M.S.Y. Huen, F. Lopitz-Otsoa, M.S. Rodríguez, V. Plans, T.M. Thomson, Nucleolar exit of RNF8 and BRCA1 in response to DNA damage, *Experimental Cell Research*. 318 (2012) 2365–2376. <https://doi.org/10.1016/j.yexcr.2012.07.003>.
- [203] R. Benyair, G.Z. Lederkremer, Common fixation-permeabilization methods cause

- artifactual localization of a type II transmembrane protein, *Microscopy* (Oxford, England). 65 (2016) 517–521. <https://doi.org/10.1093/jmicro/dfw035>.
- [204] M.L. Finch, A.M. Passman, R.P. Strauss, G.C. Yeoh, B.A. Callus, Sub-cellular localisation studies may spuriously detect the yes-associated protein, YAP, in nucleoli leading to potentially invalid conclusions of its function, *PLoS ONE*. 10 (2015) 1–15. <https://doi.org/10.1371/journal.pone.0114813>.
- [205] I.S. de Melo, M.D. Jimenez-Nuñez, C. Iglesias, A. Campos-Caro, D. Moreno-Sanchez, F.A. Ruiz, J. Bolívar, NOA36 Protein Contains a Highly Conserved Nucleolar Localization Signal Capable of Directing Functional Proteins to the Nucleolus, in *Mammalian Cells*, *PLoS ONE*. 8 (2013) 1–12. <https://doi.org/10.1371/journal.pone.0059065>.
- [206] Y. Wang, B. Chen, Y. Li, D. Zhou, S. Chen, PNRC accumulates in the nucleolus by interaction with B23/nucleophosmin via its nucleolar localization sequence, *Biochimica et Biophysica Acta - Molecular Cell Research*. 1813 (2011) 109–119. <https://doi.org/10.1016/j.bbamcr.2010.09.017>.
- [207] R. V. Intine, M. Dundr, A. Vassilev, E. Schwartz, Y. Zhao, Y. Zhao, M.L. DePamphilis, R.J. Maraia, Nonphosphorylated Human La Antigen Interacts with Nucleolin at Nucleolar Sites Involved in rRNA Biogenesis, *Molecular and Cellular Biology*. 24 (2004) 10894–10904. <https://doi.org/10.1128/mcb.24.24.10894-10904.2004>.
- [208] Y. Shav-Tal, J. Blechman, X. Darzacq, C. Montagna, B.T. Dye, J.G. Patton, R.H. Singer, D. Zipori, Dynamic Sorting of Nuclear Components into Distinct Nucleolar Caps during Transcriptional Inhibition, *Molecular Biology of the Cell*. 16 (2005) 2395–2413.
- [209] H. Mangan, M. Gailín, B. McStay, Integrating the genomic architecture of human

- nucleolar organizer regions with the biophysical properties of nucleoli, *FEBS Journal*. 284 (2017) 3977–3985. <https://doi.org/10.1111/febs.14108>.
- [210] L. Trinkle-Mulcahy, J.E. Sleeman, The Cajal body and the nucleolus: “In a relationship” or “It’s complicated”?, *RNA Biology*. 14 (2017) 739–751. <https://doi.org/10.1080/15476286.2016.1236169>.
- [211] Y.M. Lin, P.H. Chu, P. Ouyang, Ectopically expressed pNO40 suppresses ribosomal RNA synthesis by inhibiting UBF-dependent transcription activation, *Biochemical and Biophysical Research Communications*. 516 (2019) 381–387. <https://doi.org/10.1016/j.bbrc.2019.06.057>.
- [212] Anthony J. Saporita, Leonard B. Maggi, Anthony J. Apicelli, Jason D. Weber, Therapeutic Targets in the ARF Tumor Suppressor Pathway, *Current Medicinal Chemistry*. 14 (2007) 1815–1827. <https://doi.org/10.2174/092986707781058869>.
- [213] S. Rossetti, A.T. Hoogeveen, J. Esposito, N. Sacchi, Loss of MTG16a (CBFA2T3), a novel rDNA repressor, leads to increased ribogenesis and disruption of breast acinar morphogenesis, *Journal of Cellular and Molecular Medicine*. 14 (2010) 1358–1370. <https://doi.org/10.1111/j.1582-4934.2009.00982.x>.
- [214] M.A. Amin, S. Matsunaga, S. Uchiyama, K. Fukui, Depletion of nucleophosmin leads to distortion of nucleolar and nuclear structures in HeLa cells, *Biochemical Journal*. 415 (2008) 345–351. <https://doi.org/10.1042/BJ20081411>.
- [215] S. Ulbert, W. Antonin, M. Platani, I.W. Mattaj, The inner nuclear membrane protein Lem2 is critical for normal nuclear envelope morphology, *FEBS Letters*. 580 (2006) 6435–6441. <https://doi.org/10.1016/j.febslet.2006.10.060>.
- [216] D. Wang, J. Zhang, X. Jin, J. Wu, Y. Shi, Investigation of the structural stability of hUBF HMG box 5 by native-state hydrogen exchange, *Biochemistry*. 46 (2007) 1293–1302. <https://doi.org/10.1021/bi061682r>.

[217] C.G. Grummitt, F.M. Townsley, C.M. Johnson, A.J. Warren, M. Bycroft, Structural consequences of nucleophosmin mutations in acute myeloid leukemia, *Journal of Biological Chemistry*. 283 (2008) 23326–23332. <https://doi.org/10.1074/jbc.M801706200>.

# *Chapter 9*

## *Appendix*

## Compositions of the Buffers/ Reagents used in this study

### 1. 10X Phosphate Buffered Saline (PBS) pH 7.4

NaCl	80 g
Na <sub>2</sub> HPO <sub>4</sub>	16 g
NaH <sub>2</sub> PO <sub>4</sub>	4.5 g

### 2. 10X Tris buffered saline (TBS) pH 7.6

Tris	24.2 g
NaCl	80 g
Distilled water	1000 ml
Adjust the pH to 7.6 using HCl	

### 3. 1X Tris Buffered Saline containing Tween-20 (TBST)

Add 0.1% (v/v) Tween-20 to 1X TBS to prepare 1X TBST

### 4. TELT buffer for plasmid DNA extraction

Tris-Cl (pH 7.5)	50mM
EDTA (pH 8.0)	62.5mM
Triton X-100	0.4%
LiCl	2.5M

### 5. Lysis buffer for protein extraction

NaCl	125 mM
Tris (pH 7.5)	50 mM
NP-40	0.5%

Add protease inhibitor cocktail while lysate preparation

**6. 6X Sample loading dye (For 10 ml)**

1 M Tris (pH 6.8)	1.875 ml
$\beta$ -mercaptoethanol	4.5 ml
Glycerol	6 ml
10% SDS	0.69 ml
1% Bromophenol blue	0.5 ml

**7. 10 X Electrode buffer (For 1 litre)**

Tris	30.2 g
Glycine	144.12g
SDS	10 g

**8. 30% Acrylamide solution**

Acryamide	29.2g
Bis-Acrylamide	0.8g
Distilled Water	Make up volume to 100ml

**9. Transfer/Electroblotting Buffer**

Tris Base	9g
Glycine	39.5g
Methanol	600ml
10% SDS	1ml
Distilled Water	Make up volume to 3000ml

**10. Stripping Buffer**

B-Mercaptoethanol	1.63g
10% SDS	40ml
1M Tris	12.5ml
Distilled Water	Make up volume to 200ml

**11. 10X Sodium Citrate Buffer for IHC (pH: 5.8-6.0)**

Tri-Sodium Citrate	2.94 g
Distilled Water	Make up volume to 1000ml

## 12. Erythrosine B dye

0.4 g Erythrosine B powder dissolved in 100 ml of 1X PBS

## 13. 50X TAE

Tris base	242 g
Acetic acid	57.1 ml
0.5 M EDTA (pH 8.0)	100 ml
Distilled Water	Make up volume to 1000ml

## 14. 4% Paraformaldehyde (PFA)

Dissolve 4 g EM grade PFA in 50 ml distilled water. Add 1 ml 1 M NaOH. Stir gently on a heating block at 60<sup>0</sup>C until the PFA is dissolved completely. Add 10 ml of 10X PBS and allow the mixture to cool at R.T. Adjust the pH 7.4 with 1M HCl and then adjust the final volume to 100 ml with distilled water. Filter the solution through 0.45 μ filter to remove any particulate matter.

## 15. Super Optimal Broth (For 100 ml)

Tryptone	2.0 g
Yeast extract	0.5 g
0.05% NaCl	0.05 g
250mM KCl	1 ml

Autoclave and then add 1 ml of 1M MgCl<sub>2</sub> before use.

## 16. Transformation Buffer

10mM PIPES Na-Salt	0.165g
15mM CaCl <sub>2</sub>	0.11g
250mM KCl	0.932g
Adjust pH using KOH to 6.7	
Add 55mM MnCl <sub>2</sub>	0.54g

Filter sterilize the solution.

## Thesis Abstract

**Name:** Ms. Rajashree Chittaranjan Kadam

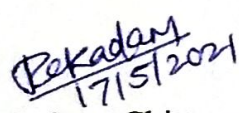
**Enrollment Number:** LIFE09201304006

**Thesis Title:** "Elucidating the Role of Clusterin in Human Oral Cancers"

Clusterin (CLU) is stress induced chaperonic glycoprotein associated with various physiological functions like cell cycle regulation, apoptosis, DNA repair, etc. The two spliced variants of CLU namely the secretory and nuclear forms serve anti- and pro-apoptotic functions respectively. Previous studies done in the lab using ribonuclease protection assay have shown downregulation of CLU transcripts in oral cancer cells unlike its overexpression in other carcinomas which prompted us further to investigate the role of CLU in oral tumorigenesis.

We demonstrated the downregulation of secretory CLU (sCLU) transcript and protein in human oral cancer tissues. Immunohistochemical analysis in oral tumor samples has shown that low expression of sCLU in the epithelium and high expression in stroma is associated with poor overall and recurrence-free survival of patients. Oral cancer cell lines showed downregulation of sCLU transcripts compared to normal tissues; however, we observed high expression of sCLU protein in oral cancer cell lines possibly due to its increased stability. Nuclear CLU (nCLU) was not detected at transcript and protein levels in oral cancer cells. In the present study, we report for the first time the RNA-dependent nucleolar localization of sCLU protein in oral cancer cell lines. sCLU has been shown to form 'nucleolar cap' like structures in response to nucleolar stress conditions which affect the ribosome biosynthesis. Interestingly, post-CLU knockdown we observed an increase in ribogenesis and proliferation which suggests its possible tumor-suppressive role in oral cancer. Also knockdown of sCLU resulted in a decrease in NPM1 and Fibrillarin levels which concomitantly result in abnormal shapes of nuclei and shrunk cytoskeletal filaments indicative of its role in nuclear shape maintenance. Further *in silico* analysis revealed the hydrophobic interaction of Phe152 residue of CLU with different nucleolar proteins like NPM1, Fibrillarin, Nucleolin, and UBF suggesting the possible chaperonic function of CLU in the stabilization of these nucleolar proteins.

Signature:

  
17/5/2021  
Student\*: Rajashree Chittaranjan Kadam

Signature:

  
17/05/21  
Guide\*: Dr. Tanuja Teni

Forwarded through:

  
17/5/2021  
Dr. Sorab N. Dalal,  
Chairperson, Academic &  
Training Programme, ACTREC

**(Dr. Sorab N. Dalal)**  
Chairperson, Academic & Training Programme  
Tata Memorial Center, ACTREC,  
Kharghar, Navi Mumbai - 410210

  
27/5/21  
Dr. S. D. Banavali,  
Dean (Academics)  
T.M.C.

PROF. S. D. BANAVALI, MD  
DEAN (ACADEMICS)  
TATA MEMORIAL CENTRE  
MUMBAI - 400 012.

\*Put name only

## Thesis Highlight

**Name of the Student:** Ms. Rajashree Chittaranjan Kadam

**Name of the CI/OCC:** TMC-ACTREC

**Enrolment No.:** LIFE09201304006

**Thesis Title:** Elucidating the Role of Clusterin in Human Oral Cancers

**Discipline:** Life Sciences

**Date of viva voce:** 17<sup>th</sup> May, 2021

The present study aimed to identify the expression of different transcript variants of CLU and its functional significance in human oral cancer cells. This is the first comprehensive study to understand the expression, localization, and intracellular function of CLU in human oral cancer tissues and cell lines. The isoform-specific qRT-PCR in oral cancer tissues and cell lines showed the presence of sCLU as the predominant isoform. The nCLU transcripts were very low/undetectable in both oral cancer tissues and cell lines. The sCLU transcript levels were significantly downregulated in oral tumors compared to their adjacent normal tissues and healthy control tissues obtained during minor dental surgeries. Similarly, we observed the downregulation of the pre-secretory form of CLU (psCLU) protein in the majority of the oral tumors compared to its adjacent normal tissue. Immunohistochemical analysis of CLU expression in oral tissue samples showed cytoplasmic staining in both epithelial and cancer-associated stromal compartments. Interestingly, low epithelial and high stromal expression of CLU was found to be associated with poor overall and recurrence-free survival of the patients, highlighting its prognostic significance. All oral cancer cell lines showed downregulation of sCLU transcripts compared to HaCaT, an immortalized skin keratinocyte cell line. However, at the protein level, all oral cancer cell lines showed the presence of a significant amount of protein possibly due to its increased stability due to heavy glycosylation.

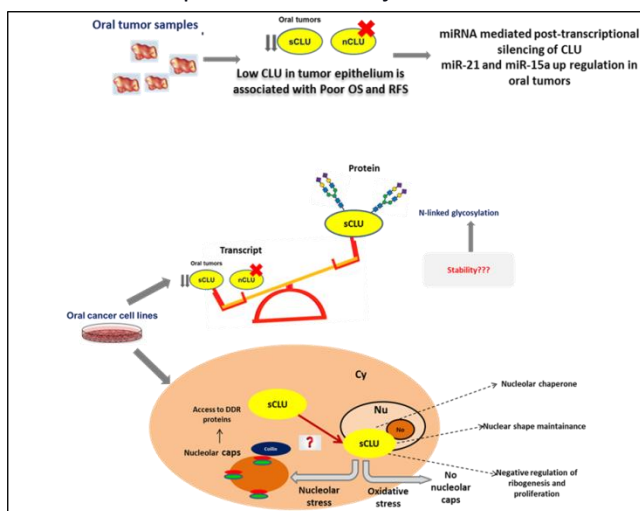


**Figure: Role of CLU in human oral cancers**

We demonstrated for the first time the nucleolar localization of CLU in oral cancer cell lines. The nucleolar localization of CLU was shown to be RNA dependent and showed response to nucleolar stress conditions as shown by nucleolar cap formation. The knockdown of CLU showed an increase in proliferation and ribosome biogenesis suggesting its possible tumor suppressor-like role. Intriguingly, we also observed altered nuclear shapes post knockdown of CLU. The knockdown of CLU resulted in a decrease in the expression of nucleolar proteins NPM1 and Fibrillarin which were earlier reported to regulate the nuclear shape possibly by maintaining the cytoskeletal structures like tubulin and actin filaments. In this study, we observed shrunk tubulin filaments in CLU silenced cells resulting in abnormal nuclear shape. This suggests the role of CLU in nuclear shape maintenance mediated by regulating the levels of nucleolar proteins like NPM1 and Fibrillarin. Further, *in silico* studies were carried out to understand the interaction between CLU and nucleolar proteins. Interestingly, docking studies revealed the involvement of the amino acid region 140-155 of sCLU in interaction with all the complexes studied. Notably, all the docking complexes showed that the Phe152 residue of sCLU is held in a hydrophobic core created by the residues of the interacting partners.